

# Electronic Supplementary Information (ESI)

## Tris-NHC-propagated self-supported polymer-based Pd catalysts for heterogeneous C–H functionalization

Tanmoy Mandal,<sup>a</sup> Tapas Kumar Dutta,<sup>b</sup> Sunit Mohanty,<sup>c</sup> and Joyanta Choudhury<sup>a\*</sup>

<sup>a</sup>Organometallics & Smart Materials Laboratory, Department of Chemistry, Indian Institute of Science Education and Research (IISER) Bhopal, Bhopal 462 066, India.

<sup>b</sup>Department of Chemistry, IISER Bhopal, Bhopal 462 066, India.

<sup>c</sup>Department of Earth and Environmental Sciences, IISER Bhopal, Bhopal 462 066, India.

E-mail: [joyanta@iiserb.ac.in](mailto:joyanta@iiserb.ac.in).

### CONTENTS

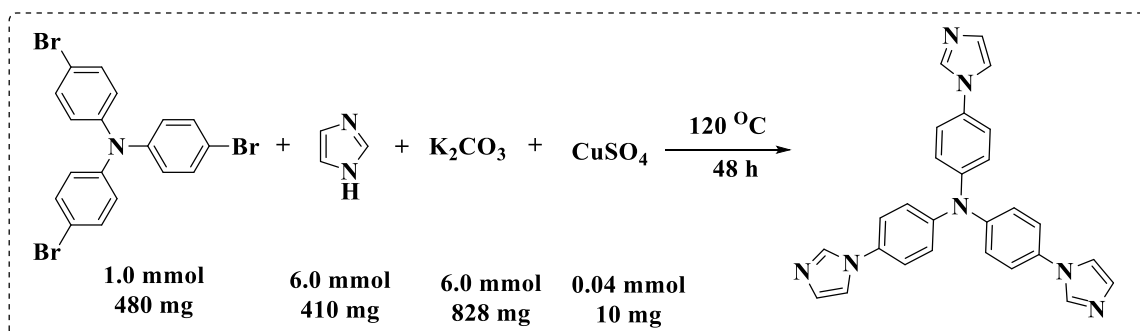
- I. General methods and materials
- II. Synthesis of ligands and polymeric materials
- III. SEM images
- IV. XPS analysis
- V. EDX analysis
- VI. FT-IR spectra
- VII. Adsorption-desorption studies
- VIII. UV-vis studies
- IX. Electrochemical studies
- X. TGA plots
- XI. Solid-state <sup>13</sup>C NMR spectra
- XII. Solution-state <sup>1</sup>H NMR spectra
- XIII. Catalytic halogenation
- XIV. Catalytic arylation
- XV. XPS and SEM analysis of the recovered catalysts
- XVI. References

## I. General methods and materials:

$^1\text{H}$  and  $^{13}\text{C}\{^1\text{H}\}$  NMR spectra were recorded in Bruker AVANCE III 400 MHz and 500 MHz NMR spectrometers. Chemical shifts ( $\delta$ ) are expressed in ppm using the residual proton resonance of the solvent as an internal standard ( $\text{CHCl}_3$ :  $\delta = 7.26$  ppm for  $^1\text{H}$  spectra, 77.36 ppm for  $^{13}\text{C}\{^1\text{H}\}$  spectra; DMSO:  $\delta = 2.50$  ppm for  $^1\text{H}$  spectra, 39.52 ppm for  $^{13}\text{C}\{^1\text{H}\}$  spectra). All coupling constants ( $J$ ) are expressed in hertz (Hz) and only given for  $^1\text{H}$ - $^1\text{H}$  couplings. The following abbreviations were used to indicate multiplicity: s (singlet), d (doublet), t (triplet), dd (doublet of doublets), dt (doublet of triplets), m (multiplet), bs (broad singlet), and bm (broad multiplet). UV-vis spectra were recorded on Agilent Technology Cary 100 UV-vis spectrophotometer. Electrochemical experiments were done using CHI 620E Electrochemical Analyzer. Thermo Gravimetric Analysis (TGA) was carried out using Perkin Elmer TGA-6000 instrument. The morphology of the materials was examined using a Carl Zeiss (Ultra Plus) field emission scanning electron microscope (FE-SEM). Energy-dispersive X-ray spectroscopy was performed using Oxford Instruments X-MaxN. XPS analysis was conducted in PHI 5000 Versa Probe II instrument from FEI Inc. at IIT Kanpur, India. ICP-MS was performed with induced coupled plasma Mass spectrometer (ICP-MS) Thermo iCAP Q facility at the EES Department, IISER Bhopal. GC-MS were recorded with an Agilent 7890A GC coupled with an Agilent 5975C MS system. Solid-state NMR spectroscopy was performed on JEOL Model ECX400 Proton freq: 400 MHz instruments at IISc Bangalore, India. FTIR measurements were recorded on Shimadzu and Perkin-Elmer instruments. Solvents and reagents were obtained from commercial suppliers and used without further purification. Deuterated solvents were purchased from Aldrich.  $\text{Pd}(\text{OAc})_2$  was purchased from Johnson Matthey and used as received without further purification.

## II. Synthesis of ligands and polymeric materials:

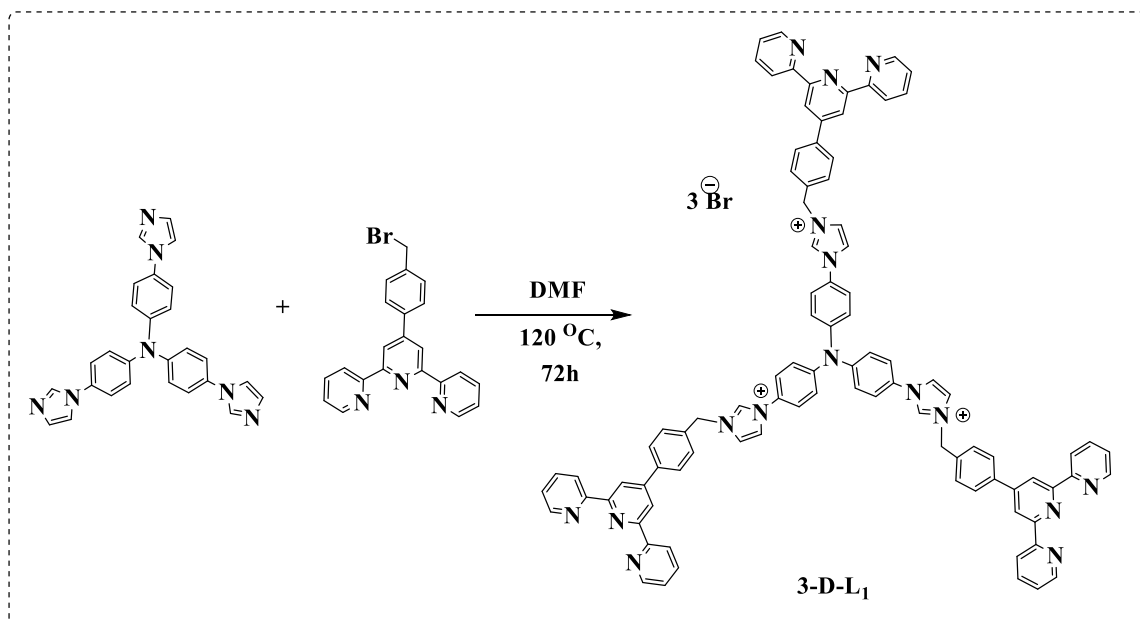
### i. Synthesis of tris (4-(1H-imidazol-1-yl) phenyl) amine:



**Scheme S1:** Synthesis of tris (4-(1H-imidazol-1-yl) phenyl) amine

Tris (4-bromophenyl) amine (480 mg, 1.0 mmol), imidazole (410 mg, 6.0 mmol), potassium carbonate (828 mg, 6.0 mmol) and copper sulfate (10 mg, 0.04 mmol) were heated at 120 °C for 48 h in a pressure tube. A off-white solid was formed which was filtered using G4 bed. and was washed with water, toluene and then by using ether to afford the desired product. Yield = 85 %. <sup>1</sup>H NMR (400 MHz, DMSO-d<sub>6</sub>) δ 8.20 (s, 3H), 7.70 (s, 3H), 7.62 (d, 6H), 7.18 (d, 6H), 7.10 (s, 3H).

**ii. Synthesis of 3D-L<sub>1</sub>:**

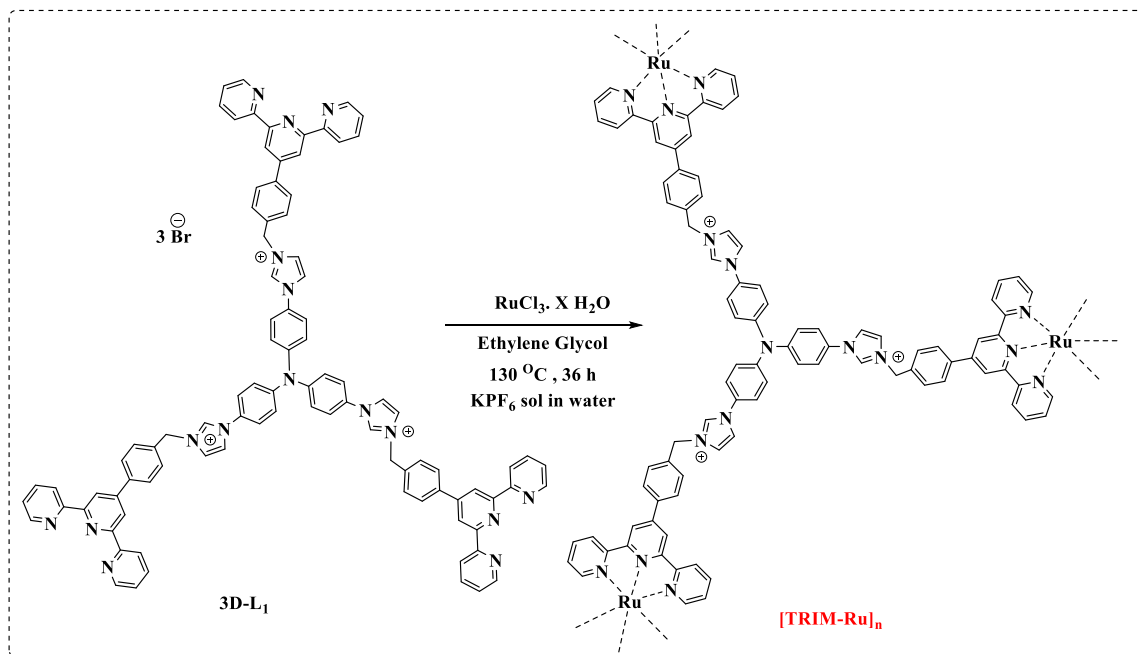


**Scheme S2:** Synthesis of **3D-L<sub>1</sub>**

Tris (4-(1H-imidazol-1-yl) phenyl) amine (271 mg, 0.6 mmol) and 4'-(4-(bromomethyl) phenyl)-2, 2':6', 2''-terpyridine (1.47 g, 3.65 mmol) were dissolved in 15 mL DMF and stirred at 120 °C for 72 h. Then the reaction mixture was allowed to cool to room temperature which results in a deep brown colored solution. This solution was added to acetone (70 mL) in a drop-wise manner with vigorous stirring which results in a large amount of white-grey color precipitate. Then it was then filtered and washed with diethyl ether to furnish the product as an off-white powder. Yield = 90%. The product was characterized by <sup>1</sup>H NMR spectroscopy and by matching with literature report.

<sup>1</sup>H NMR (400 MHz, DMSO-d<sub>6</sub>) δ 10.15 (s, 3H), 8.80 – 8.65 (m, 18H), 8.38 (s, 3H), 8.14 (s, 3H), 8.09 – 8.02 (m, 12H), 7.81 (d, 6H), 7.73 (d, 6H), 7.67 (s, 6H), 7.34 (d, 6H), 5.66 (s, 6H).

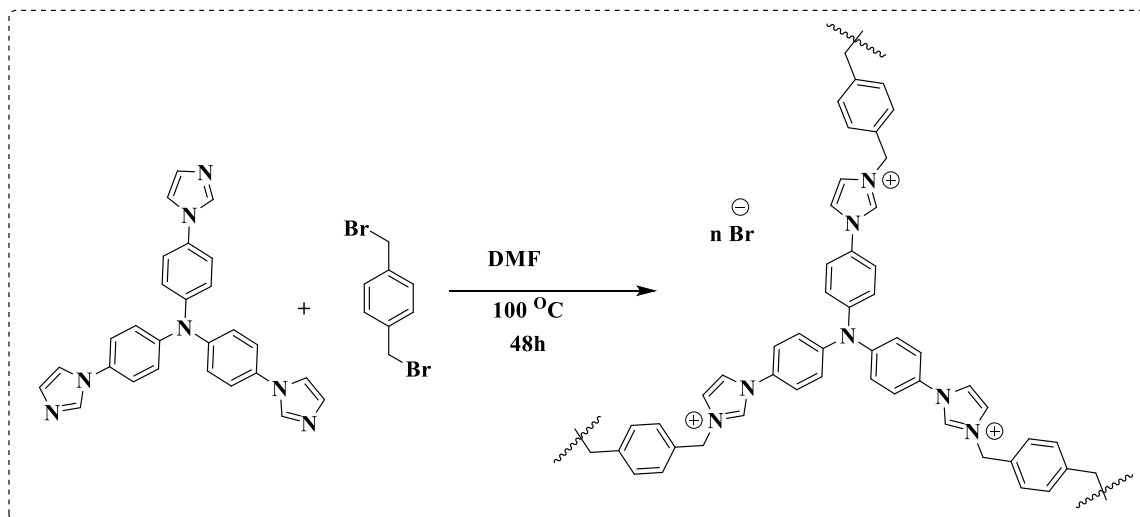
iii. Synthesis of [TRIM-Ru]<sub>n</sub>:



Scheme S3: Synthesis of [TRIM-Ru]<sub>n</sub>

(0.1 mmol, 165.0 mg) **3D-L<sub>1</sub>** and 1.5 equivalent of RuCl<sub>3</sub>·3H<sub>2</sub>O (0.15 mmol, 32.0 mg) were taken in a Schlenk tube. 5 mL of ethylene glycol was added to this and the reaction mixture was stirred at 130 °C for 36 h. After this time the reaction mixture turned to a deep blood-red colored solution with some red colored precipitate. Thereafter the reaction mixture was cooled to room temperature and an excess solution of aqueous KPF<sub>6</sub> was added to this. Immediately, a red-colored precipitate was formed. The precipitate was filtered by using G4 bed and washed well with a lot of water and methanol. At last, the precipitate was washed with diethyl ether and the red-colored solid was collected which was further dried under vacuo. Yield = 180 mg. The product was partially soluble in acetonitrile and slightly more soluble in DMSO. With the product, UV-vis spectroscopy and electrochemistry experiments were performed which confirmed the binding of Ru with the ligand **3D-L<sub>1</sub>**.

iv. Synthesis of [TRIM-Org]<sub>n</sub>:



Scheme S4: Synthesis of [TRIM-Org]<sub>n</sub>

Tris(4-(1H-imidazol-1-yl)phenyl)amine (133.0 mg, 0.3 mmol) and 1,4-bis(bromomethyl)benzene (119.0 mg, 0.45 mmol) were dissolved in 5 mL DMF and stirred at 100 °C for 48 h. In the meantime, white precipitate appeared. Then the reaction mixture was allowed to cool to room temperature and filtered by using G4 bed. The precipitate was washed with methanol, DCM, and at last with diethyl ether to result in an off-white powder. The product was insoluble in common organic solvents except in DMSO where it showed very little solubility.

v. Synthesis of [TRIM-Ru-Pd]<sub>n</sub>:

[TRIM-Ru]<sub>n</sub> (100.0 mg), palladium acetate (0.22 mmol, 50.0 mg), and potassium iodide (1.0 mmol, 166.0 mg) were mixed in a Schlenk tube. 5.0 mL DMSO was added to this, and the solution was heated to 80 °C for 16 h. Then the reaction mixture was cooled and 30.0 mL DCM was added to this. The red precipitate was filtered using G4 bed and washed well using water, DCM, methanol, and at last by dry diethyl ether. The solid was dried under vacuo. A red-colored solid was isolated. Yield = 120 mg.

**vi. Synthesis of [TRIM-Org-Pd]<sub>n</sub>:**

[TRIM-Org]<sub>n</sub> (95.7 mg), palladium acetate (0.3 mmol, 67.0 mg), and potassium iodide (1.0 mmol, 166.0 mg) were mixed in a Schlenk tube. 5.0 mL DMSO was added to this, and the solution was heated to 80 °C for 16 h. Then the reaction mixture was cooled and 30.0. mL DCM was added to this. The precipitate was filtered using G4 bed and washed well using DCM, methanol and at last by diethyl ether. The solid was dried under vacuo. A yellow-brown colored powder was isolated. Yield = 120 mg.

### III. SEM images:

#### 1. SEM images of [TRIM-Ru]<sub>n</sub>:

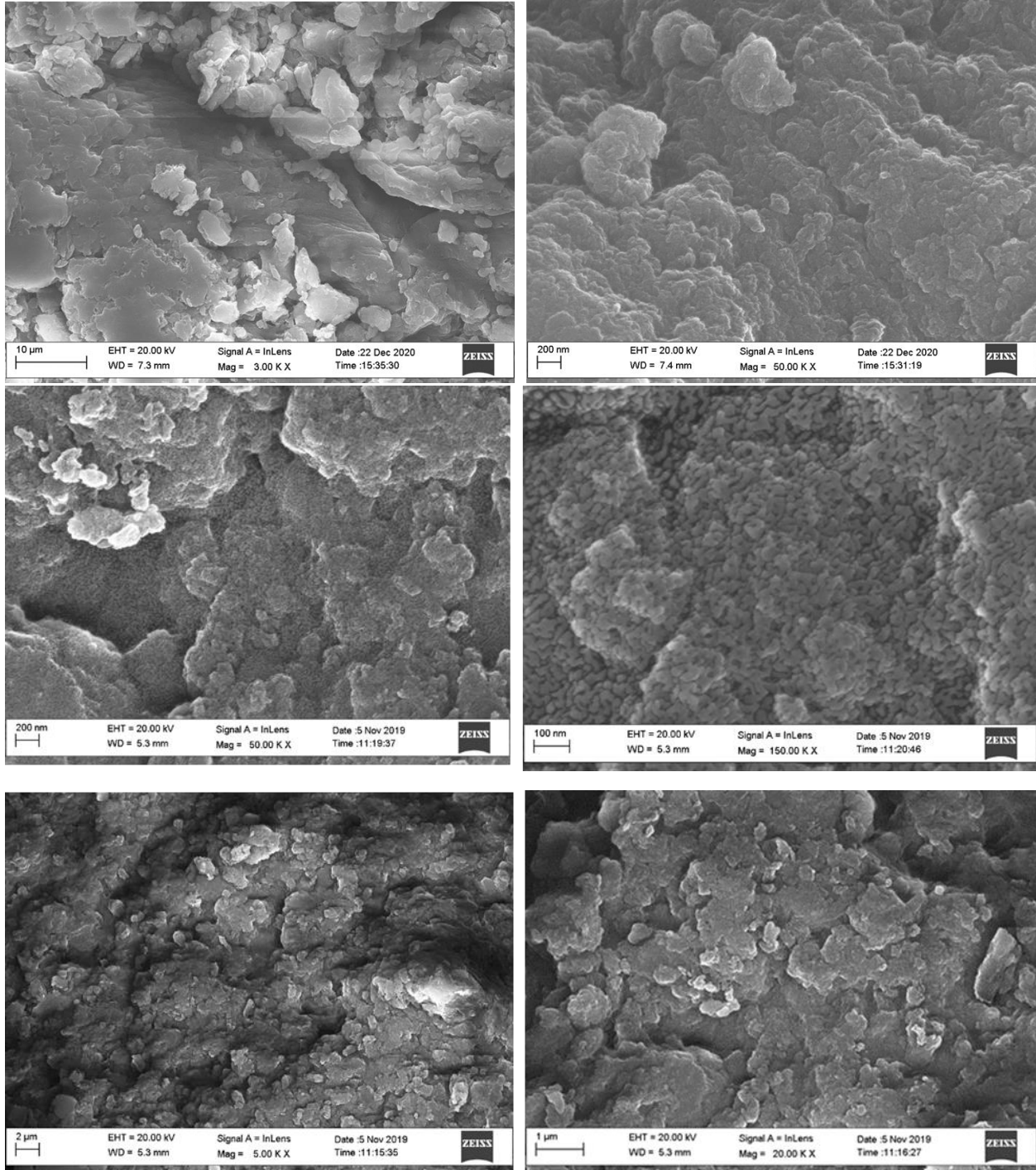
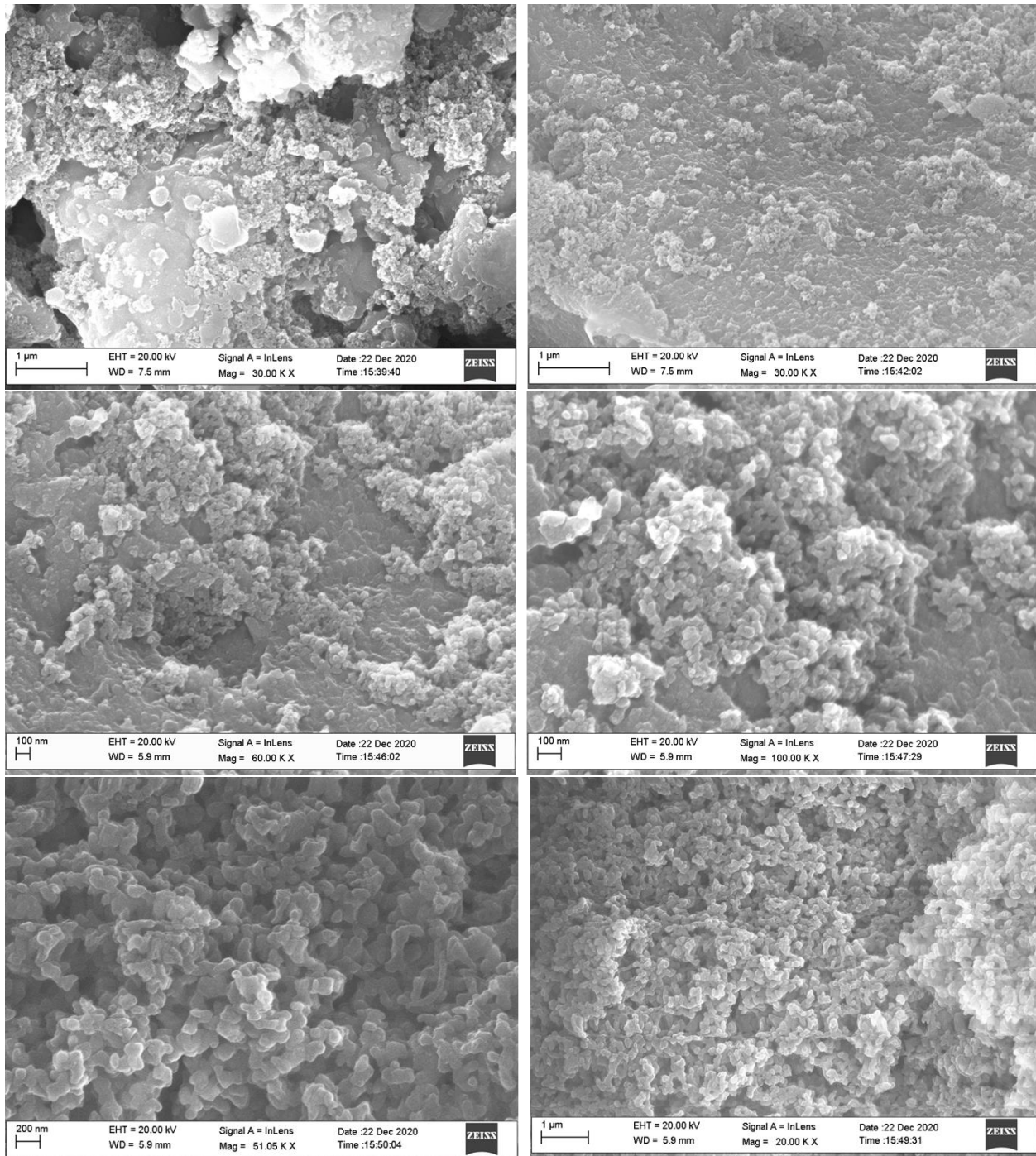


Figure S1: SEM images of [TRIM-Ru]<sub>n</sub>

## 2. SEM images of [TRIM-Ru-Pd]<sub>n</sub>:



**Figure S2:** SEM images of [TRIM-Ru-Pd]<sub>n</sub>



3. SEM images of [TRIM-Org]<sub>n</sub>:

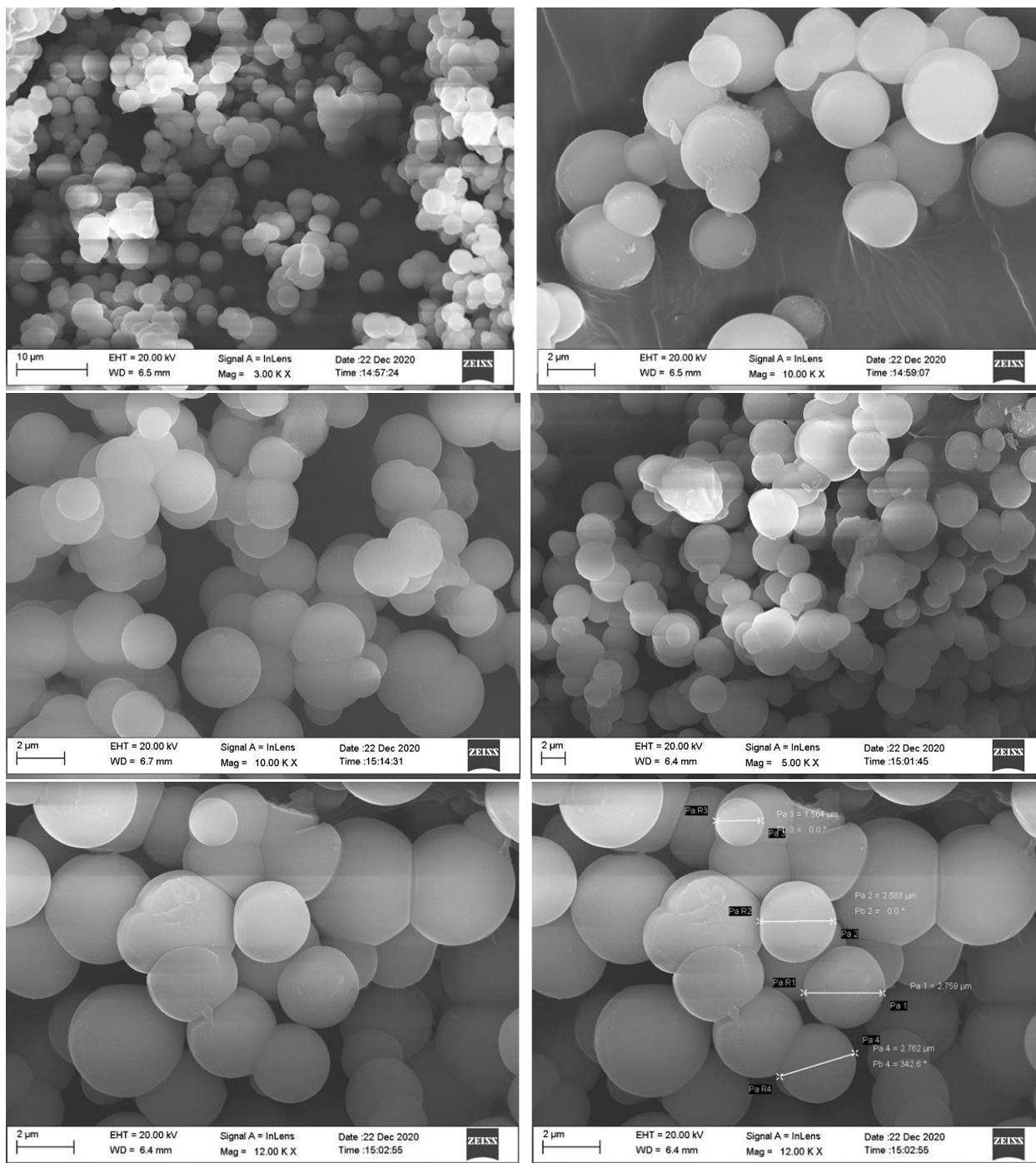


Figure S3: SEM images of [TRIM-Org]<sub>n</sub>

#### 4. SEM images of [TRIM-Org-Pd]<sub>n</sub>:

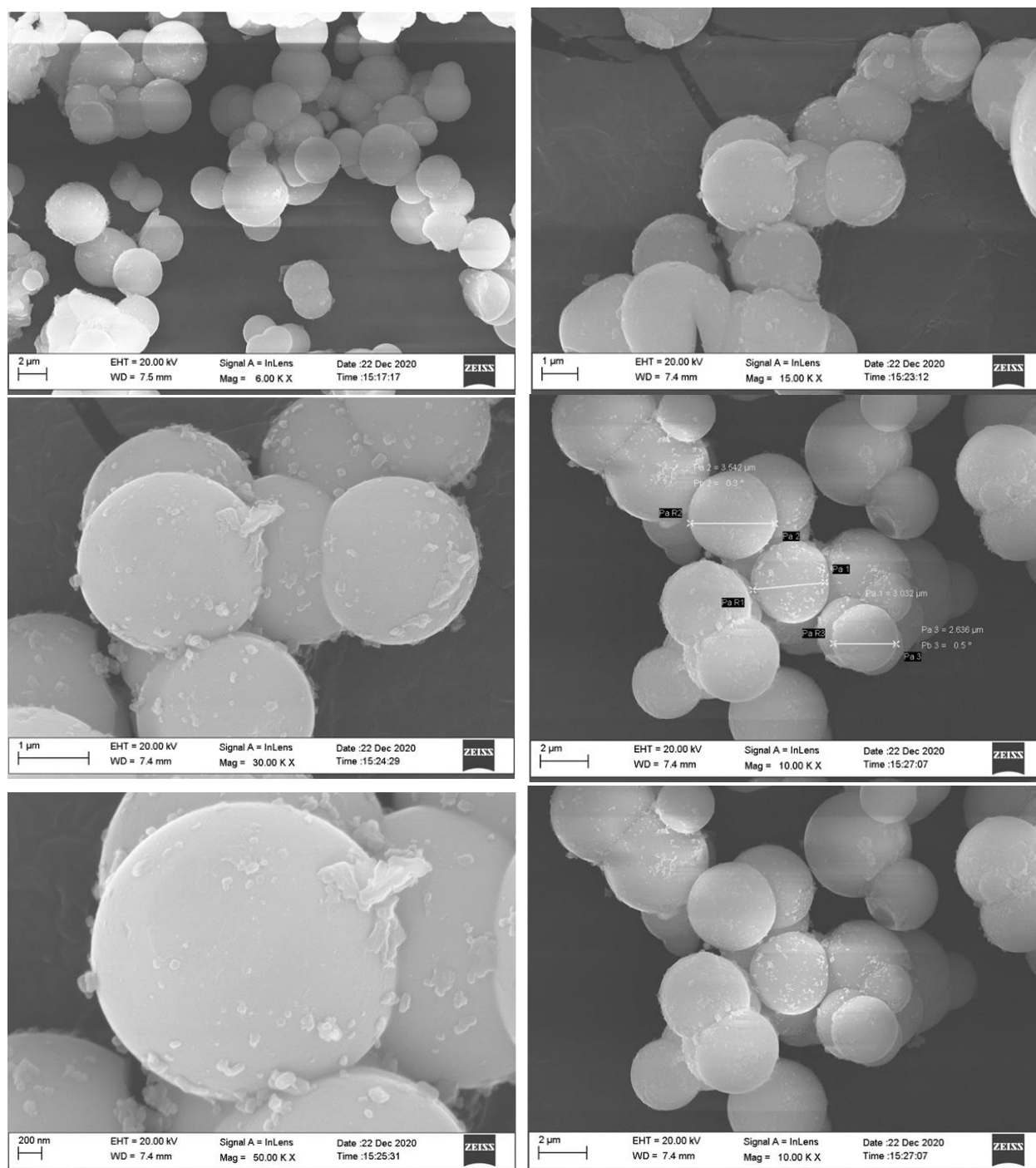


Figure S4: SEM images of [TRIM-Org-Pd]<sub>n</sub>

#### IV. XPS analysis:

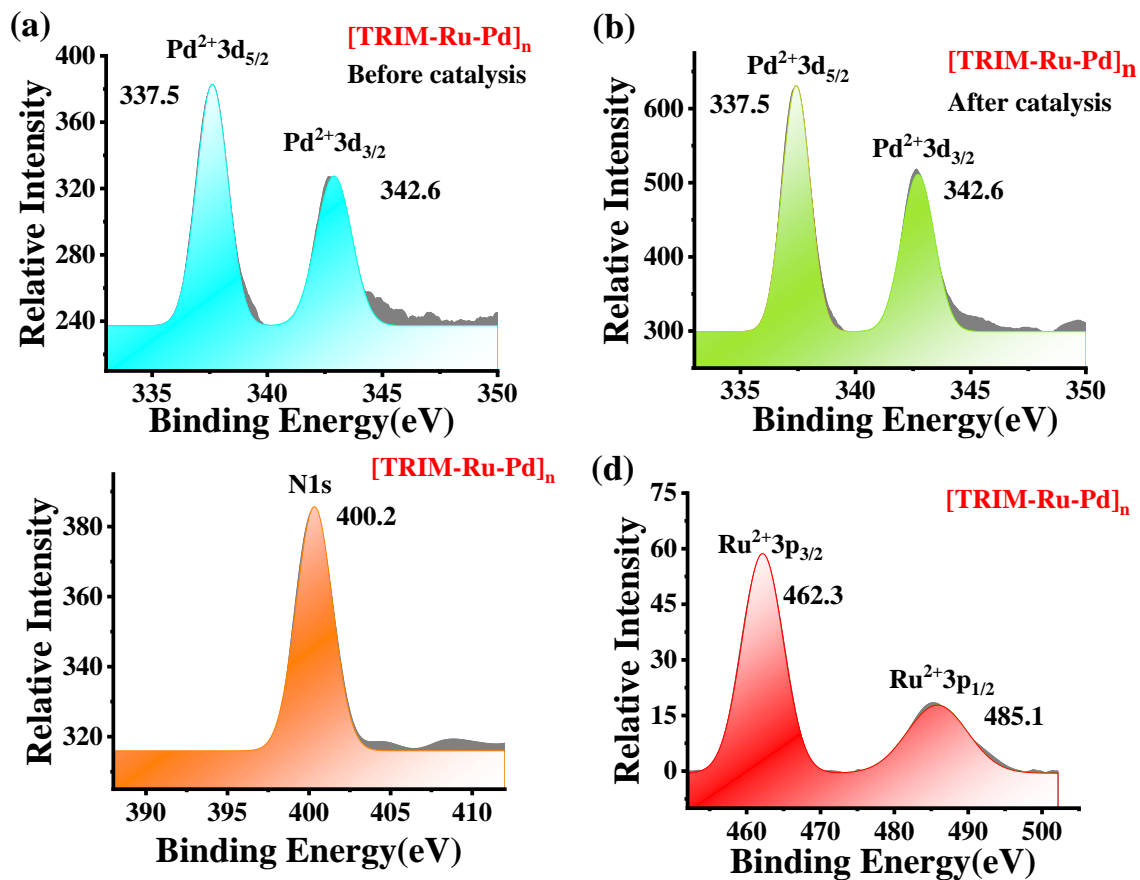
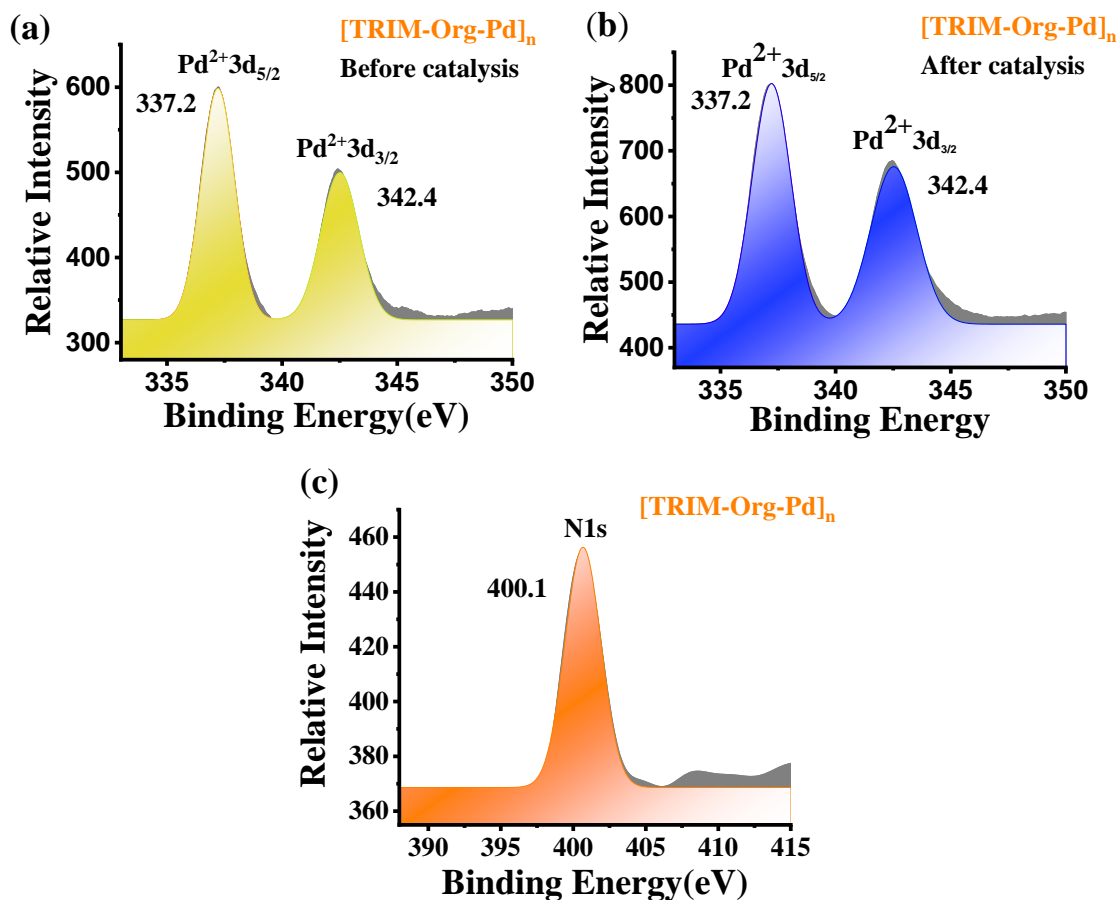


Figure S5: XPS data of the compound  $[\text{TRIM-Ru-Pd}]_n$ ; (a) XPS of Pd<sup>2+</sup> (freshly prepared Pd catalyst) (a) XPS of Pd<sup>2+</sup> (after recycling) (c) XPS of Nitrogen (d) XPS of Ru<sup>2+</sup>.

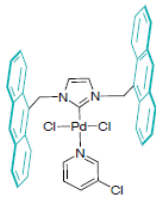
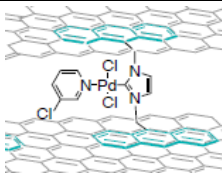
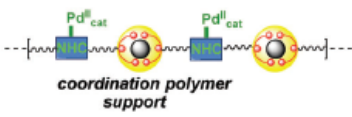
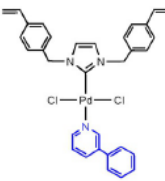


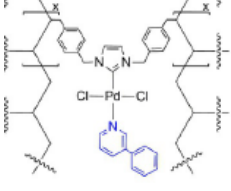
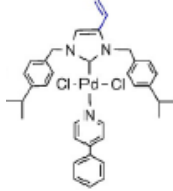
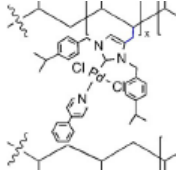

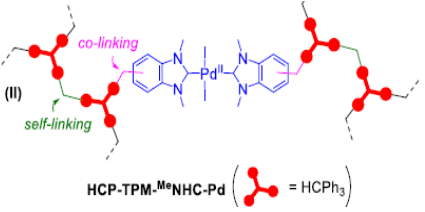
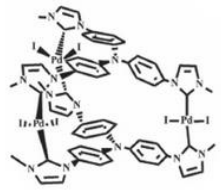
**Figure S6:** XPS data of the compound [TRIM-Org-Pd]<sub>n</sub>; (a) XPS of Pd<sup>2+</sup> (Newly prepared Pd catalyst) (a) XPS of Pd<sup>2+</sup> (after recycling) (c) XPS of Nitrogen.

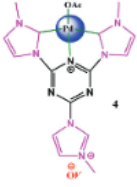
**Discussion:** The X-ray photoelectron spectroscopic (XPS) investigation showed the Pd 3d core-level binding energy values in [TRIM-Ru-Pd]<sub>n</sub> and [TRIM-Org-Pd]<sub>n</sub> as 337.5 and 337.2 eV for 3d<sub>5/2</sub> and 342.6 and 342.4 eV for 3d<sub>3/2</sub> respectively, confirming the presence of Pd<sup>II</sup> in these materials, in accordance with the energy values reported in literature. Furthermore, the above energy values were found to be significantly lower by 0.9–1.2 eV (in case of [TRIM-Ru-Pd]<sub>n</sub>) and by 1.2–1.5 eV (in case of [TRIM-Org-Pd]<sub>n</sub>) for the 3d<sub>5/2</sub> level, and by 1.2 eV (in case of [TRIM-Ru-Pd]<sub>n</sub>) and by 1.4 eV (in case of [TRIM-Org-Pd]<sub>n</sub>) for the 3d<sub>3/2</sub> level, as compared to the respective energy values in Pd(OAc)<sub>2</sub> (338.4–338.7 eV for 3d<sub>5/2</sub> and 343.8 eV for 3d<sub>3/2</sub>). These results suggested an enhanced electron density around the Pd<sup>II</sup> centre in [TRIM-Ru-Pd]<sub>n</sub> and [TRIM-Org-Pd]<sub>n</sub> which can be correlated to the presence of Pd<sup>II</sup>–NHC bonding, as the NHC ligands are known to be strong  $\sigma$ -donors. The Pd<sup>II</sup>–NHC bonds in [TRIM-Ru-Pd]<sub>n</sub> and [TRIM-Org-Pd]<sub>n</sub> were expectedly formed via the reaction of Pd(OAc)<sub>2</sub> with the imidazolium moieties present in the polymers [TRIM-Ru]<sub>n</sub> and [TRIM-Org]<sub>n</sub> respectively. There were two possibilities from the above metalation reaction – a mono-NHC species, Pd<sup>II</sup>–NHC or a bis-NHC species, NHC–Pd<sup>II</sup>–NHC. Based on the trend in the binding energy values, [TRIM-Ru-Pd]<sub>n</sub> and [TRIM-Org-Pd]<sub>n</sub> are expected to contain Pd<sup>II</sup>–NHC and NHC–Pd<sup>II</sup>–NHC moieties respectively. Notably, the deconvolution analysis of the Pd peaks in both the XP spectra of [TRIM-Ru-Pd]<sub>n</sub> and [TRIM-Org-Pd]<sub>n</sub> signified the absence of any free or encapsulated Pd(OAc)<sub>2</sub> in the polymeric materials. Finally, the absence of a peak near 335.0 eV which is the characteristic peak for the 3d<sub>5/2</sub> level of Pd<sup>0</sup>, suggested that there was no metallic Pd<sup>0</sup> nanoparticles or Pd<sup>0</sup> complex in

[TRIM-Ru-Pd]<sub>n</sub> and [TRIM-Org-Pd]<sub>n</sub>. Additionally, in case of [TRIM-Ru-Pd]<sub>n</sub>, the presence of Ru<sup>II</sup> was easily characterized through XPS by analyzing the 3p level binding energy peak which shows characteristic doublets in the range of 461.0–465.0 eV for 3p<sub>3/2</sub> and 483.0–487.0 eV for 3p<sub>1/2</sub>. Thus, the XP spectrum of [TRIM-Ru-Pd]<sub>n</sub> showed the Ru<sup>II</sup> 3p core level binding energy value of 462.3 eV for 3p<sub>3/2</sub> and 485.1 eV for 3p<sub>1/2</sub> which matched with the reported values. Nitrogen XPS was also investigated for both the materials. For [TRIM-Ru-Pd]<sub>n</sub>, although two different but close peaks were expected due to the presence of two different types of N environments, the appearance of only one peak at 400.3 eV characteristic of the N<sub>1s</sub> level energy, suggested that the binding energy values of the two types of N atoms were modulated to very similar probably due to metal coordination at both the sites (viz., Ru–terpyridine and Pd–NHC), and therefore could not be differentiated. For [TRIM-Org-Pd]<sub>n</sub>, as expected, only one N<sub>1s</sub> peak was observed at 400.2 eV.

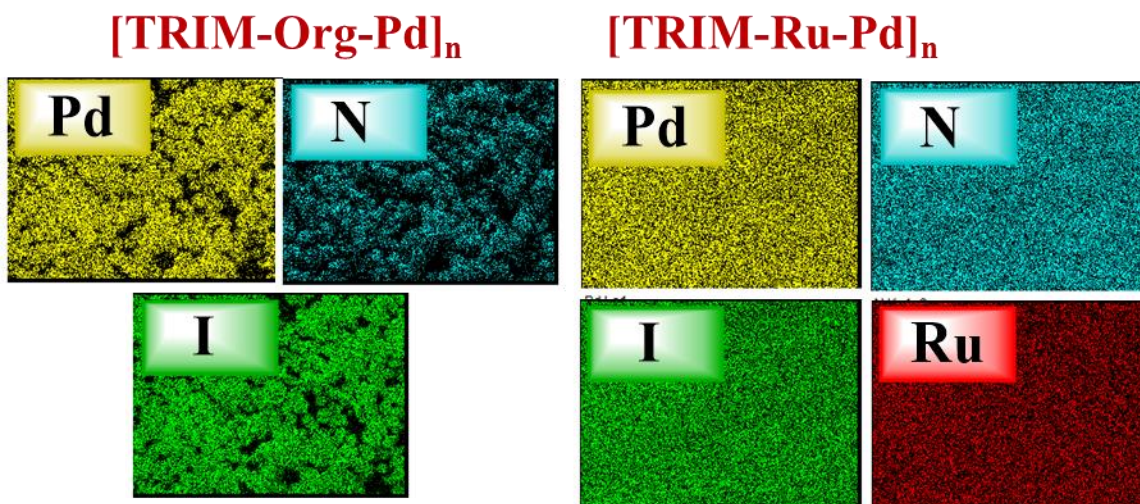
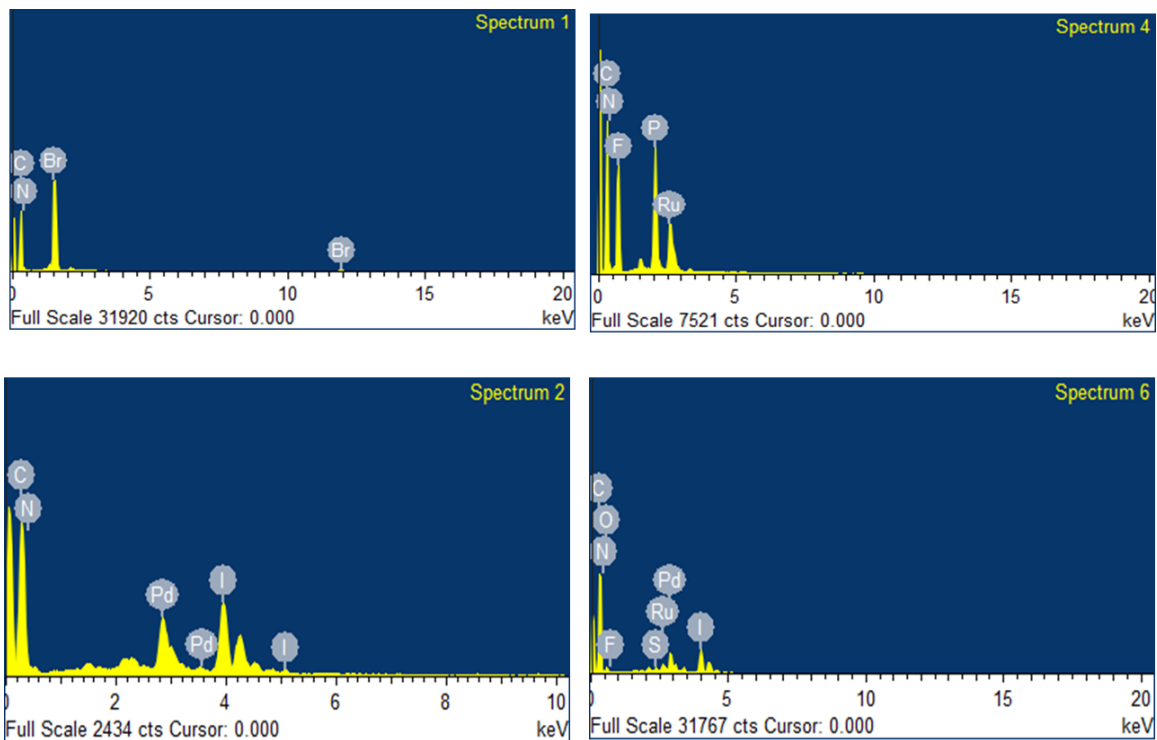
- Some reported XPS-derived binding energy values for mono-NHC-Pd<sup>II</sup> and bis-NHC-Pd<sup>II</sup> species

Entry	Pd <sup>2+</sup> 3d <sub>5/2</sub>	Pd <sup>2+</sup> 3d <sub>3/2</sub>	Ref.
<b>Mono-NHC-Pd<sup>II</sup></b>			
	337.9	343.4	<i>Eur. J. Inorg. Chem.</i> <b>2018</b> , 4742–4746
	337.6	343.1	<i>Eur. J. Inorg. Chem.</i> <b>2018</b> , 4742–4746
 coordination polymer support	337.6	342.8	<i>Chem. Commun.</i> , <b>2017</b> , 53, 3185–3188
	340	345.5	<i>Chem. Eur. J.</i> <b>2017</b> , 23, 8457 – 8465

	340	345.5	<i>Chem. Eur. J.</i> <b>2017</b> , <i>23</i> , 8457 – 8465
	338.3	343.6	<i>Chem. Eur. J.</i> <b>2019</b> , <i>25</i> , 13591 – 13597
	338.3	343.6	<i>Chem. Eur. J.</i> <b>2019</b> , <i>25</i> , 13591 – 13597
	337.7	342.9	<i>ACS Omega</i> <b>2018</b> , <i>3</i> , 15217–15228
<b>Bis-NHC-Pd<sup>II</sup></b>			
 HCP-TPM-M <sup>n</sup> NHC-Pd (HCPPh <sub>3</sub> )	337.2	342.5	<i>Organometallics</i> <b>2021</b> , <i>40</i> , 2443–2449
	337.1	340.0	<i>Small</i> <b>2015</b> , <i>11</i> , 3642–3647

	337.2	342.6	<i>New J. Chem.</i> , <b>2021</b> , <i>45</i> , 11662–11671
---	-------	-------	---

*V. EDX analysis plot of all the polymeric materials:*



**Figure S7:** EDX analysis of (a) [TRIM-Org]<sub>n</sub> (spectrum 1), (b) [TRIM-Ru]<sub>n</sub> (spectrum 4), (c) [TRIM-Ru-Pd]<sub>n</sub> (spectrum 2), and (d) [TRIM-Ru-Pd]<sub>n</sub> (spectrum 6), and the corresponding elemental mappings.



## VI. FT-IR spectra of the polymeric materials:

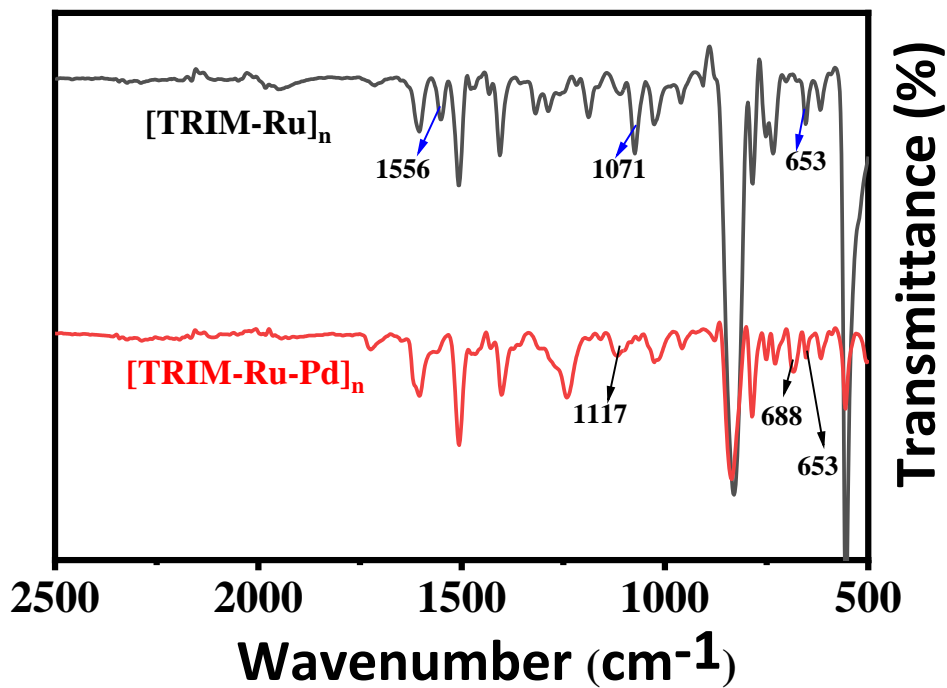


Figure S8: FT-IR spectra of [TRIM-Ru]<sub>n</sub> and [TRIM-Ru-Pd]<sub>n</sub>.

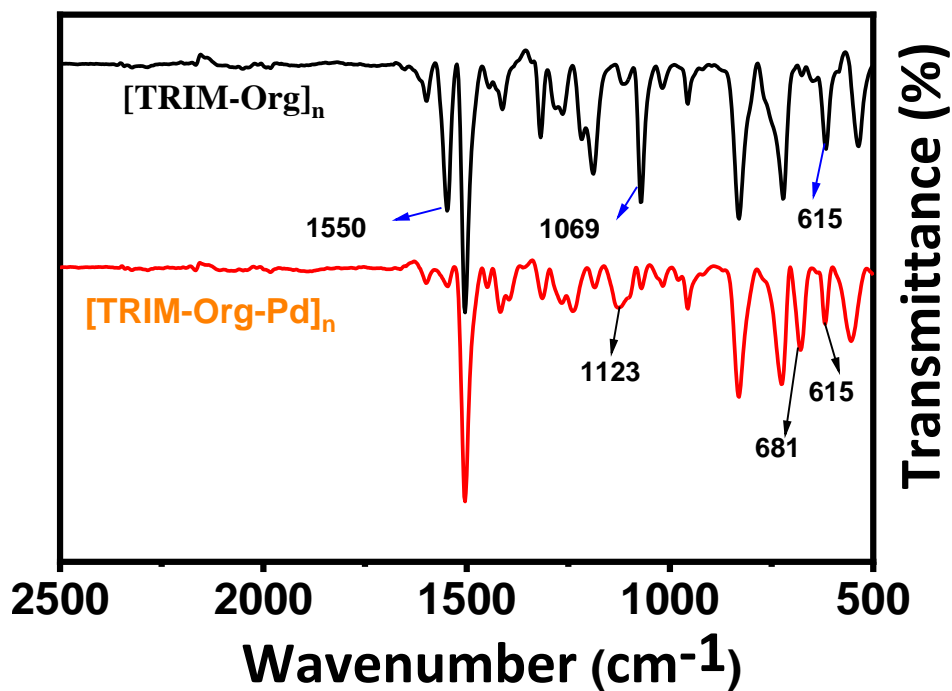
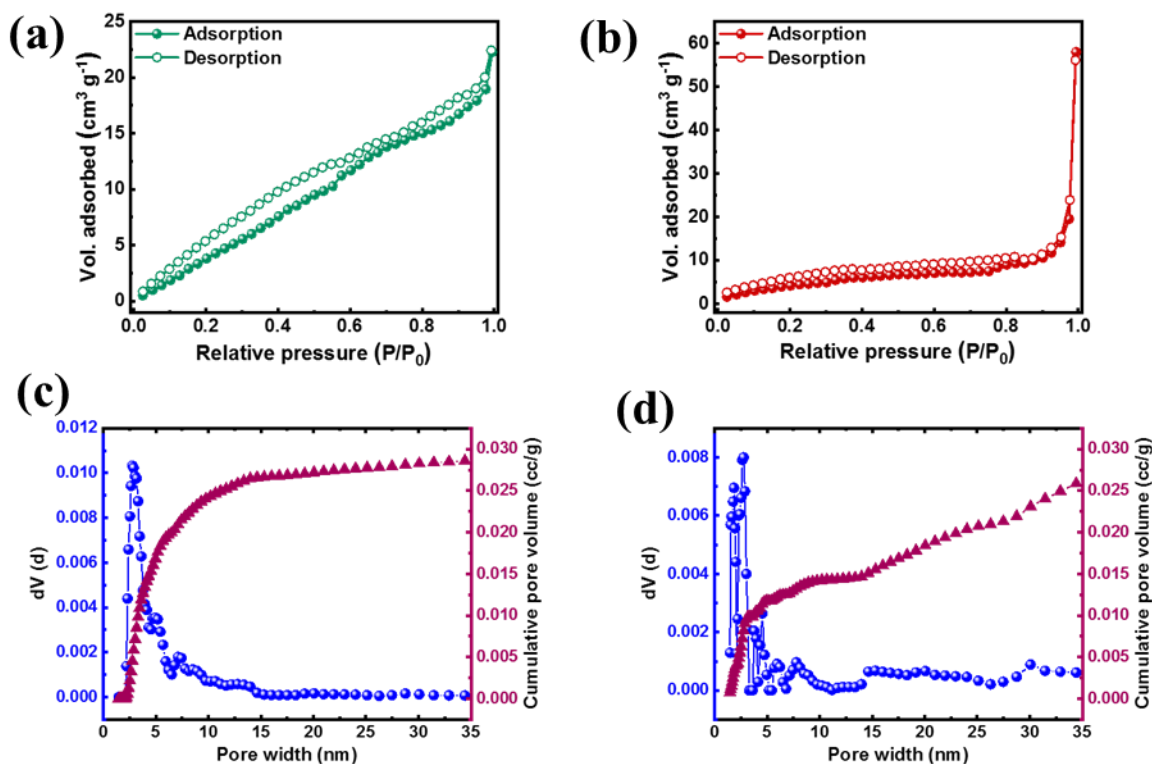


Figure S9: FT-IR spectra of [TRIM-Org]<sub>n</sub> and [TRIM-Org-Pd]<sub>n</sub>.

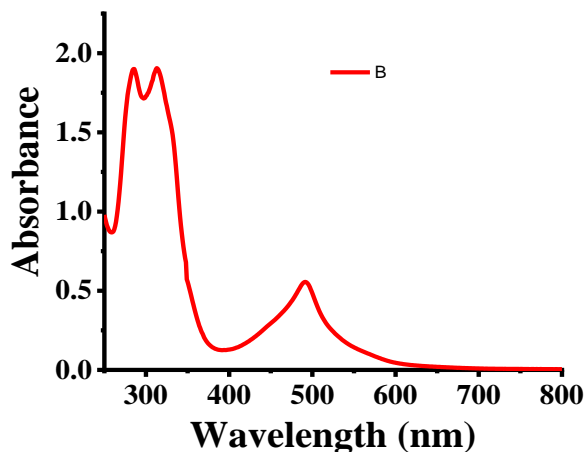
## VII. N<sub>2</sub> adsorption-desorption analysis:



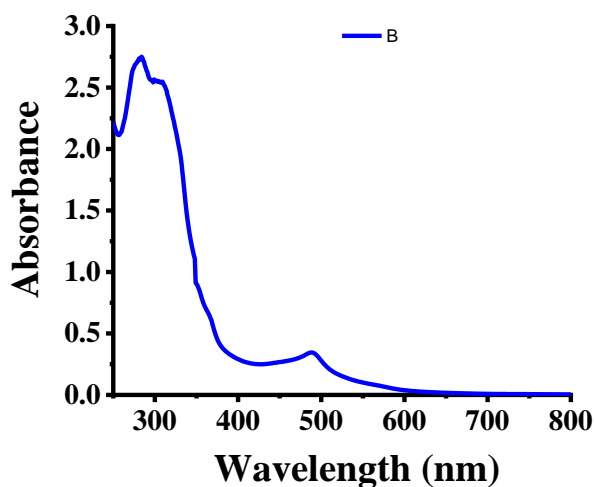
**Figure S10:** N<sub>2</sub> gas sorption analysis and pore size distribution of [TRIM-Org-Pd]<sub>n</sub> (a and c respectively) and [TRIM-Ru-Pd]<sub>n</sub> (b and d respectively).

## VIII. UV-vis studies of [TRIM-Ru]<sub>n</sub> and [TRIM-Ru-Pd]<sub>n</sub>:

UV-vis spectroscopy was performed to detect the presence of [Ru<sup>II</sup>(terpy)] chromophoric group in the backbone of both the Ru-based polymers [TRIM-Ru]<sub>n</sub> and [TRIM-Ru-Pd]<sub>n</sub>. For that DMSO was chosen as a solvent. 2.0 mg of the solid material was taken in a glass vial and 3.0 mL of DMSO was added to this. A red-colored solution was observed along with some insoluble particles. This solution was taken for the UV-vis spectroscopic measurement. The characteristic MLCT band of the [Ru<sup>II</sup>(terpy)] chromophore, present in [TRIM-Ru]<sub>n</sub> and [TRIM-Ru-Pd]<sub>n</sub> was observed at ~490 nm.



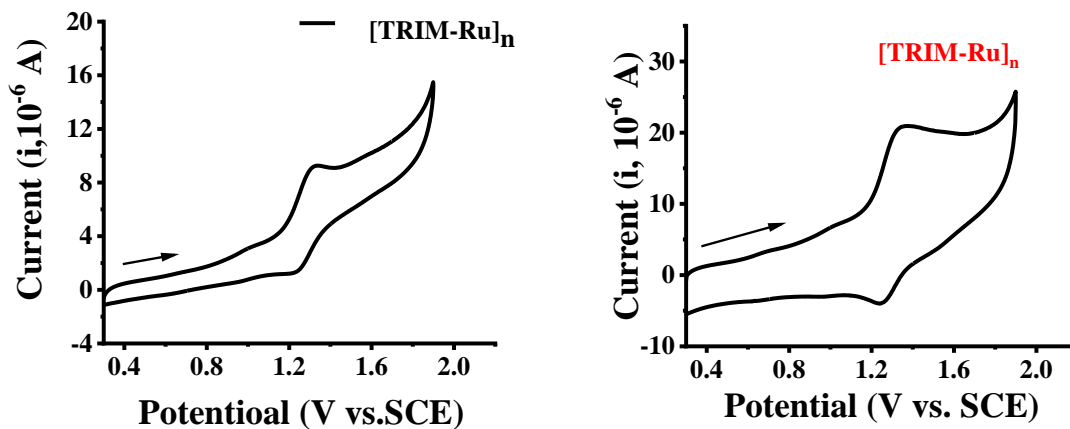
**Figure S11:** UV-vis spectrum of [TRIM-Ru]<sub>n</sub> in DMSO solution.



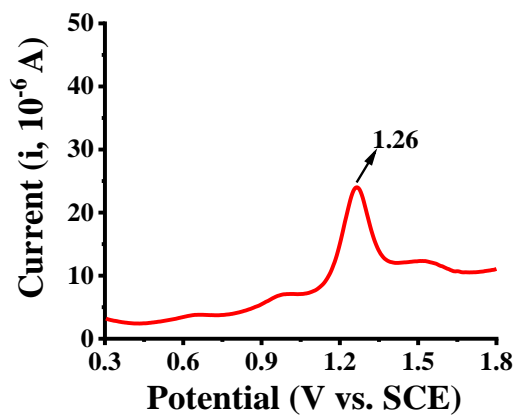
**Figure S12:** UV-vis spectrum of [TRIM-Ru-Pd]<sub>n</sub> in DMSO solution.

### ***IX. Electrochemical studies of [TRIM-Ru]<sub>n</sub>:***

An electrochemical study was also performed with the [TRIM-Ru]<sub>n</sub> polymer in acetonitrile. For that 3.0 mg material was taken in 3.0 mL acetonitrile and the mixture was stirred properly. Then the soluble portion was separated and 114 mg of <sup>n</sup>Bu<sub>4</sub>NPF<sub>6</sub> was added to the solution as a supporting electrolyte. To perform the cyclic voltammetry, Pt disc was used as a working electrode, SCE was used as reference electrode, and Pt wire was used as counter electrode. For external calibration standard; ferrocene ( $E_{1/2}$  of F<sub>c</sub>/F<sub>c</sub><sup>+</sup> couple was 0.37 V vs SCE) was used. The Ru<sup>II/III</sup> redox couple present in the material showed a quasi-reversible peak due to the presence of Ru<sup>II</sup>(terpy)<sub>2</sub> unit. The  $E_{1/2}$  value was found to be 1.26 V (versus SCE) which was similar value as that for other such complexes.



**Figure S13:** CV of [TRIM-Ru]<sub>n</sub> in acetonitrile solution at a scan rate of 10 mV (left). CV of [TRIM-Ru]<sub>n</sub> in acetonitrile solution at a scan rate of 50 mV (right). Supporting electrolyte: nBu<sub>4</sub>NPF<sub>6</sub>, working electrode: Pt disc; reference electrode: SCE; counter electrode: Pt wire; scan rate: 100 mV/sec; external calibration standard: ferrocene ( $E_{1/2}$  of Fc/Fc<sup>+</sup> couple was 0.37 V vs SCE).



**Figure S14:** DPV of [TRIM-Ru]<sub>n</sub> in acetonitrile solution.

### X. TGA of [TRIM-Ru-Pd]<sub>n</sub> and [TRIM-Org-Pd]<sub>n</sub>:

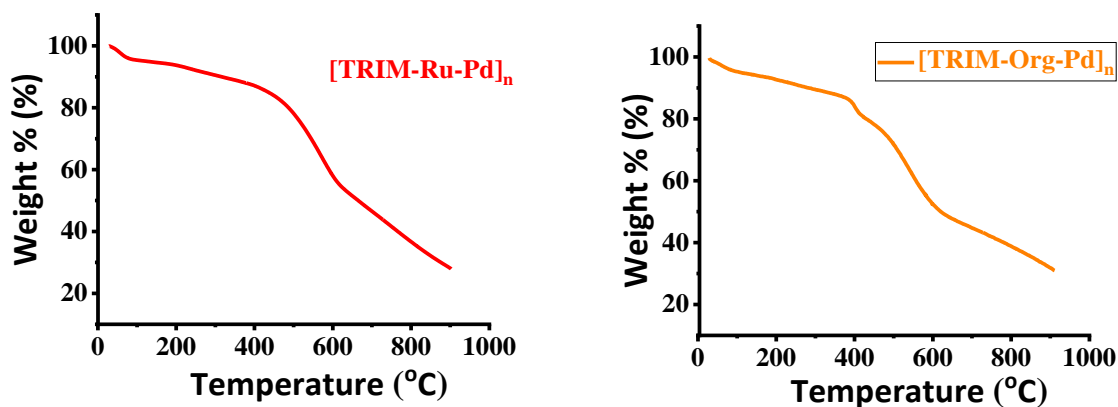


Figure S15: TGA plot of the compound [TRIM-Ru-Pd]<sub>n</sub> and [TRIM-Org-Pd]<sub>n</sub>.

### XI. Solid state <sup>13</sup>C NMR spectra:

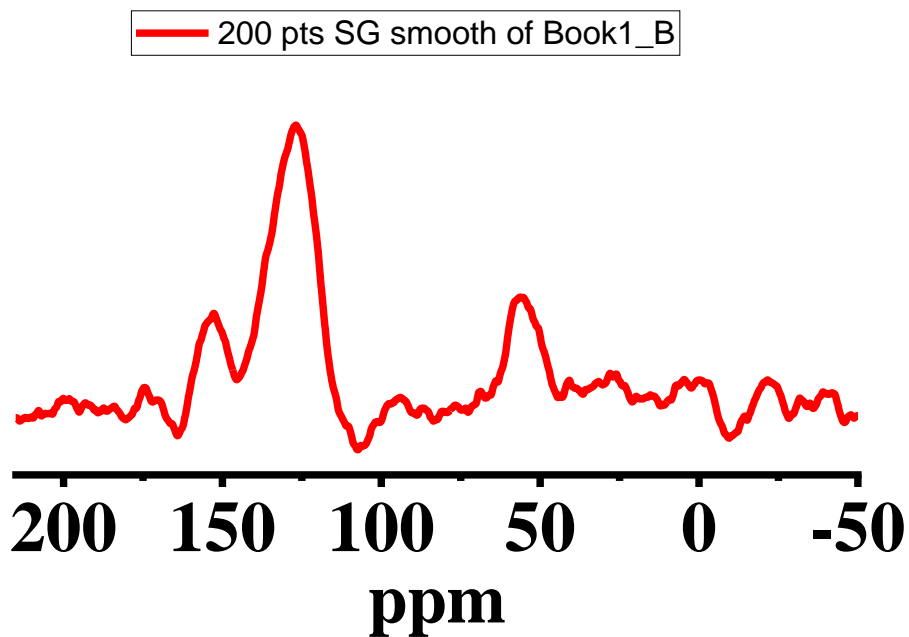


Figure S16: Solid state CP-MAS <sup>13</sup>C NMR spectrum of [TRIM-Ru]<sub>n</sub>.

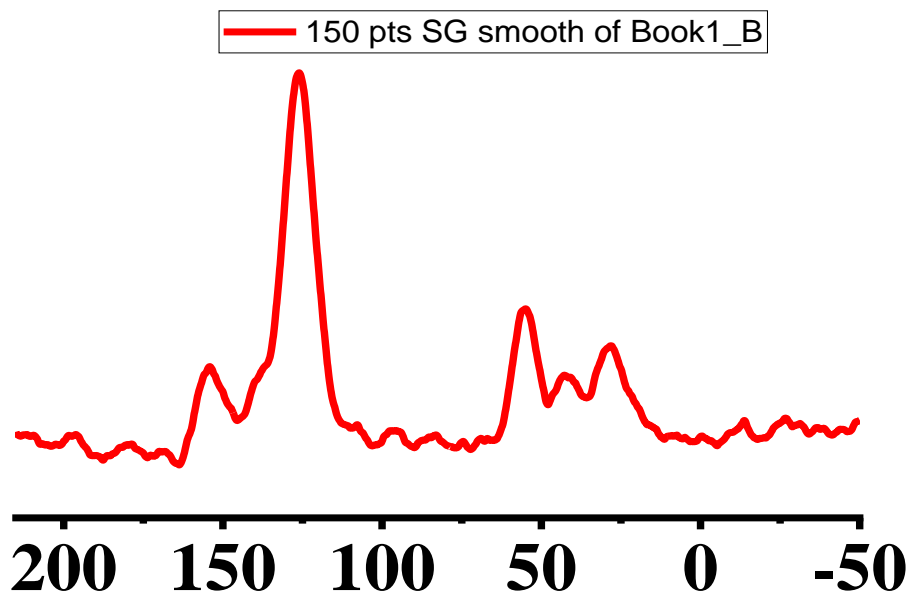


Figure S17: Solid-state CP-MAS  $^{13}\text{C}$  NMR spectrum of  $[\text{TRIM-Ru-Pd}]_n$ .

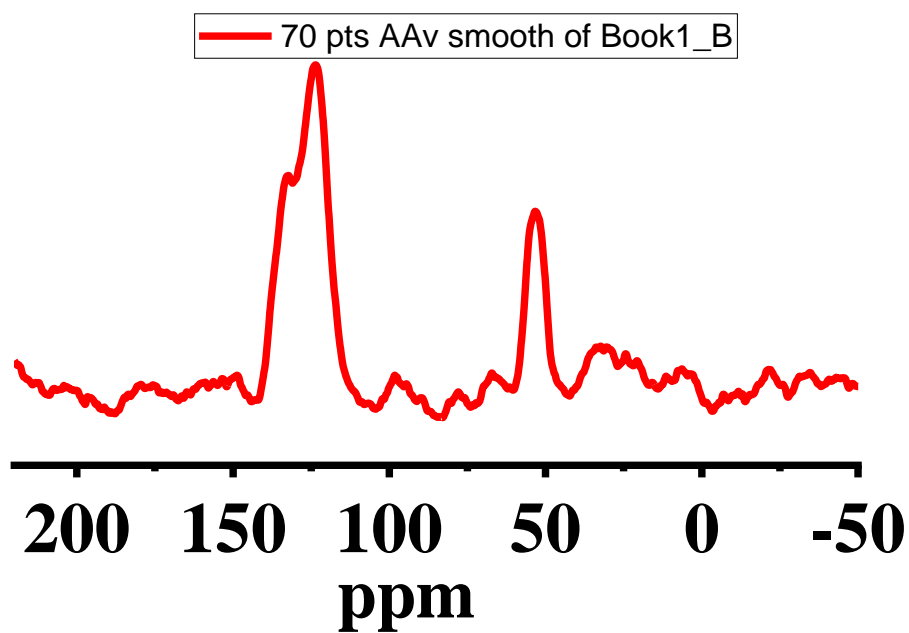


Figure S18: Solid state CP-MAS  $^{13}\text{C}$  NMR spectrum of  $[\text{TRIM-Org}]_n$ .

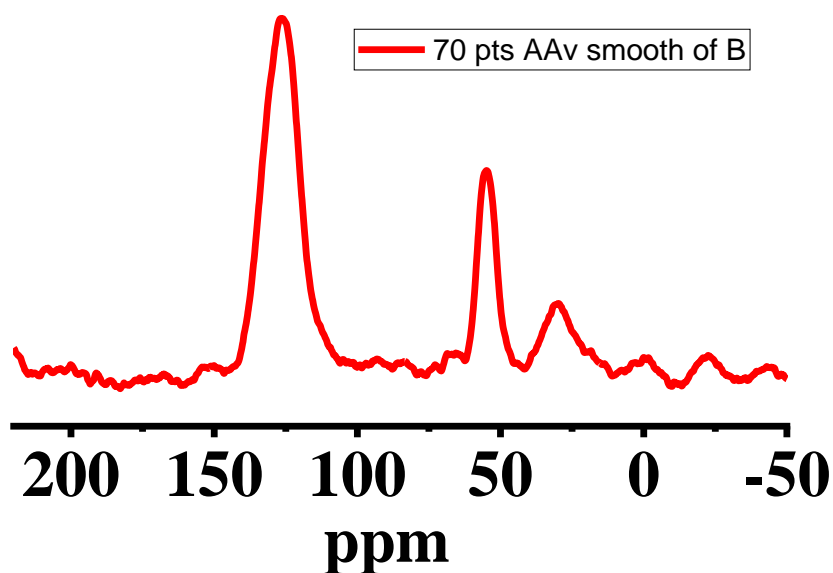


Figure S19: Solid state CP-MAS  $^{13}\text{C}$  NMR spectrum of  $[\text{TRIM-Org-Pd}]_n$

## XII. Solution state $^1\text{H}$ NMR spectra of $[\text{TRIM-Ru}]_n$ and $[\text{TRIM-Ru-Pd}]_n$ :

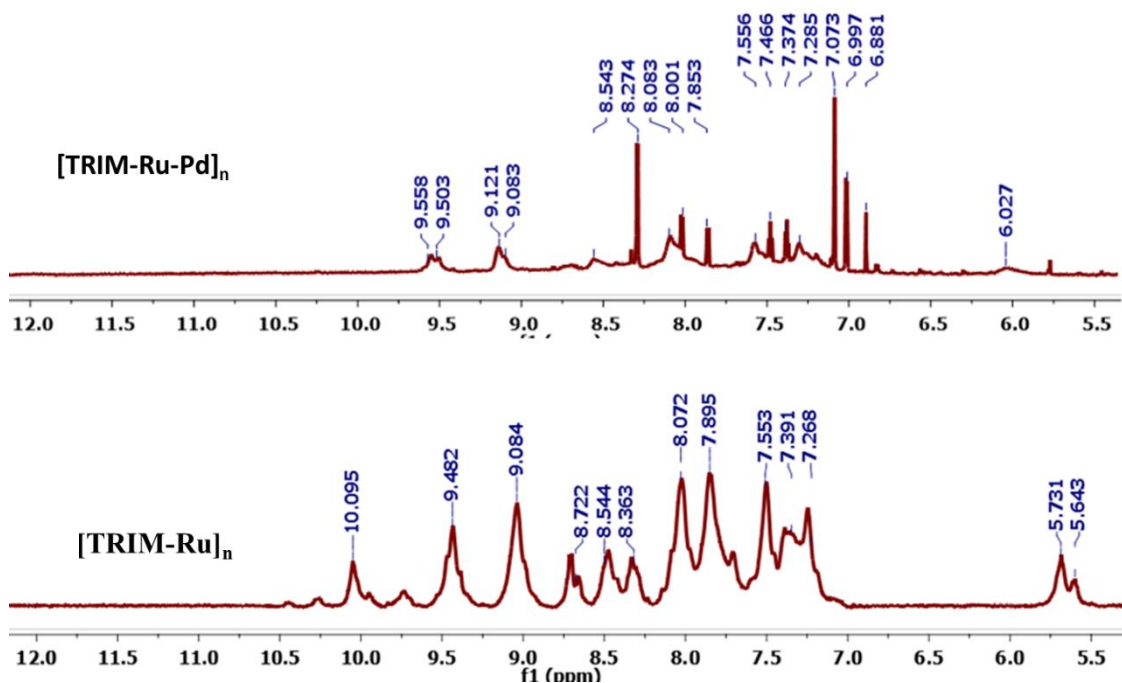


Figure S20: Solution-state  $^1\text{H}$  NMR spectra of  $[\text{TRIM-Ru}]_n$  and  $[\text{TRIM-Ru-Pd}]_n$ . (500 MHz,  $\text{DMSO-d}_6$ )

### XIII. Catalytic halogenation:

- Reported results on directed halogenation reaction under heterogeneous conditions:

**Halogenation reaction:**

NXS = N-chlorosuccinimide (X = Cl); N-bromosuccinimide (X = Br); N-iodosuccinimide (X = I)

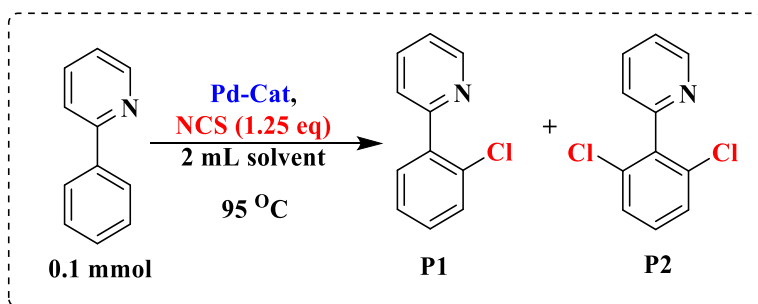
Entry, Reference	Product	Catalyst	Pd loading	Yield	Solvent, temperature, Time
1 Ref S1		Pd(II)/MWCNT	10 mol%	X= Cl (55%) X= Br (40%)	ACN, 100 °C, 6 h
2 Ref S1		Pd(II)/MWCNT	5 mol%	X= Br (89%)	ACN, 100 °C, 1.5 h
3 Ref S2		UIO-66-PdTCAT	5 mol%	X= Cl (95%) X= Br (97%)	ACN, 85 °C, 24 h
4 Ref S3		Pd@MOF	4 mol%	X= I (81%)	AcOH, 50 °C, 7 h
5 Ref S3		Pd@MOF	4 mol%	X= Cl (99%) X= Br (98%)	AcOH, 50 °C, 8 h AcOH, 50 °C, 2 h
6 Ref S4		Ru-CP-Pd	1.5 mol%	X= Cl (63%) X= Br (55%)	ACN, 95 °C, 16 h
7 Ref S5		Pd NPs	3 mol%	X= Cl (99%) X= Br (99%)	C <sub>6</sub> H <sub>6</sub> , 120 °C, 3 h
8 Ref S6		NHC-Pd polymer-supported	5 mol%	X= Cl (90%)	AcOH/Ac <sub>2</sub> O, 100 °C, 24 h
9 Ref S7		Poly-salen-Pd	5 mol%	X= Cl (71%) X= Br (90%)	ACN, 100 °C, 24 h
10 Ref S8		Pd(II)/COF	1 mol%	X= Cl (76%) X= Br (80%)	ACN, 80 °C
11 Ref S9		HCP-Pd-NHC	5 mol%	X= Cl (70%) X= Br (55%)	ACN, 95 °C, 24 h
12 Ref S9		HCP-Pd-NHC	5 mol%	X= Cl (70%) X= Br (55%)	ACN, 95 °C, 24 h



### A. Directed halogenation:

For directed halogenation reaction, arene (0.1 mmol), NCS/NBS (0.125 mmol) and [TRIM-Ru-Pd]<sub>n</sub> catalyst (5 mol % Pd) were placed in pressure tube. 2 mL solvent was added and the pressure tube was capped tightly. Resulting solution was stirred at different 95 °C for 12 h. After that the reaction mixture was cooled and PhCl was added as an internal standard. Then 0.250 mL reaction mixture was taken, diluted with ethyl acetate and injected to GC for yield calculation. The products were further verified by GCMS analysis.

#### 1. Reaction optimization for directed halogenation using 2-phenyl pyridine:



**Scheme S5:** Reaction condition for solvent optimization of 2 phenyl pyridine for chlorination reaction.

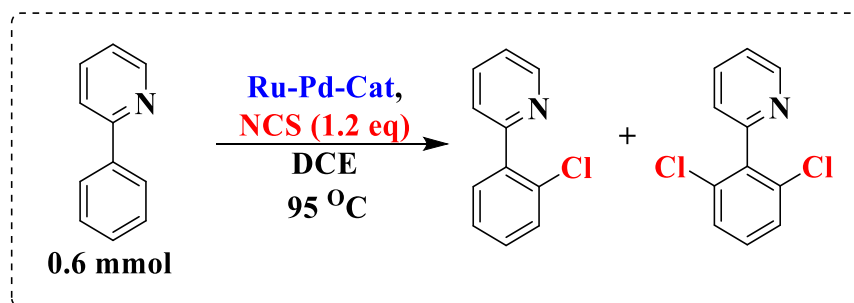
#### Solvent optimization:

Entry	Time (h)	Solvent	Reactant Conversion (%)	Yield (%) P1	Yield (%) P2
1	12	THF	37	34	2
2	12	ACN	82	74	8
3	12	Water	28	27	1
4	12	Methanol	23	19	4
5	12	Ethanol	21	17	4
6	12	Chloroform	25	21	1
7	12	DCE	92	84	8
8	12	Toluene	50	45	5
9	12	1,4 Dioxane	25	20	5
10	12	DMF	32	28	4

### Temperature optimization:

Entry	Time (h)	Temperature (°C)	Reactant Conversion (%)	Yield (%) P1	Yield (%) P2
1	6	50	10	9	1
2	6	75	15	12	3
3	6	95	40	37	3
4	6	110	46	43	3
5	6	130	46	41	4

### 2. Reusability Test:



**Scheme S6:** Reaction condition for recyclability experiment.

Recyclability experiment was performed by taking both the polymeric Pd catalysts. For that 2-phenylpyridine was chosen as a model substrate and DCE was used as a solvent. 2-phenylpyridine (0.085 mL, 0.60 mmol), NCS (100 mg, 0.75 mmol) and 5 mol % Pd catalyst were taken in 5 mL of DCE. The mixture was stirred at 95 °C in sealed tube for 16 h. After cooling to room temperature, the catalyst was separated from reaction mixture by centrifugation and washed with 3 times by using DCM and DCE. The filtrate part was injected to GC. The catalyst was then used for the next set of reaction, and the procedure was repeated for desired times.

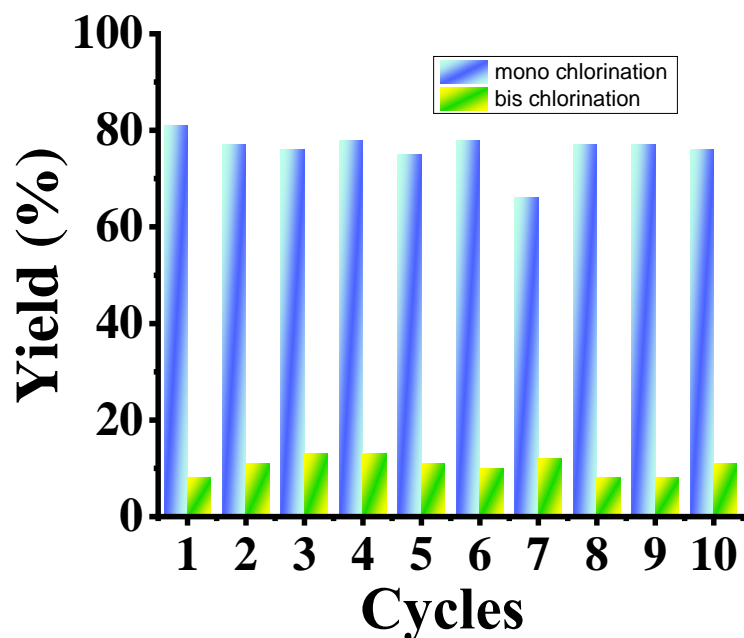


Figure S21: Recyclability experiment using  $[\text{TRIM-Ru-Pd}]_n$  catalyst.

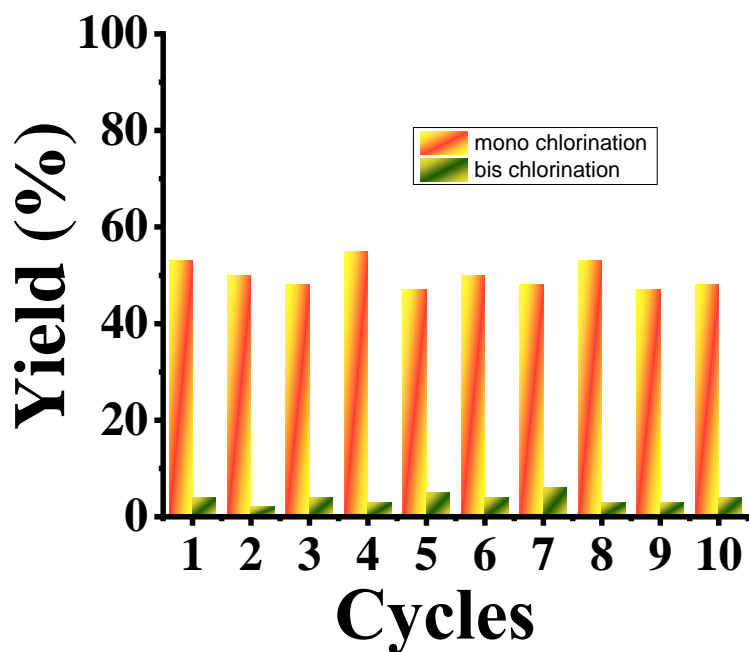
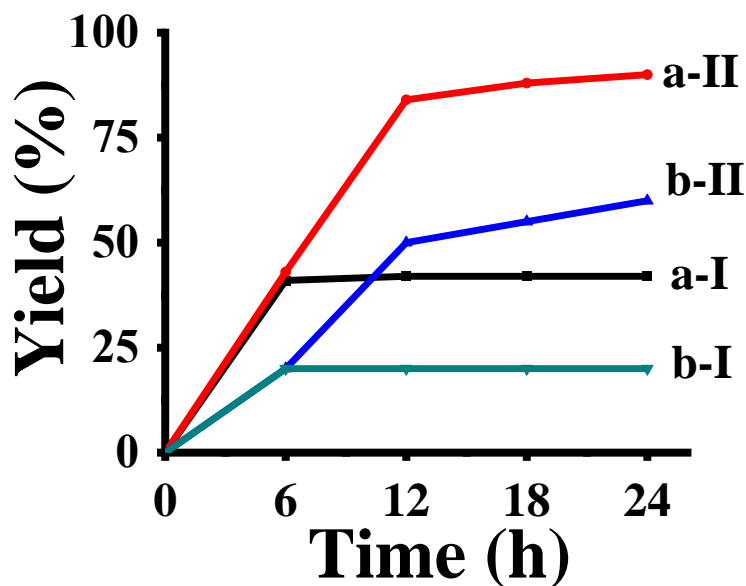


Figure S22: Recyclability experiment using  $[\text{TRIM-Org-Pd}]_n$  catalyst.

### 3. Hot filtration Test:

Hot filtration experiments were performed with both the catalysts. For this, two parallel experiments were set for each catalyst. Arene (0.10 mmol), NCS (0.125 mmol), and 5 mol % Pd catalyst were taken in pressure tube and 2 mL DCE was added to the mixture. The reaction was performed in the same oil bath at the

desired temperature. After 6 h, from one pressure tube, the solid catalyst was separated by centrifuging. Then the filtrate was transferred to the pressure tube and the reaction is continued whereas in other cases the reaction is continued without any disturbance. Yield was monitored using chlorobenzene as an internal standard. The same set of reactions was performed with both the polymeric Pd catalysts.



**Figure S23:** Hot filtration experiment using both [TRIM-Ru-Pd]<sub>n</sub> and [TRIM-Org-Pd]<sub>n</sub> catalysts.

#### 4. Substrate scope:

For directed halogenation reaction, different arenes (0.1 mmol), NCS/NBS (0.125 mmol), and polymeric Pd catalyst (5.0 mol % Pd) were placed in a pressure tube. 2.0 mL DCE was added and the pressure tube was capped tightly. The mixture was stirred at 95 °C in a sealed tube for 24 h. After the reaction, the catalyst was separated through centrifugation and the reaction mixture was injected into GCMS for product characterization. Column chromatography was also performed to isolate the desired product.

#### <sup>1</sup>H NMR data of the halogenated products:

After the catalysis experiment, the catalyst was separated through centrifugation from the reaction mixture and then the product was isolated through column chromatography. Finally, the products were characterized by <sup>1</sup>H NMR spectroscopy analysis which were matched with the literature reports.

**2-(2-chlorophenyl)pyridine:** <sup>1</sup>H NMR (400 MHz, CDCl<sub>3</sub>) 8.75 – 8.70 (1 H, m), 7.76 (1 H, td, *J* = 7.7, 1.8), 7.65 (1 H, d, *J* = 7.9), 7.59 (1 H, dd, *J* = 7.0, 2.4), 7.48 (1 H, dd, *J* = 7.6, 1.7), 7.35 (2 H, td, *J* = 7.1, 1.9), 7.30 (1 H, dd, *J* = 6.1, 1.4).

**2-(2-bromophenyl)pyridine:**  $^1\text{H}$  NMR (500 MHz,  $\text{CDCl}_3$ ) 8.71 (2 H, d,  $J = 5.8$ ), 7.77 (2 H, t,  $J = 7.7$ ), 7.68 (2 H, d,  $J = 9.1$ ), 7.60 (2 H, d,  $J = 7.9$ ), 7.54 (2 H, d,  $J = 7.6$ ), 7.41 (2 H, t,  $J = 7.5$ ), 7.32 – 7.28 (2 H, m), 7.28 – 7.24 (3 H, m).

**2-(2-chlorophenyl) thiophene:**  $^1\text{H}$  NMR (500 MHz,  $\text{CDCl}_3$ ) 7.50 (2 H, d,  $J = 8.0$ ), 7.37 (2 H, t,  $J = 7.6$ ), 7.29 (1 H, t,  $J = 7.4$ ), 7.07 (1 H, d,  $J = 3.9$ ), 6.89 (1 H, d,  $J = 3.9$ ).

**2-(2-bromophenyl) thiophene:**  $^1\text{H}$  NMR (500 MHz,  $\text{CDCl}_3$ ) 7.52 (2 H, d,  $J = 7.5$ ), 7.37 (2 H, t,  $J = 7.6$ ), 7.29 (1 H, t,  $J = 7.4$ ), 7.04 (2 H, dd,  $J = 11.7, 3.8$ ).

**10-chlorobenzo[h]quinoline:**  $^1\text{H}$  NMR (500 MHz,  $\text{CDCl}_3$ ) 9.11 (1 H, dd,  $J = 4.3, 1.9$ ), 8.17 (1 H, dd,  $J = 8.0, 1.9$ ), 7.82 (2 H, dd,  $J = 7.8, 2.0$ ), 7.77 (1 H, d,  $J = 8.8$ ), 7.69 (1 H, d,  $J = 8.8$ ), 7.55 (2 H, ddd,  $J = 7.7, 5.9, 1.6$ ).

**10-bromobenzo[h]quinoline:**  $^1\text{H}$  NMR (500 MHz,  $\text{CDCl}_3$ ) 9.11 (1 H, dd,  $J = 4.3, 1.8$ ), 8.18 (1 H, dd,  $J = 8.0, 1.8$ ), 7.83 (2 H, dd,  $J = 7.7, 5.2$ ), 7.78 (1 H, d,  $J = 8.8$ ), 7.70 (1 H, d,  $J = 8.8$ ), 7.59 – 7.53 (2 H, m).

**2-(2-chloro-4, 6-difluorophenyl) pyridine:**  $^1\text{H}$  NMR (400 MHz,  $\text{CDCl}_3$ ) 8.75 (1 H, d,  $J = 4.5$ ), 7.80 (1 H, td,  $J = 7.7, 1.7$ ), 7.41 – 7.32 (2 H, m), 7.11 – 7.05 (1 H, m), 6.87 (1 H, td,  $J = 9.0, 2.5$ ).

**2-(2-bromo-4, 6-difluorophenyl) pyridine:**  $^1\text{H}$  NMR (500 MHz,  $\text{CDCl}_3$ ) 8.75 (1 H, d,  $J = 5.4$ ), 7.80 (1 H, td,  $J = 7.7, 1.8$ ), 7.38 – 7.32 (2 H, m), 7.27 – 7.24 (1 H, m), 6.94 – 6.88 (1 H, m).

**2-(2-chlorophenyl) pyrimidine:**  $^1\text{H}$  NMR (500 MHz,  $\text{CDCl}_3$ ) 8.89 (2 H, d,  $J = 4.9$ ), 7.73 (1 H, dd,  $J = 5.9, 3.5$ ), 7.52 – 7.49 (1 H, m), 7.40 – 7.37 (2 H, m), 7.30 (1 H, t,  $J = 4.9$ ).

**2-(2-bromophenyl) pyrimidine:**  $^1\text{H}$  NMR (500 MHz,  $\text{CDCl}_3$ ) 8.89 (2 H, d,  $J = 4.9$ ), 7.73 – 7.68 (2 H, m), 7.43 (1 H, t,  $J = 7.5$ ), 7.33 – 7.28 (2 H, m).

**2-(2-chlorophenyl)-4-methylpyridine:**  $^1\text{H}$  NMR (400 MHz,  $\text{CDCl}_3$ ) 8.59 (1 H, s), 7.58 – 7.31 (5 H, m), 7.18 (1 H, s), 2.43 (3 H, s).

**2-(2-bromophenyl)-4-methylpyridine:**  $^1\text{H}$  NMR (500 MHz,  $\text{CDCl}_3$ ) 8.56 (1 H, d,  $J = 5.0$ ), 7.66 (1 H, d,  $J = 8.1$ ), 7.50 (1 H, d,  $J = 9.0$ ), 7.39 (1 H, t,  $J = 7.3$ ), 7.24 (1 H, d,  $J = 7.4$ ), 7.12 (1 H, d,  $J = 3.7$ ), 2.42 (3 H, s).

**1-(2-chlorophenyl)-N-phenylmethanimine:**  $^1\text{H}$  NMR (400 MHz,  $\text{CDCl}_3$ ) 8.91 (1 H, s), 8.24 (1 H, dd,  $J = 7.4, 1.9$ ), 7.39 (4 H, ddd,  $J = 6.9, 5.9, 1.6$ ), 7.36 – 7.33 (1 H, m), 7.24 (3 H, d,  $J = 8.3$ ).

**1-(2-Bromophenyl)-N-phenylmethanimine:**  $^1\text{H}$  NMR (500 MHz,  $\text{CDCl}_3$ ) 8.87 (1 H, s), 8.25 (1 H, dd,  $J = 7.8, 1.6$ ), 7.63 (1 H, dd,  $J = 8.0, 1.0$ ), 7.42 (3 H, dt,  $J = 7.3, 5.3$ ), 7.33 (1 H, td,  $J = 7.7, 1.8$ ), 7.29 – 7.25 (3 H, m).

**1-(2-chlorophenyl)-1H-pyrazole:**  $^1\text{H}$  NMR (400 MHz,  $\text{CDCl}_3$ ) 7.88 (1 H, d,  $J = 2.4$ ), 7.75 (1 H, d,  $J = 1.6$ ), 7.58 (1 H, dd,  $J = 7.9, 1.7$ ), 7.52 (1 H, dd,  $J = 7.9, 1.6$ ), 7.36 (2 H, dtd,  $J = 9.2, 7.5, 1.6$ ), 6.48 – 6.47 (1 H, m).

**1-(2-bromophenyl)-1H-pyrazole:**  $^1\text{H}$  NMR (500 MHz,  $\text{CDCl}_3$ ) 7.93 (1 H, s), 7.67 (1 H, s), 7.64 (2 H, d,  $J = 8.5$ ), 7.48 – 7.43 (2 H, m), 7.32 (1 H, t,  $J = 7.4$ ).

**1-(2-chlorophenyl)-2-phenyldiazene:**  $^1\text{H}$  NMR (400 MHz,  $\text{CDCl}_3$ ) 7.98 (2 H, d,  $J = 8.0$ ), 7.70 (1 H, dd,  $J = 7.9, 1.8$ ), 7.55 – 7.51 (4 H, m), 7.42 – 7.33 (2 H, m).

**1-(2 bromophenyl)-2-phenyldiazene:**  $^1\text{H}$  NMR (500 MHz,  $\text{CDCl}_3$ ) 7.98 (2 H, d,  $J = 7.9$ ), 7.75 (1 H, dd,  $J = 3.1, 1.9$ ), 7.68 (1 H, dd,  $J = 8.0, 1.6$ ), 7.57 – 7.49 (3 H, m), 7.40 (1 H, t,  $J = 8.0$ ), 7.35 – 7.31 (1 H, m).

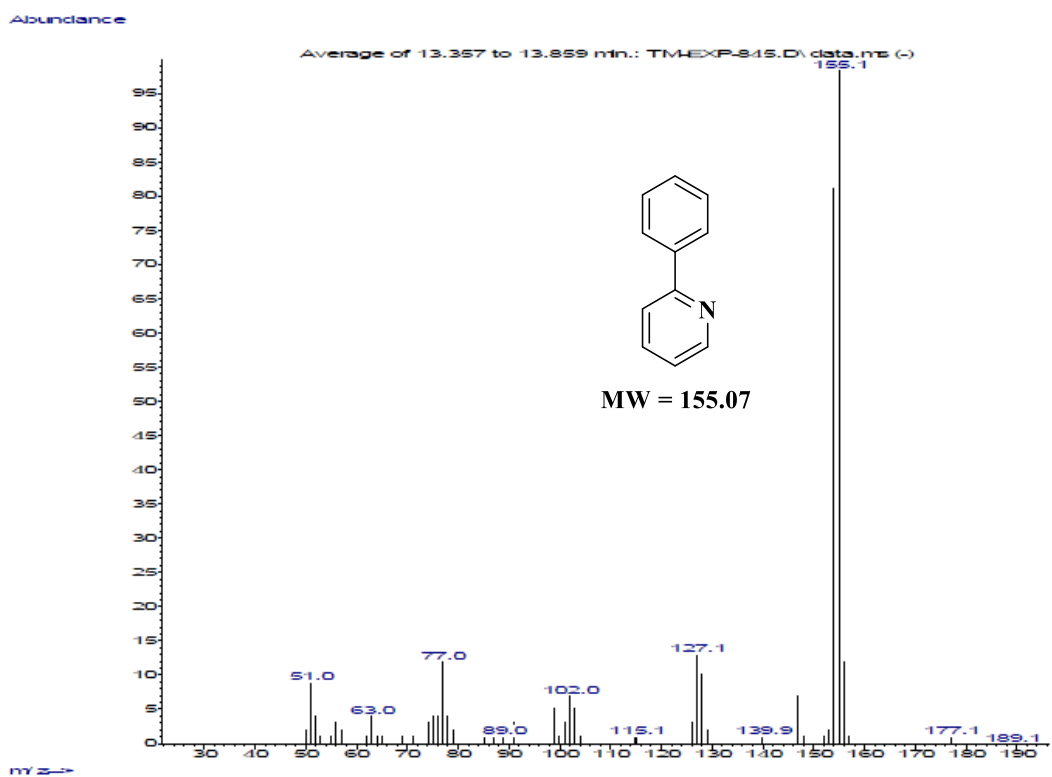
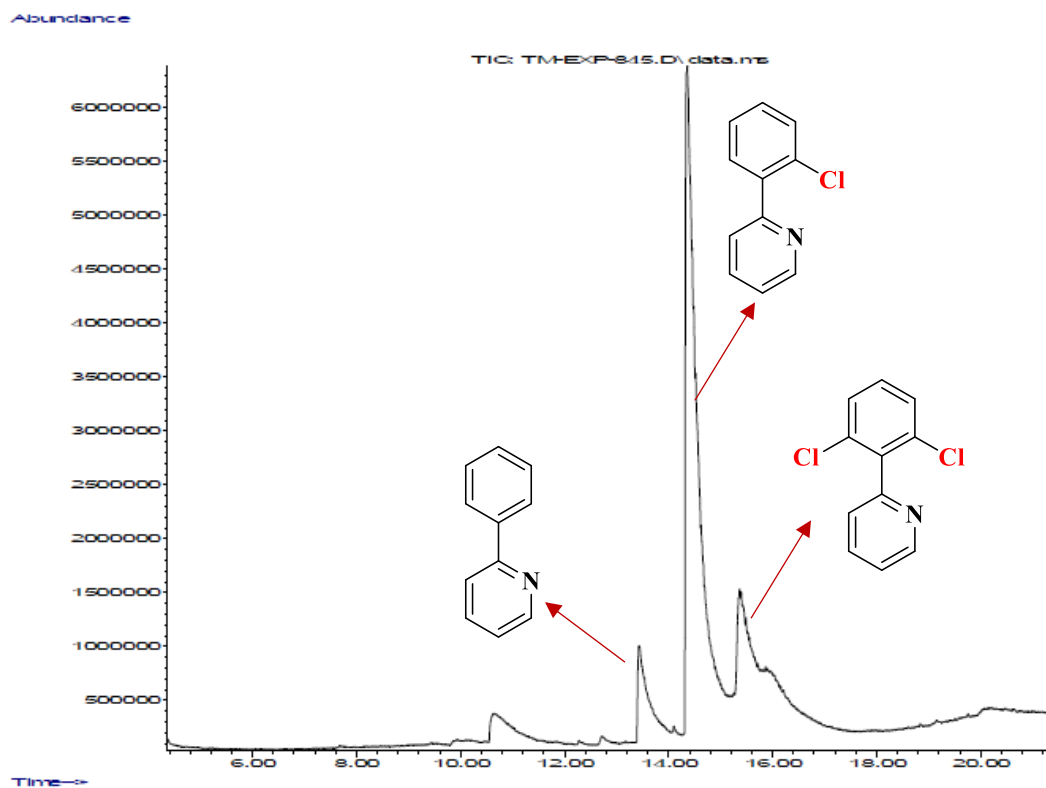
**2-(2-chloro-4-methoxyphenyl) pyridine:**  $^1\text{H}$  NMR (400 MHz,  $\text{CDCl}_3$ ) 8.71 (1 H, d,  $J = 4.3$ ), 7.78 (1 H, t,  $J = 8.2$ ), 7.68 (1 H, d,  $J = 7.9$ ), 7.58 (1 H, d,  $J = 8.6$ ), 7.31 – 7.27 (1 H, m), 7.02 (1 H, d,  $J = 2.5$ ), 6.93 (1 H, dd,  $J = 8.6, 2.5$ ), 3.85 (3 H, s).

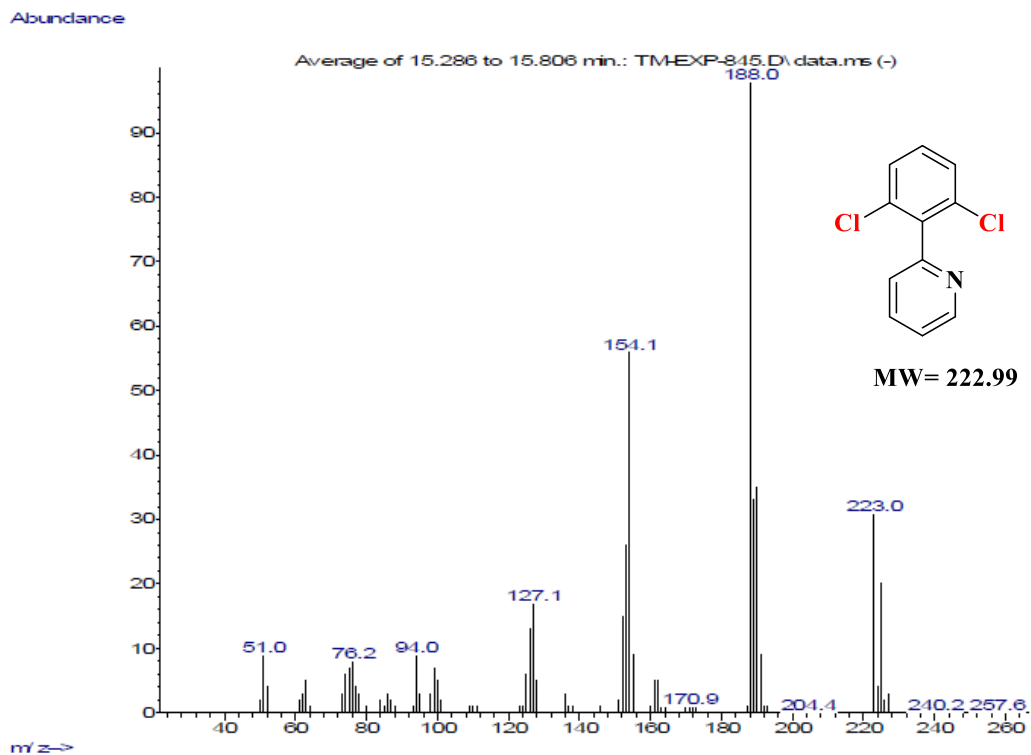
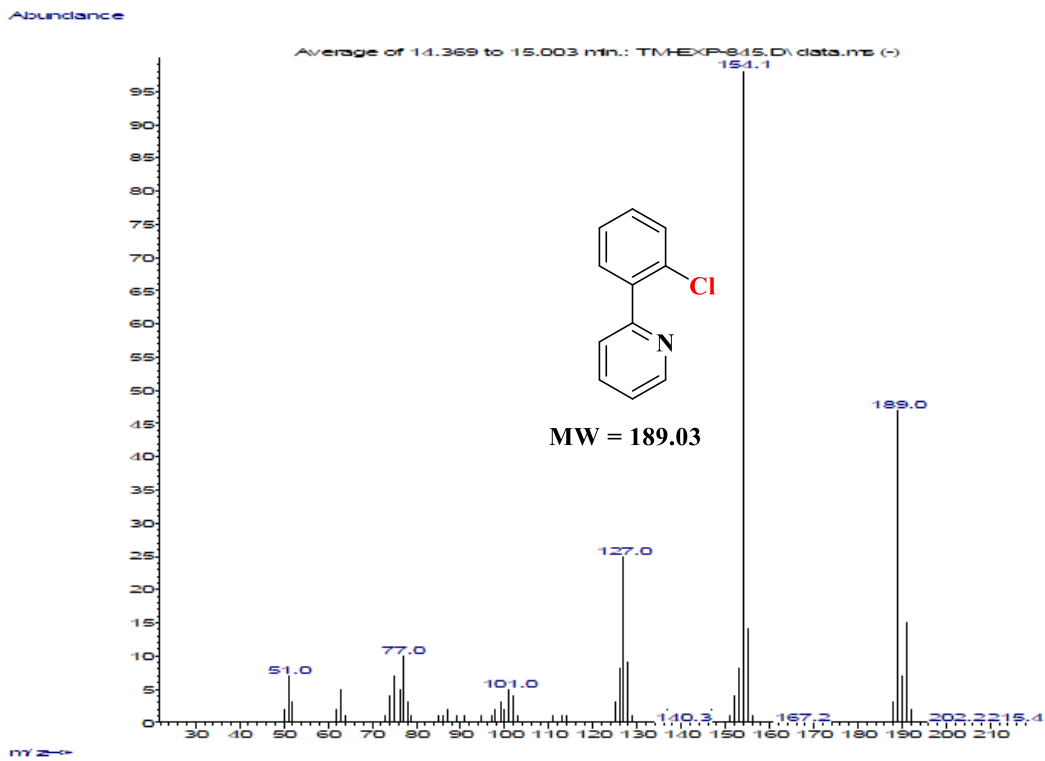
**2-(2-brmo-4-methoxyphenyl) pyridine:**  $^1\text{H}$  NMR (500 MHz,  $\text{CDCl}_3$ ) 8.66 (1 H, d,  $J = 4.6$ ), 8.23 (1 H, d,  $J = 2.1$ ), 7.94 (1 H, t,  $J = 7.7$ ), 7.76 – 7.65 (2 H, m), 7.23 – 7.16 (1 H, m), 7.03 – 6.97 (4 H, m), 3.96 (3 H, s).

**(2-(2-chloro-4-(trifluoromethyl) phenyl) pyridine:**  $^1\text{H}$  NMR (400 MHz,  $\text{CDCl}_3$ ) 8.75 (1 H, d,  $J = 4.7$ ), 7.81 (1 H, t,  $J = 7.7$ ), 7.78 – 7.72 (2 H, m), 7.68 (1 H, d,  $J = 7.9$ ), 7.63 (1 H, d,  $J = 7.9$ ), 7.37 – 7.33 (1 H, m).

**2-(2-bromo-4-(trifluoromethyl) phenyl) pyridine:**  $^1\text{H}$  NMR (500 MHz,  $\text{CDCl}_3$ ) 8.74 (1 H, d,  $J = 4.6$ ), 7.95 (1 H, s), 7.81 (1 H, t,  $J = .7$ ), 7.67 (2 H, s), 7.62 (1 H, d,  $J = 7.8$ ), 7.39 – 7.32 (1 H, m).

- Selected GC-MS profile of the halogenation reaction:

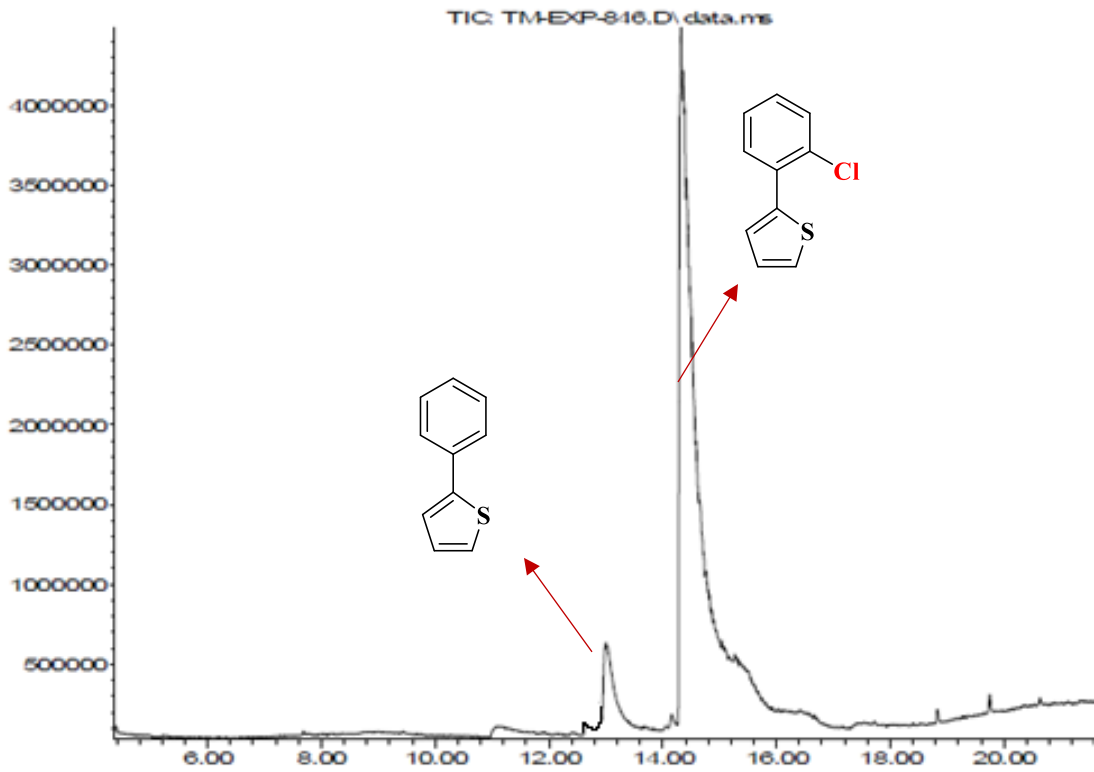




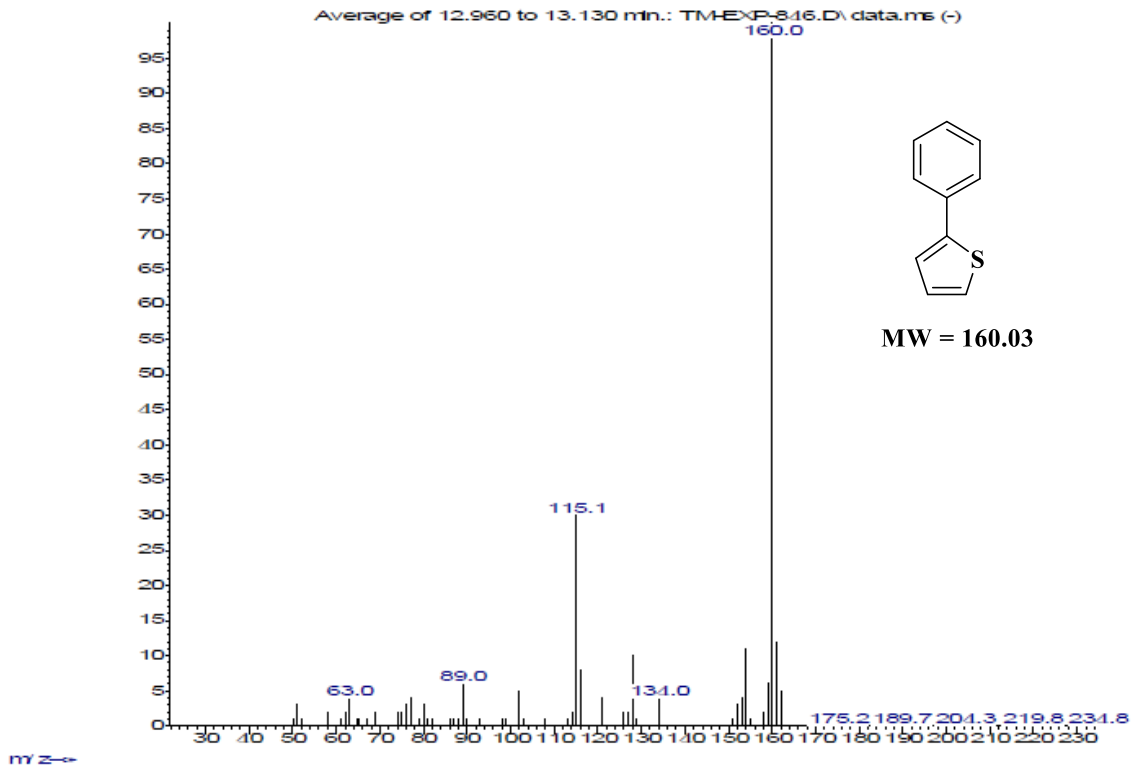
**Figure S24.** GCMS profile for the chlorination of 2-phenylpyridine.

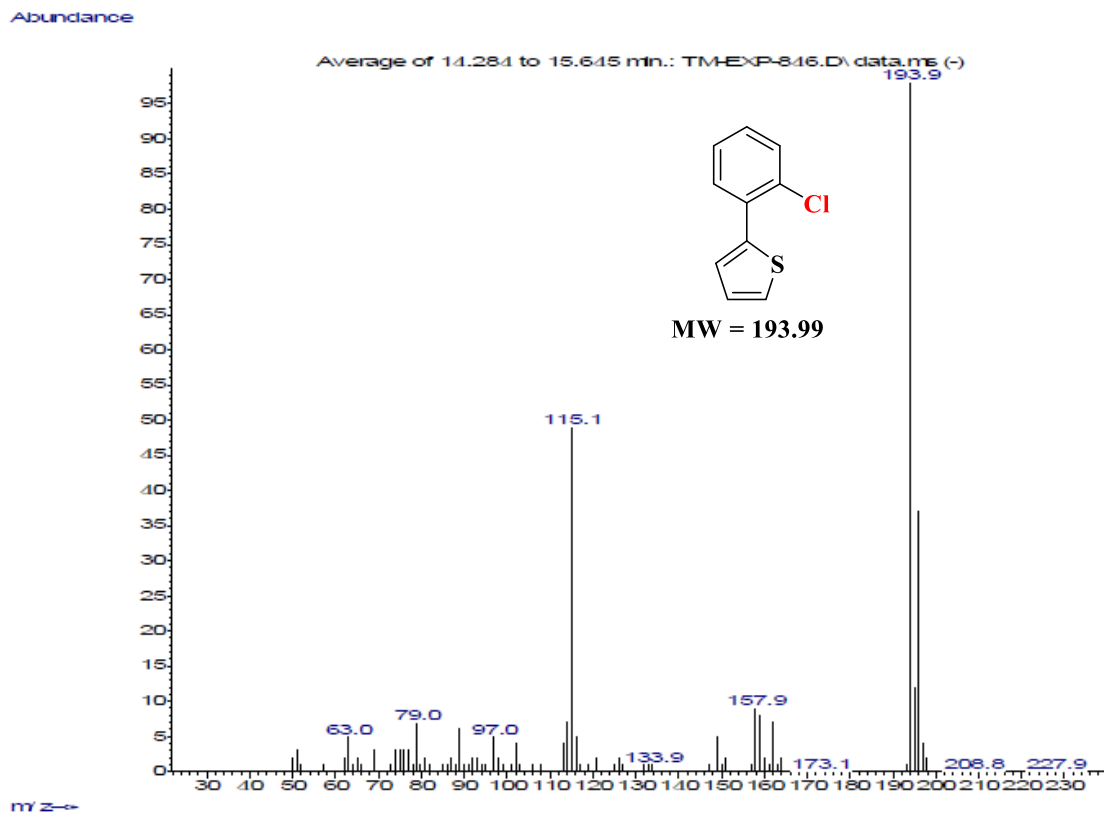


Abundance

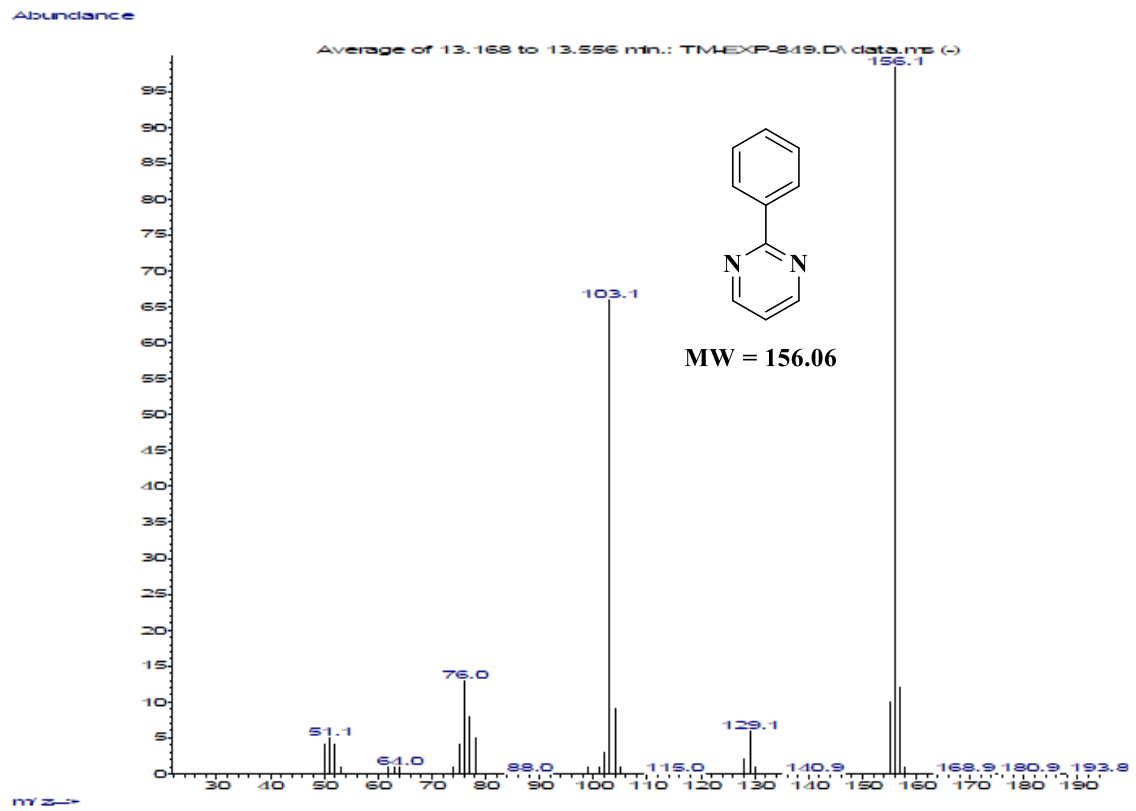
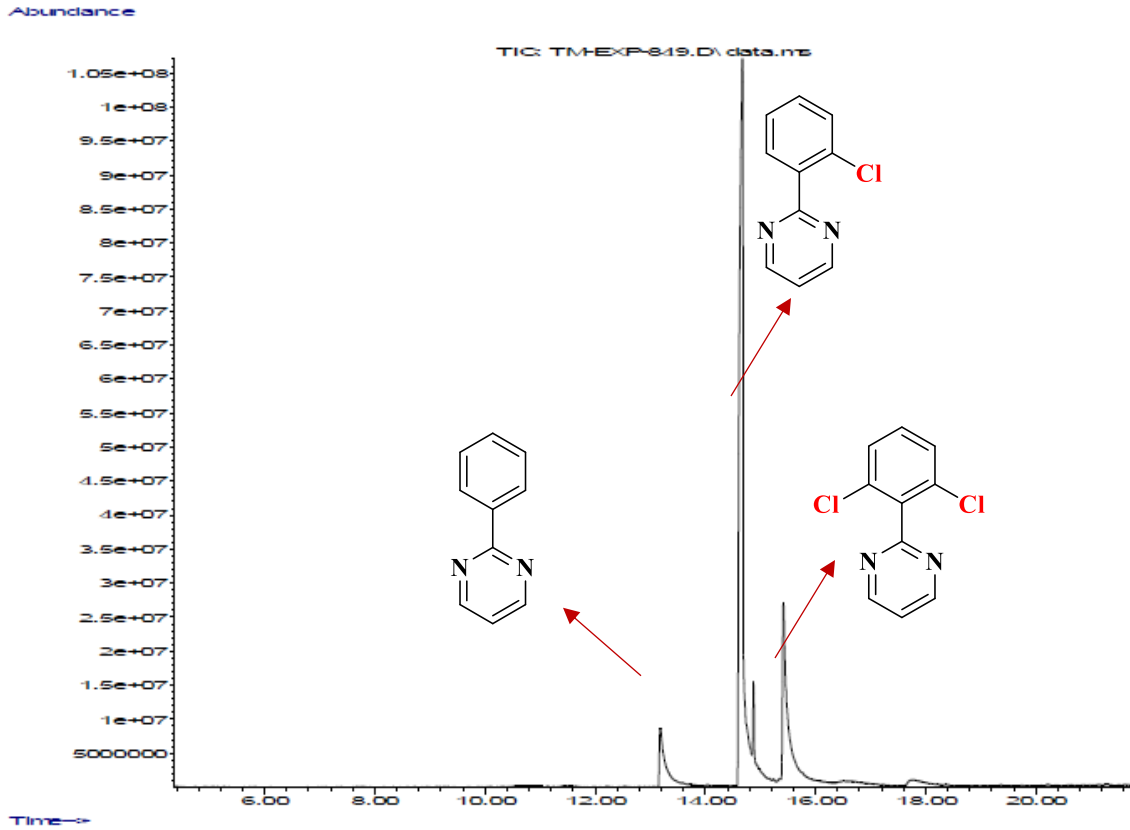


Abundance





**Figure S25.** GCMS profile for the chlorination of 2-phenylthiophene.



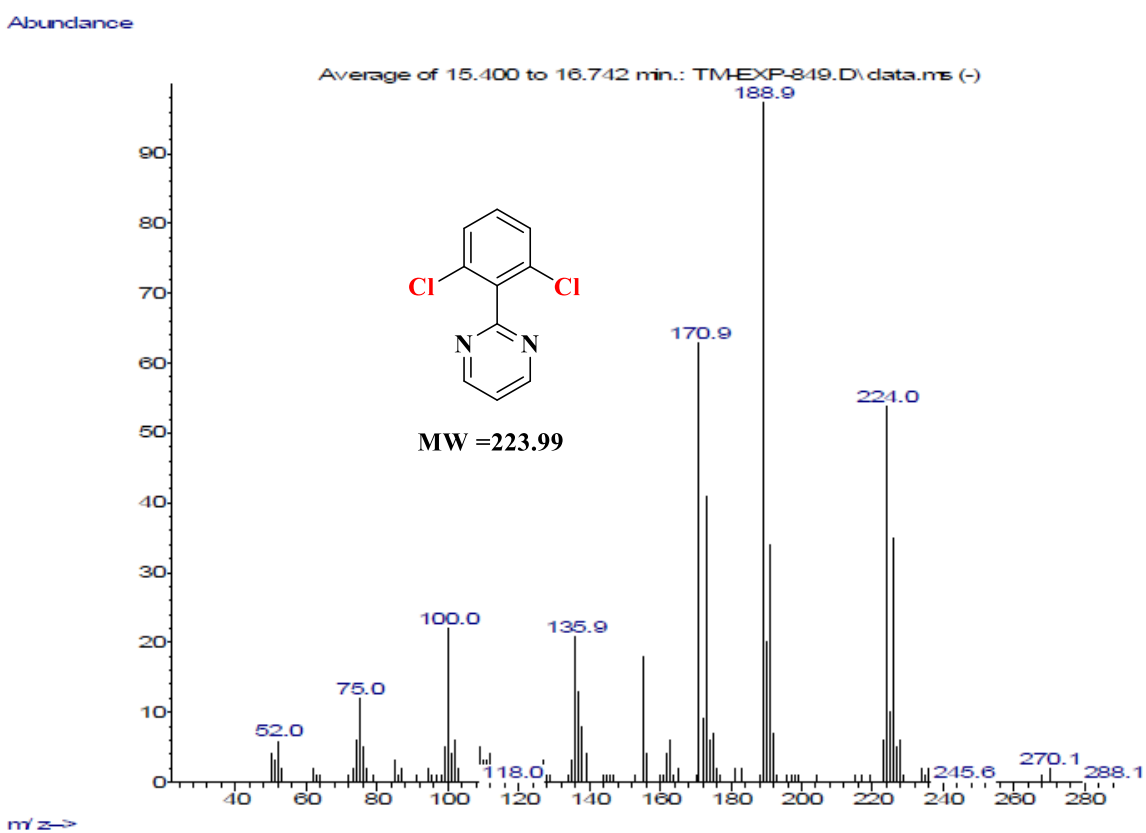
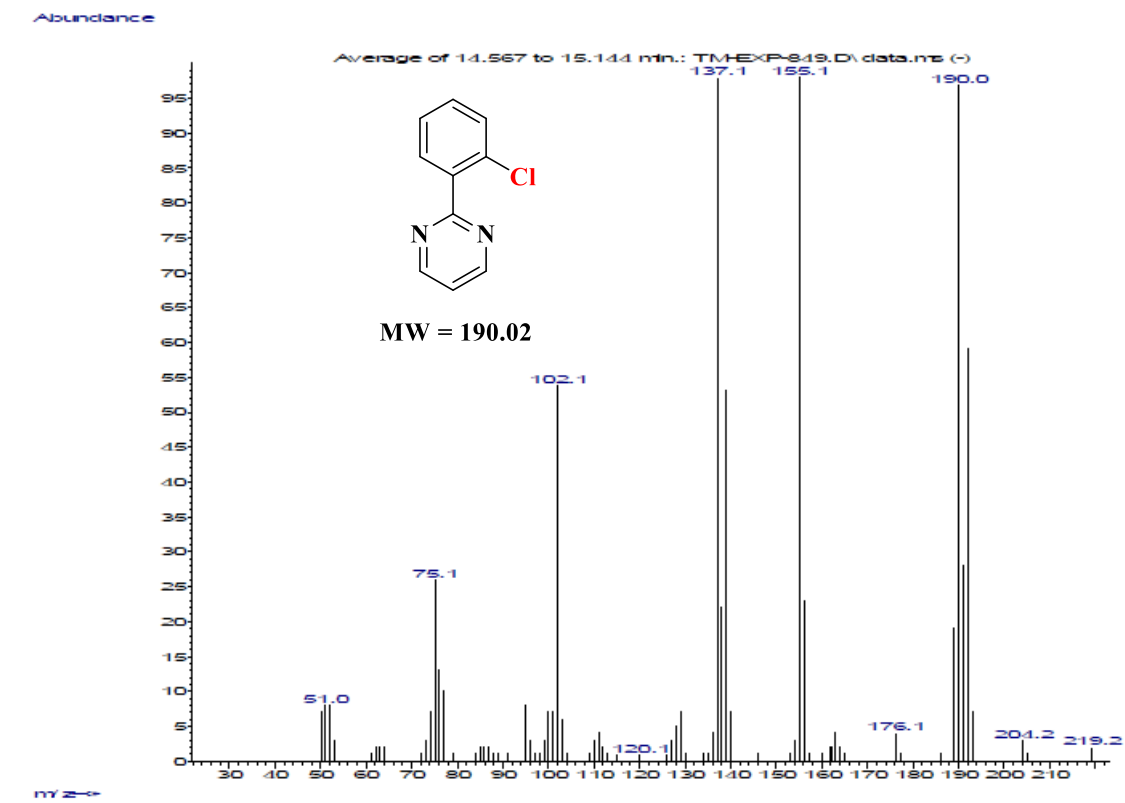
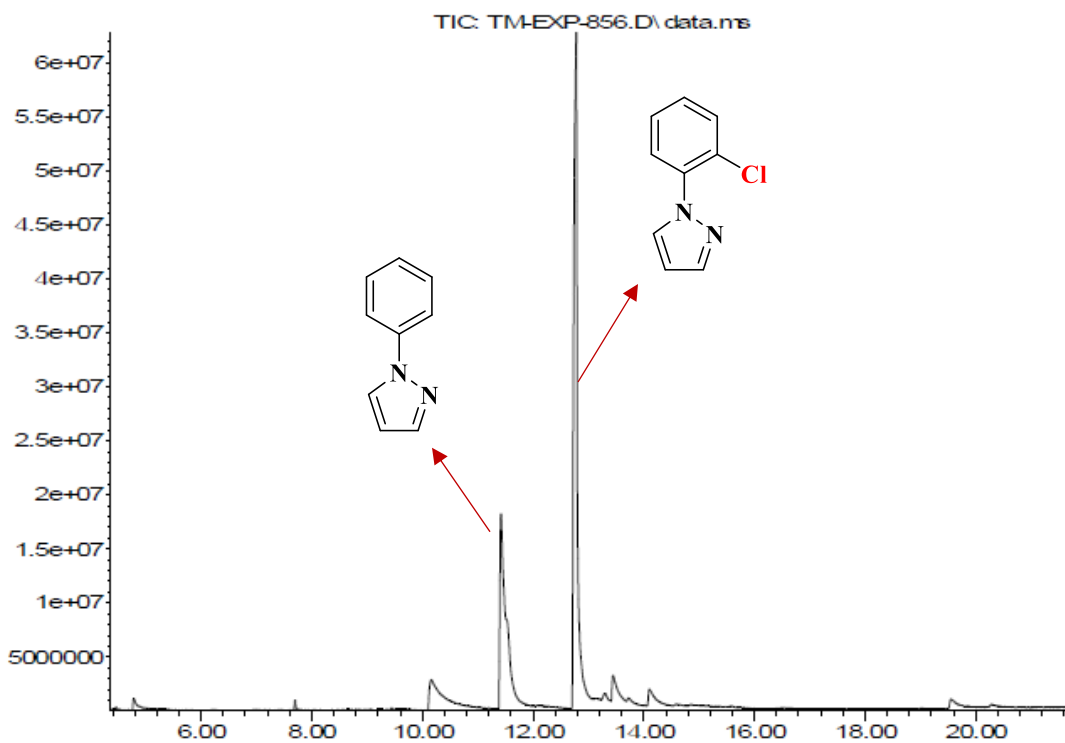
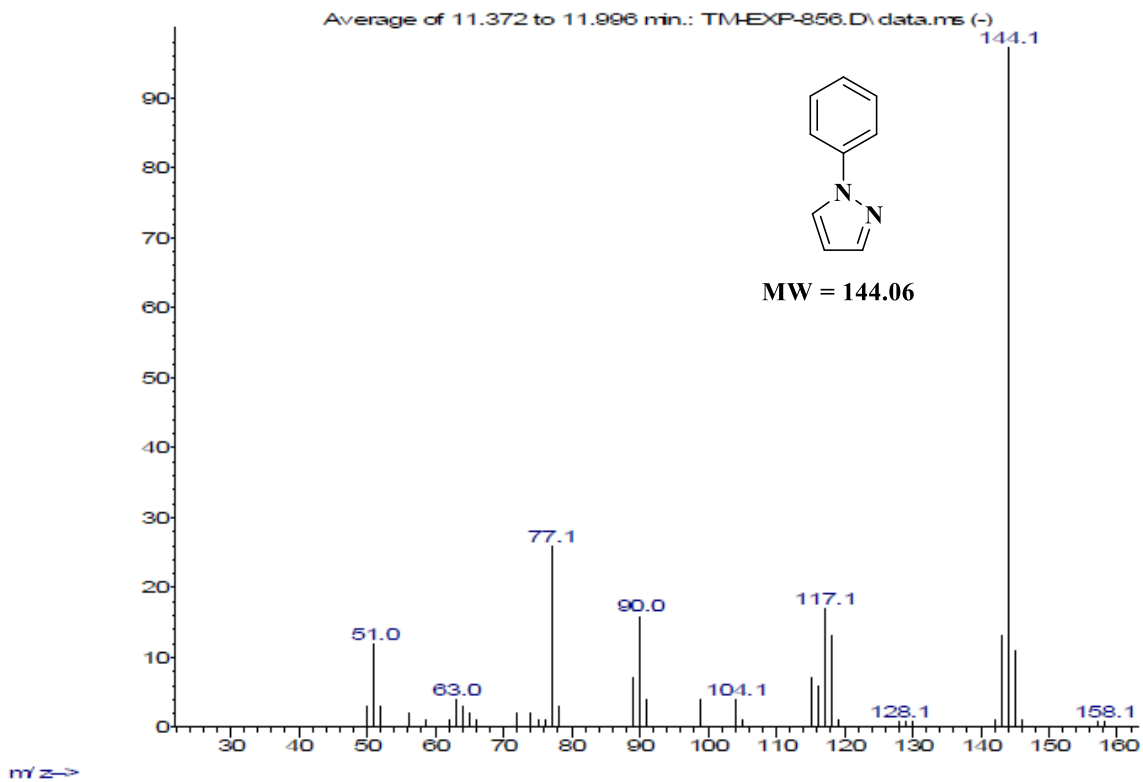


Figure S26. GCMS profile for the chlorination of 2-phenylpyrimidine.

Abundance



Abundance



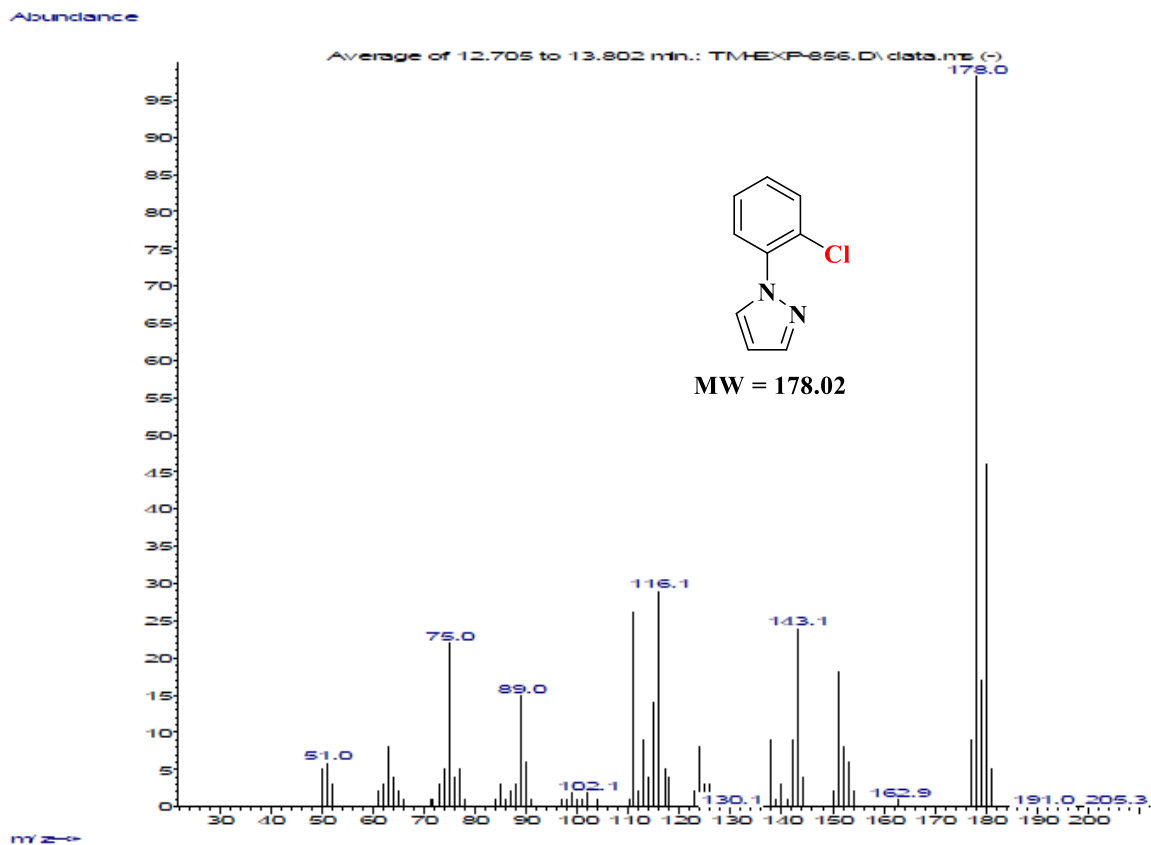
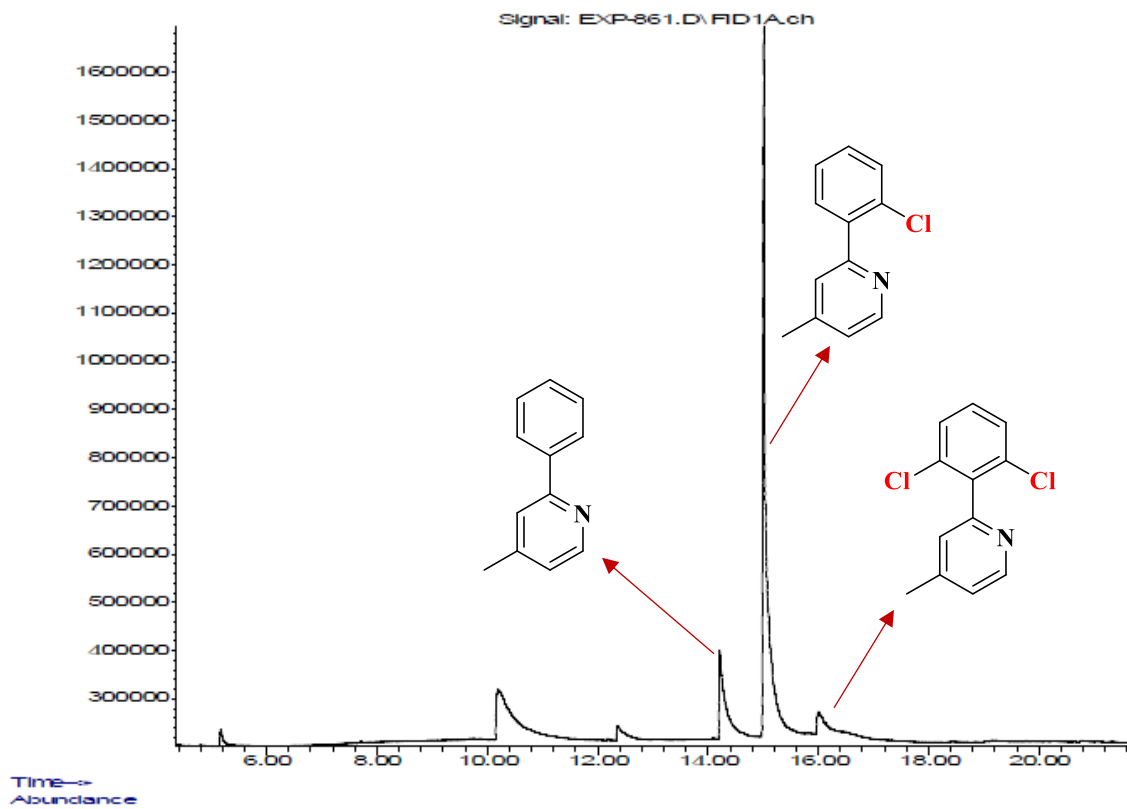
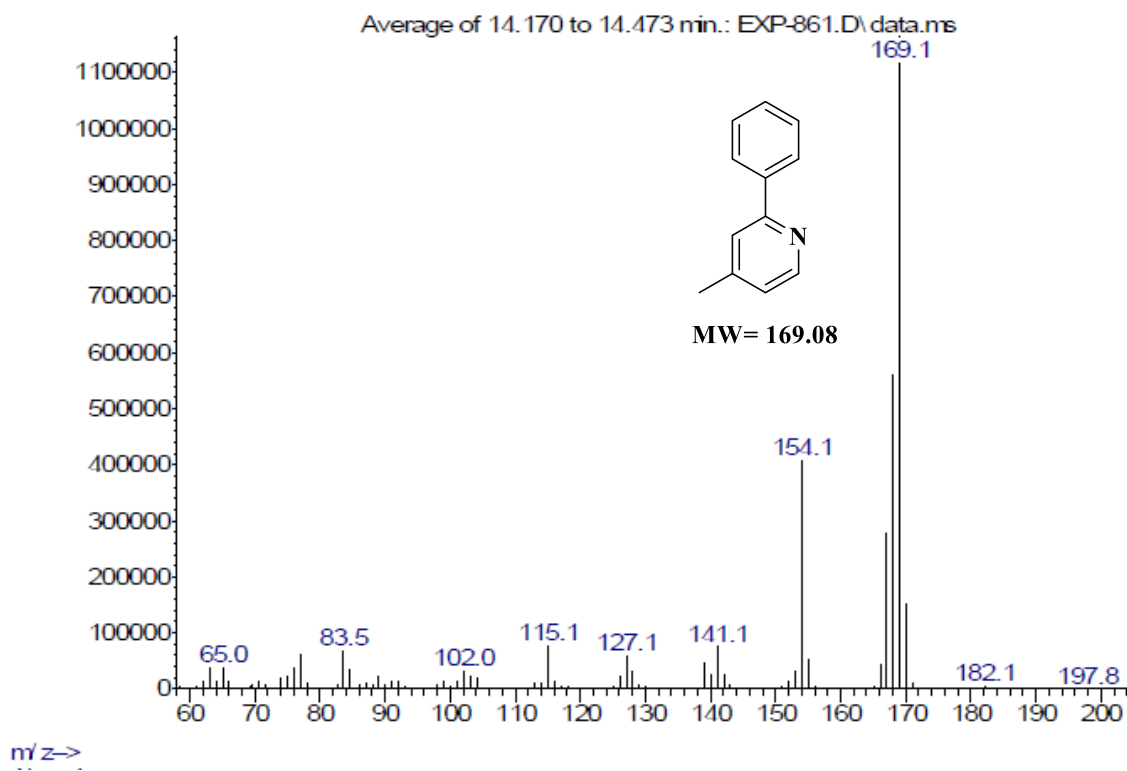
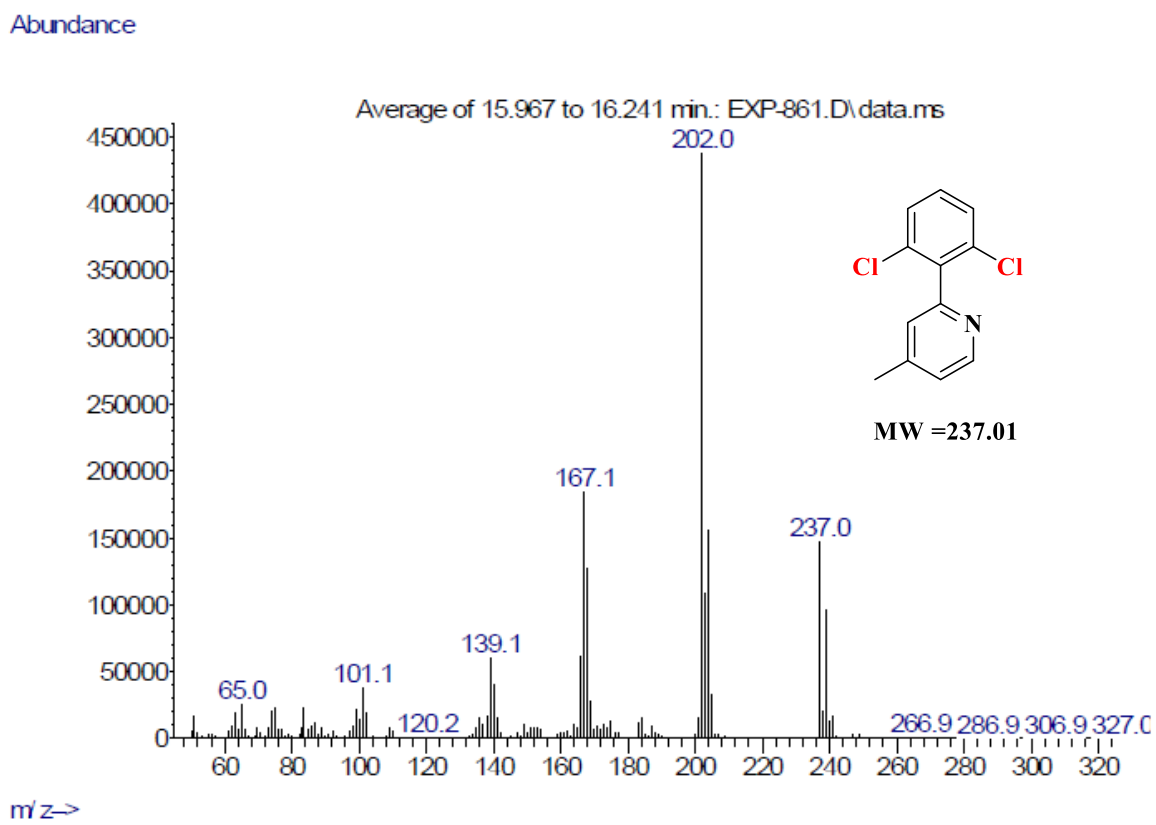
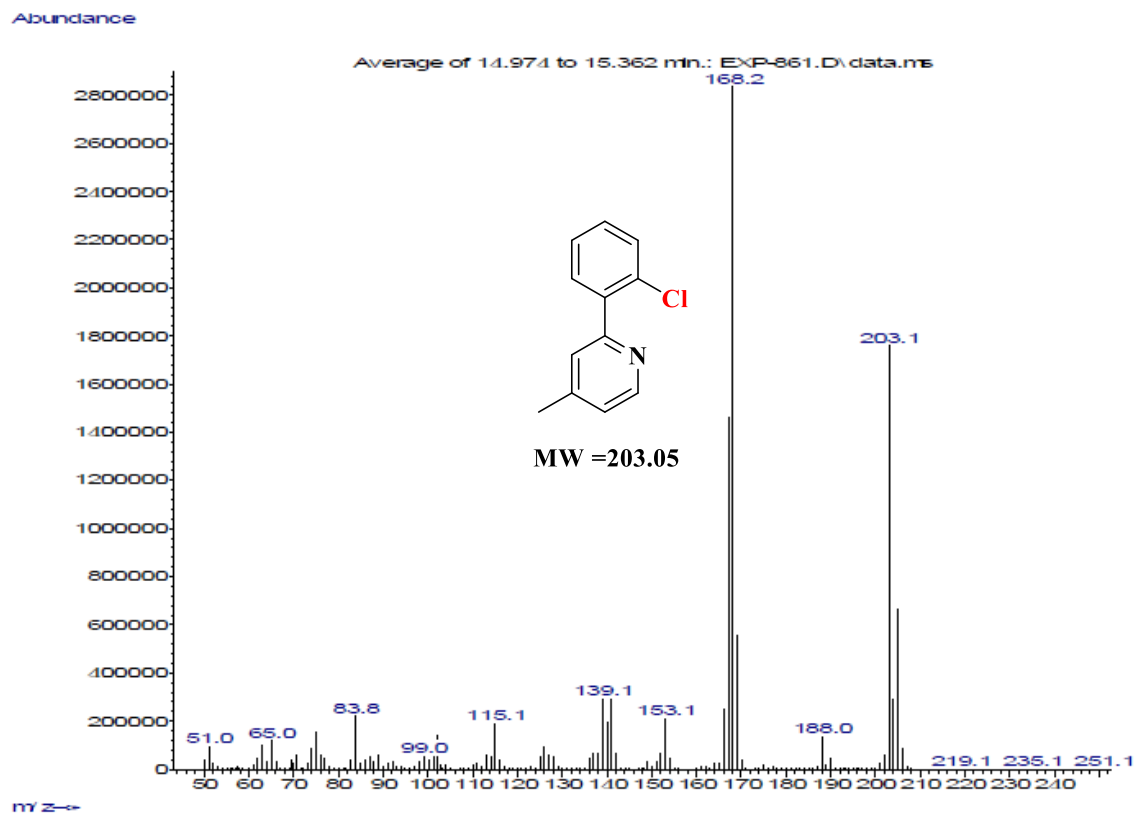


Figure S27. GCMS profile for the chlorination of 1-phenylpyrazole.



Abundance

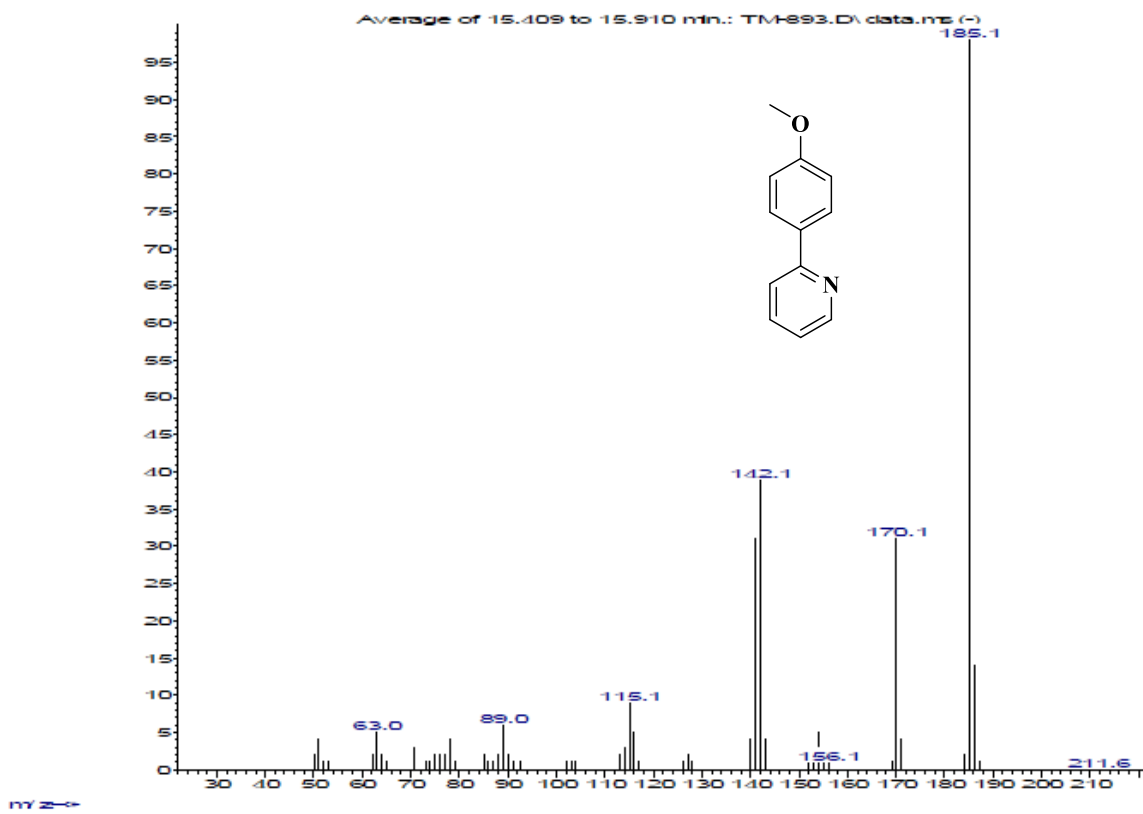
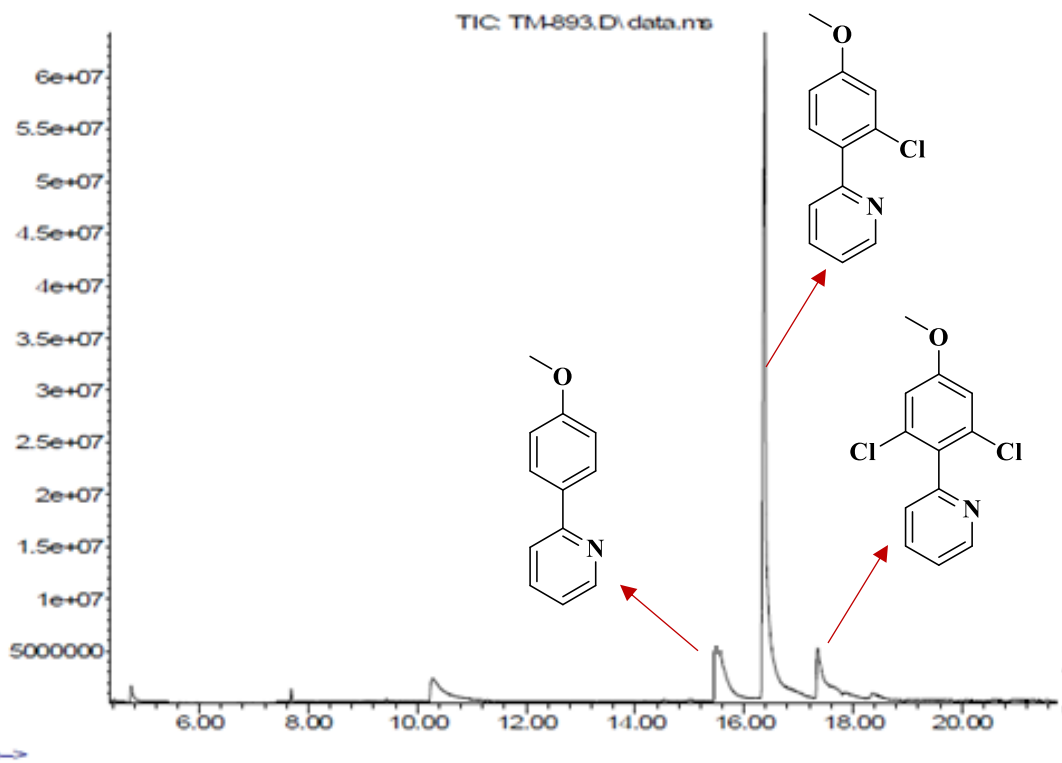




**Figure S28.** GCMS profile for the chlorination of 4-methyl-2-phenylpyridine.



Abundance



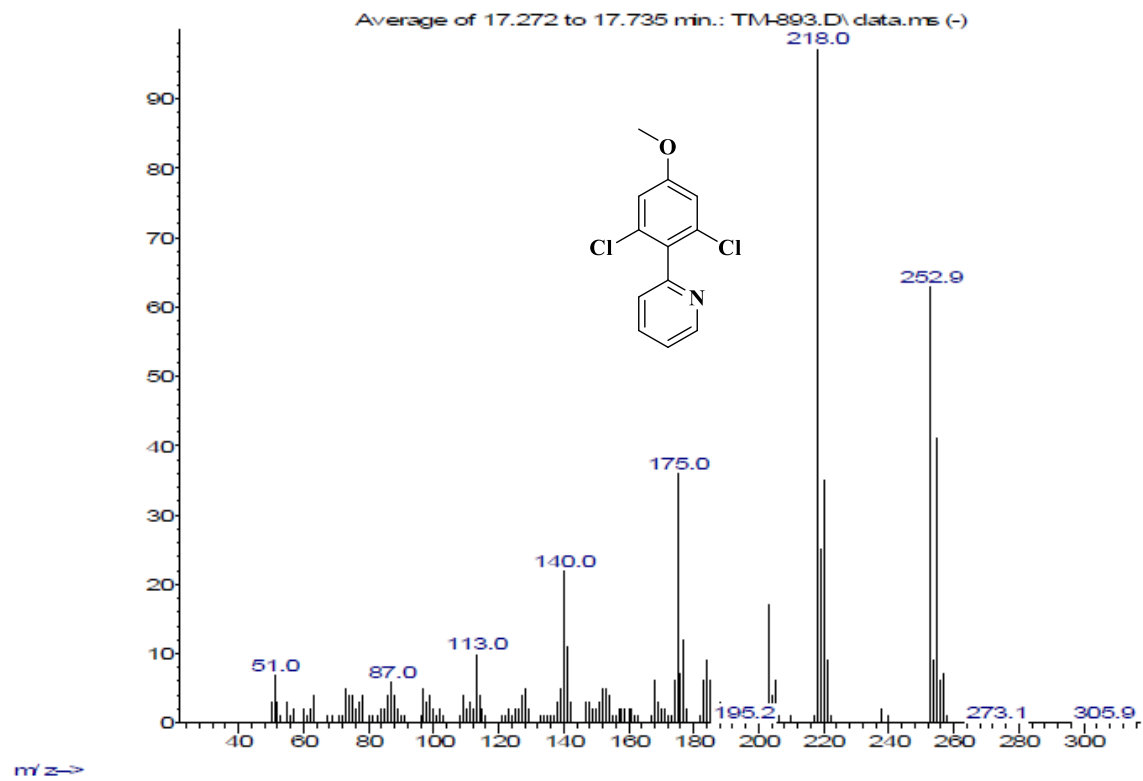
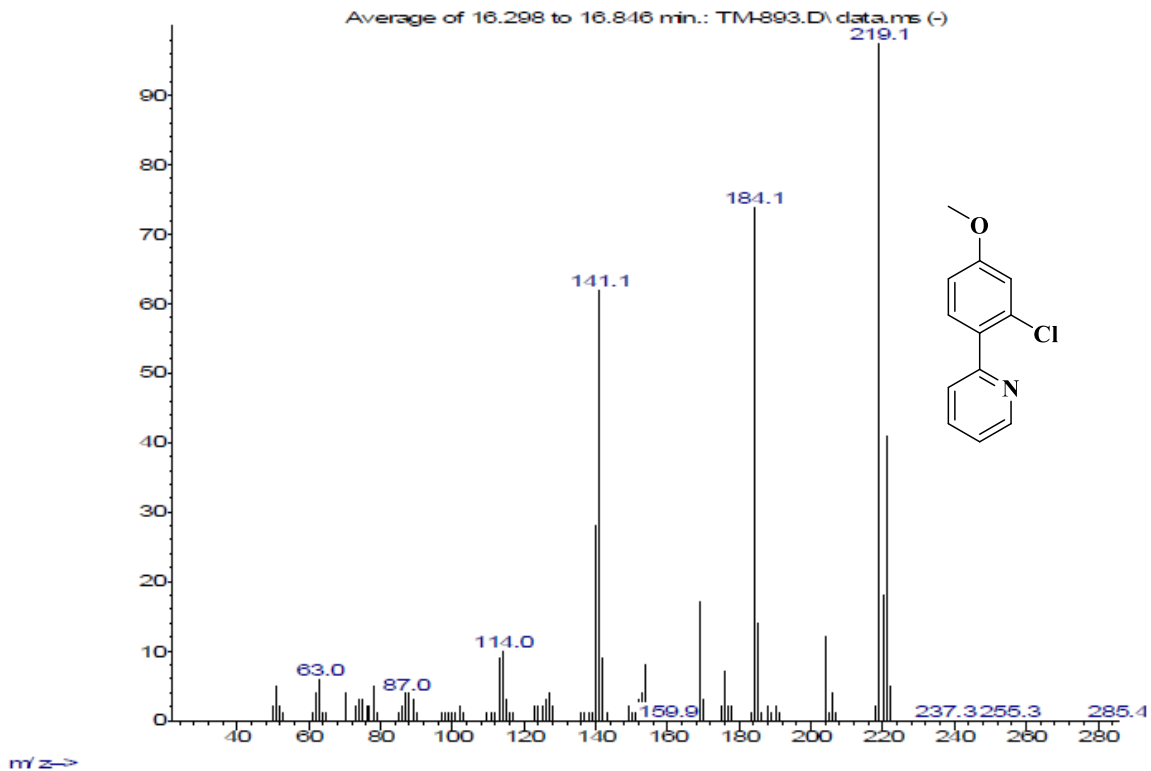
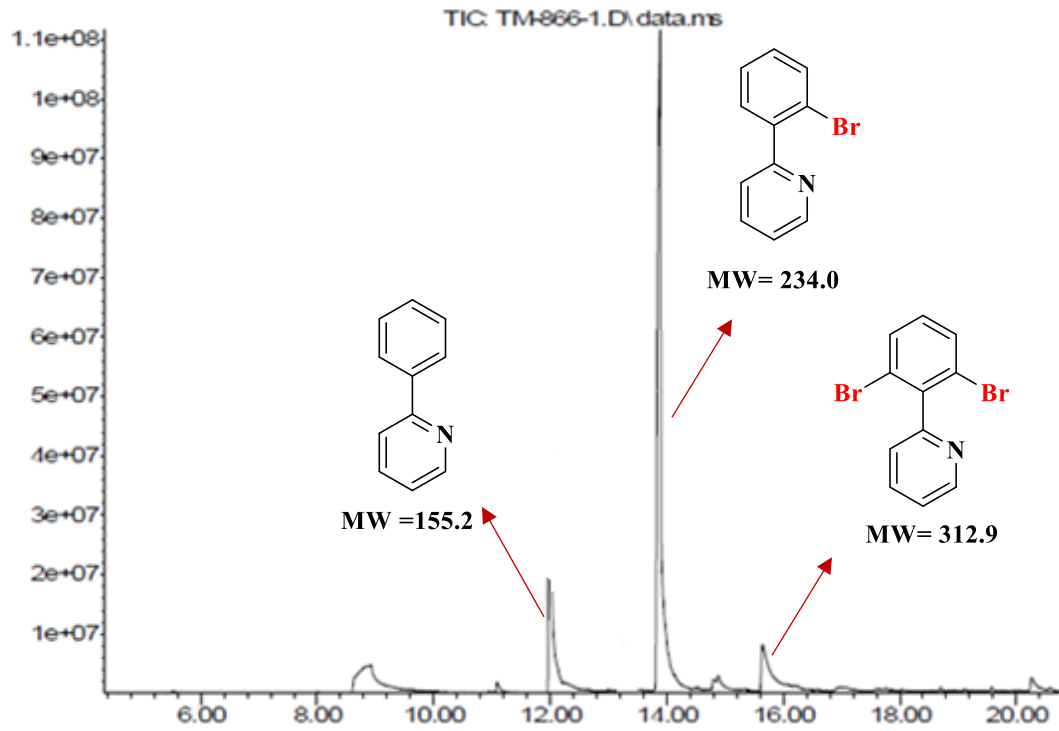
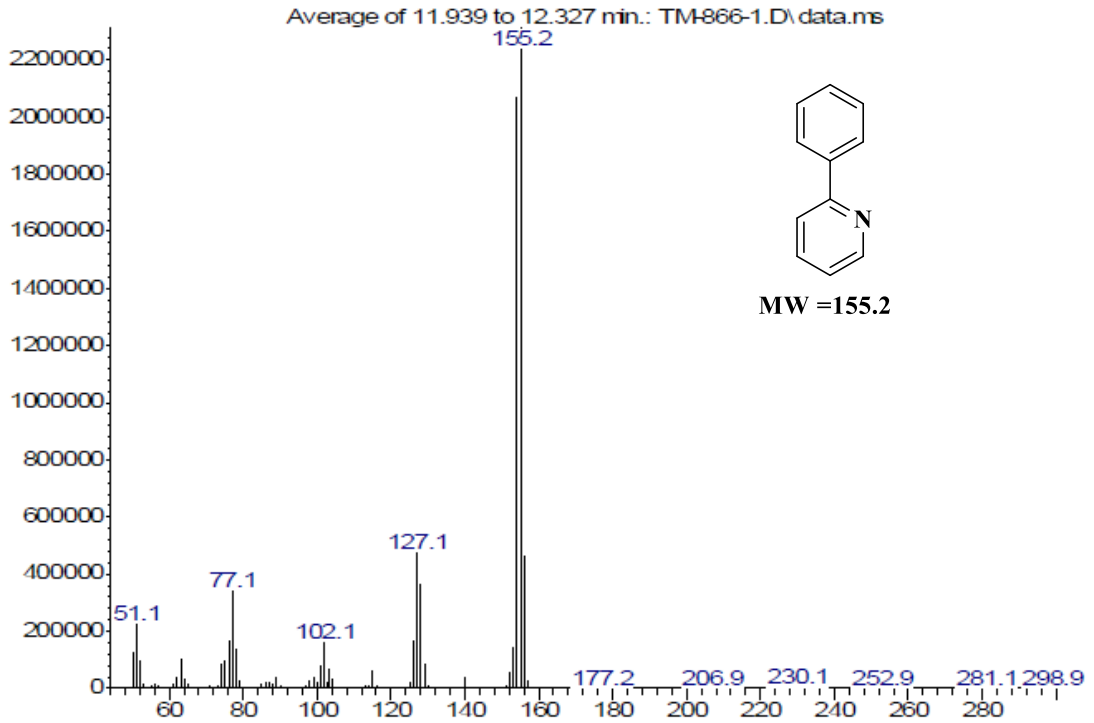


Figure S29. GCMS profile for the chlorination of 2-(4-methoxyphenyl) pyridine.

Abundance



Time→  
Abundance



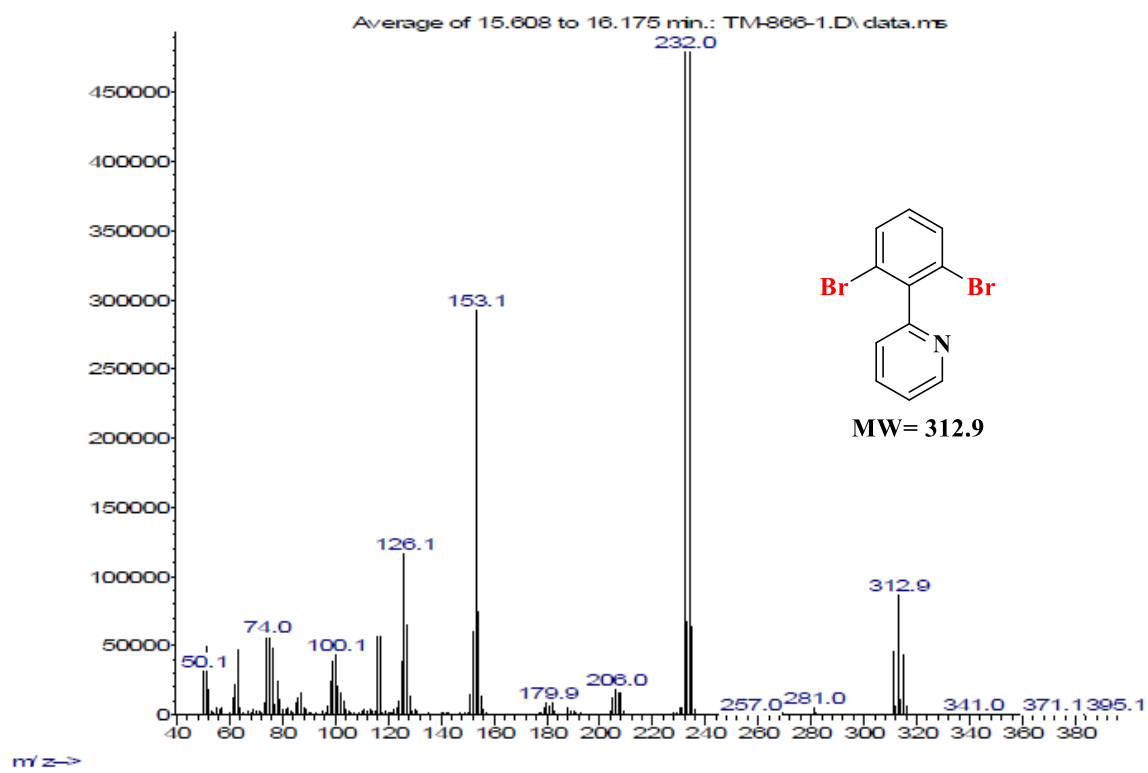
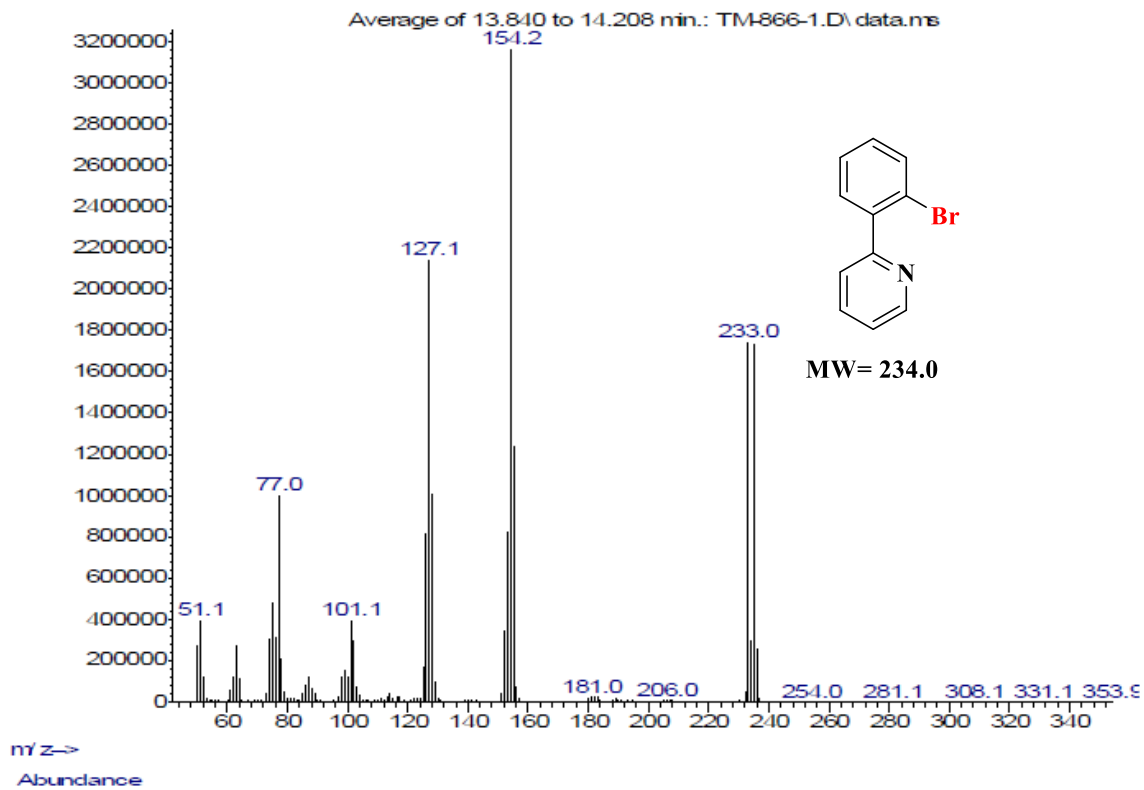
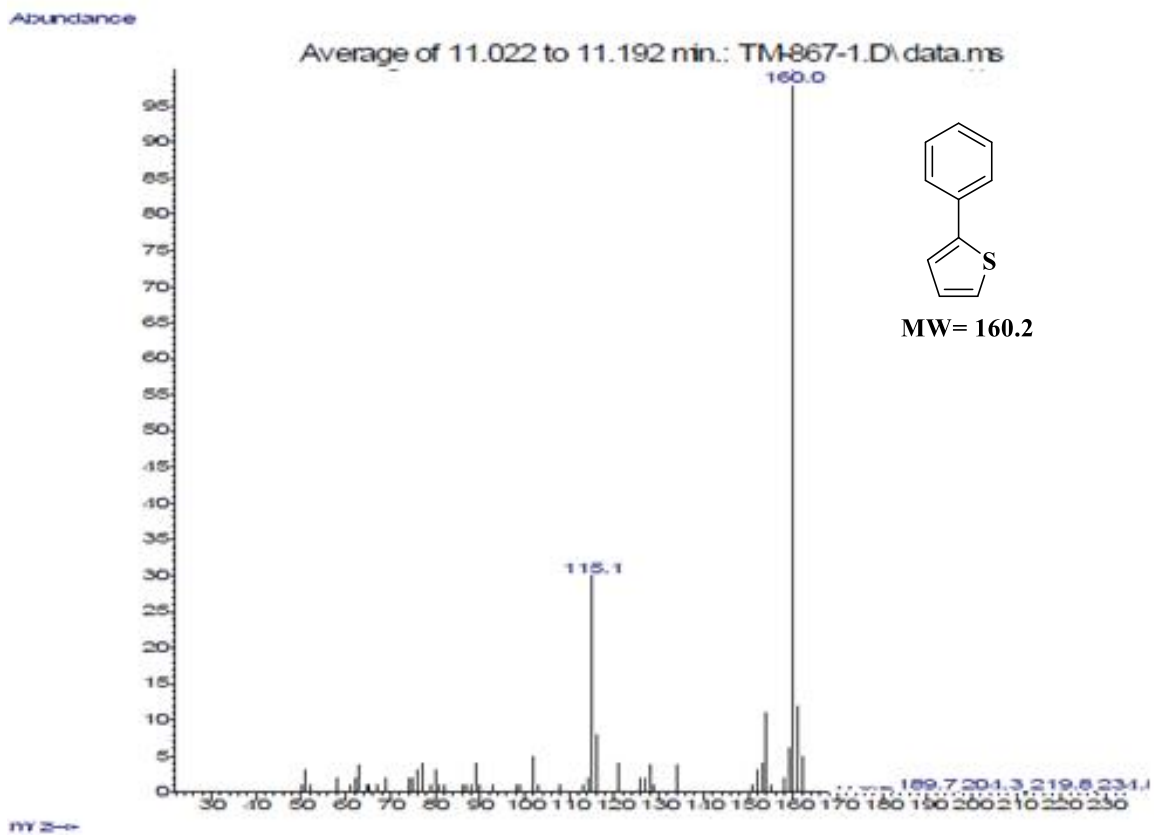
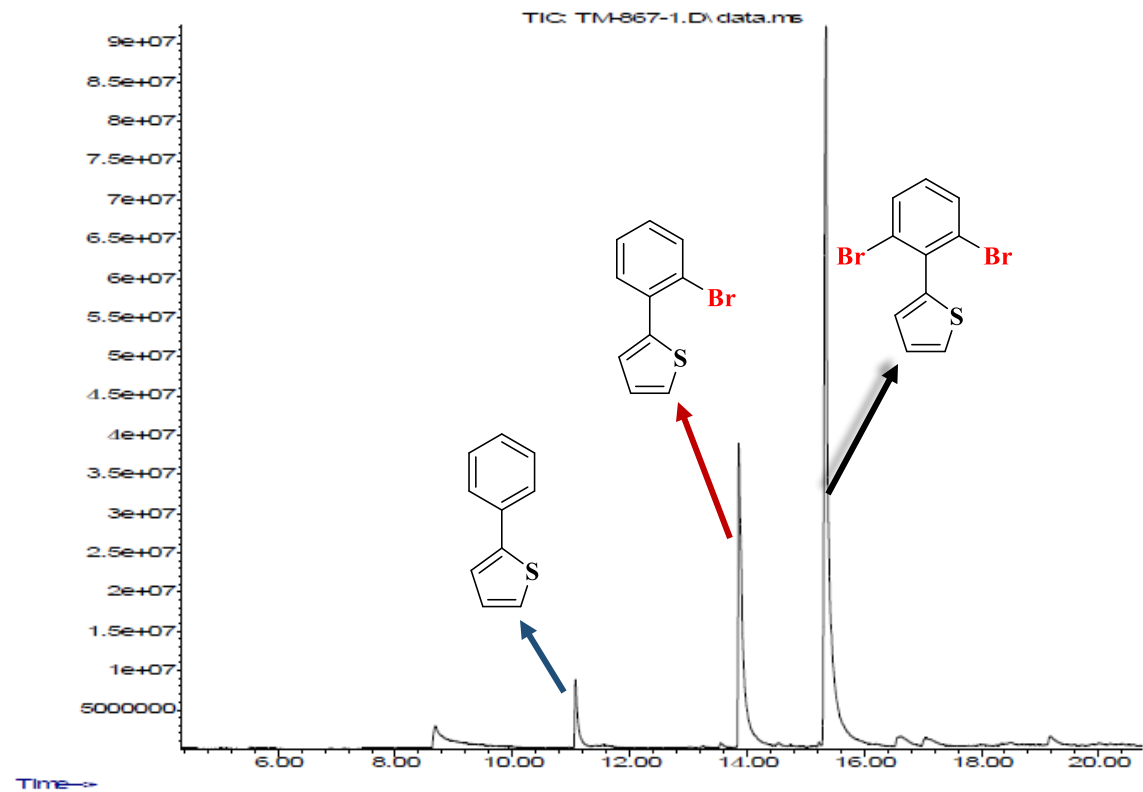


Figure S30. GCMS profile for the bromination of 2-phenylpyridine.



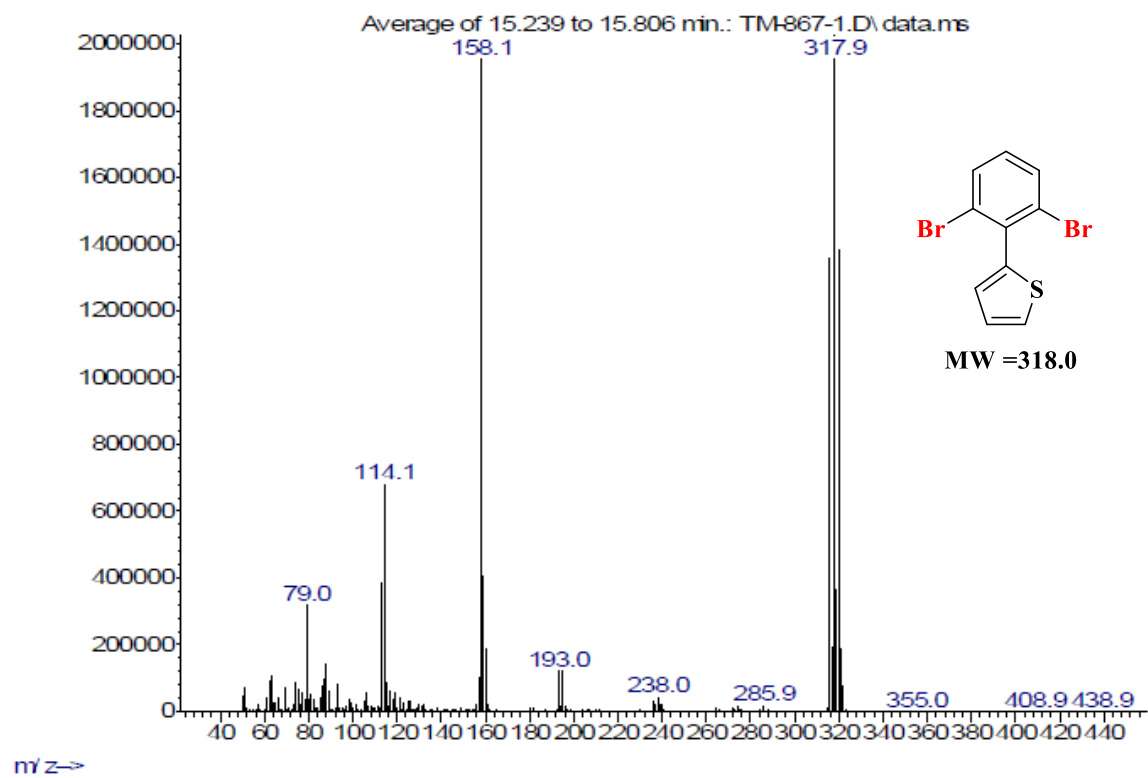
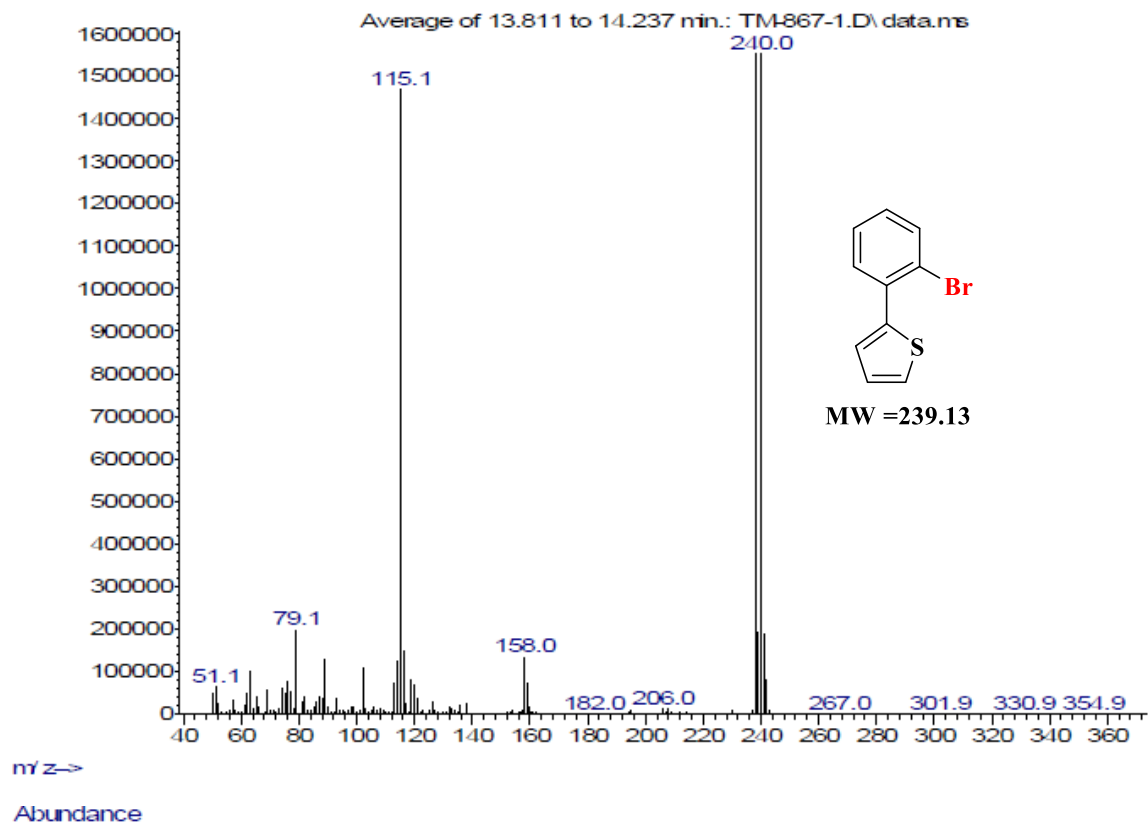
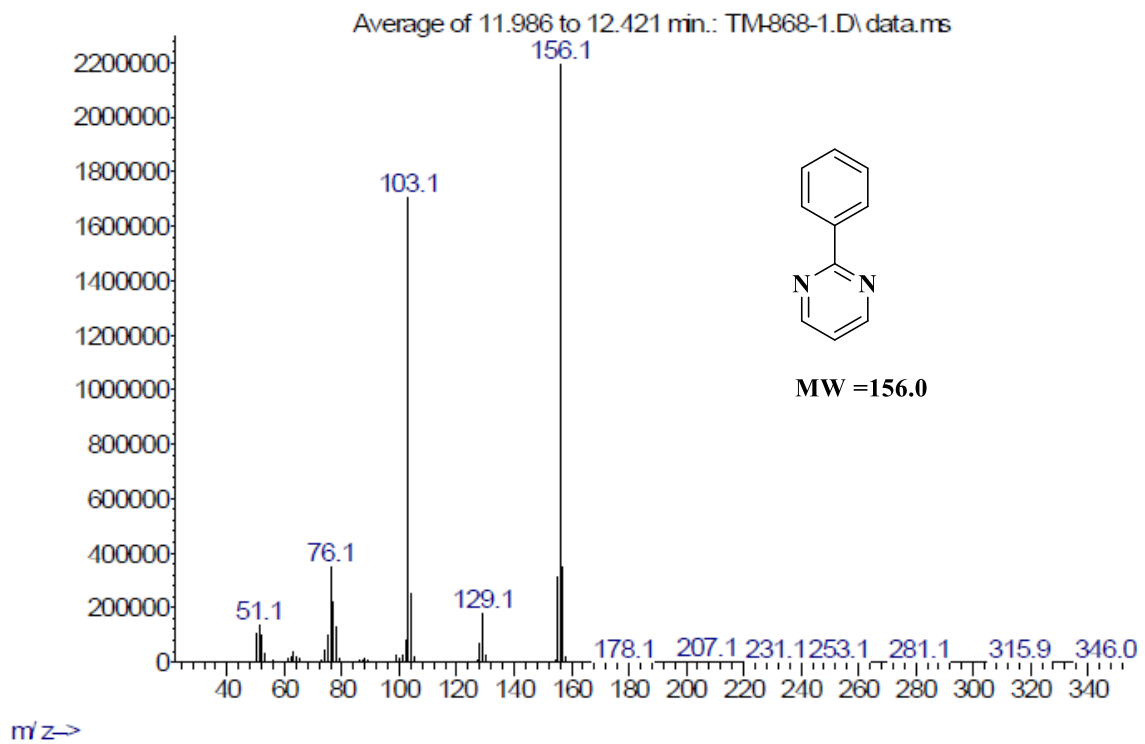
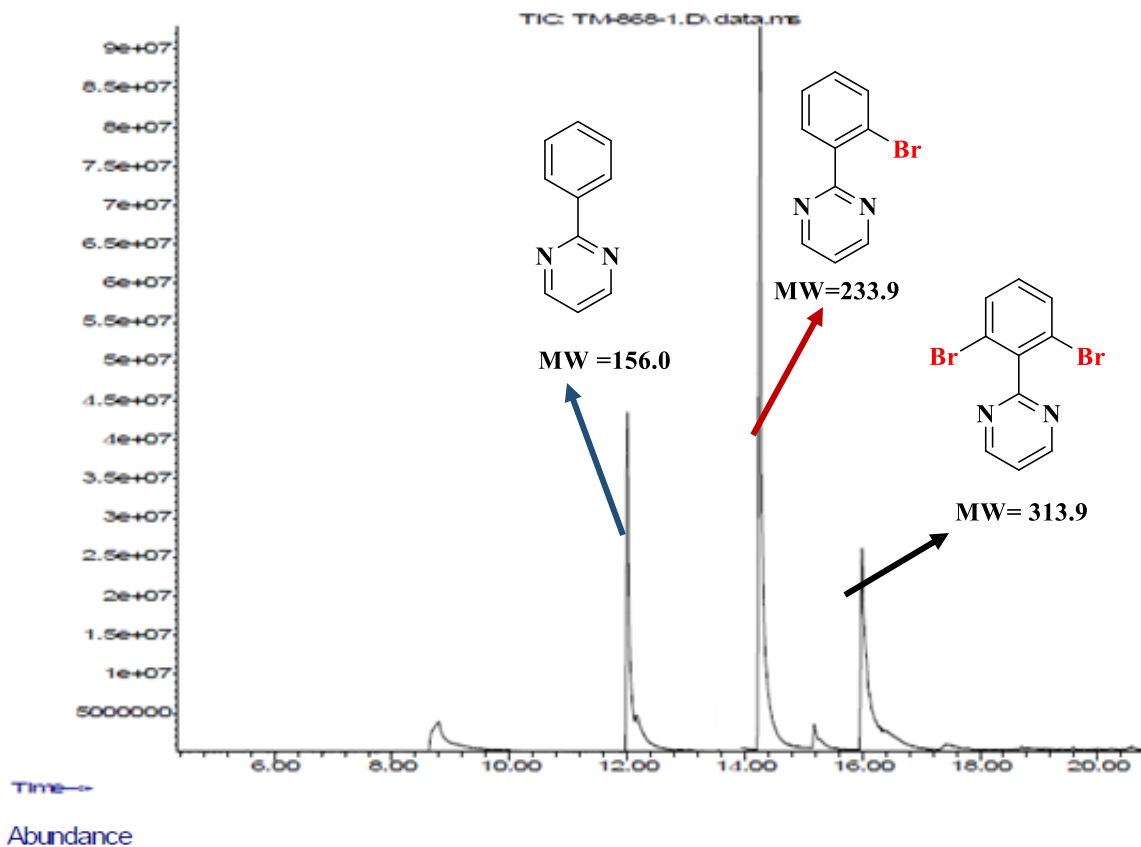
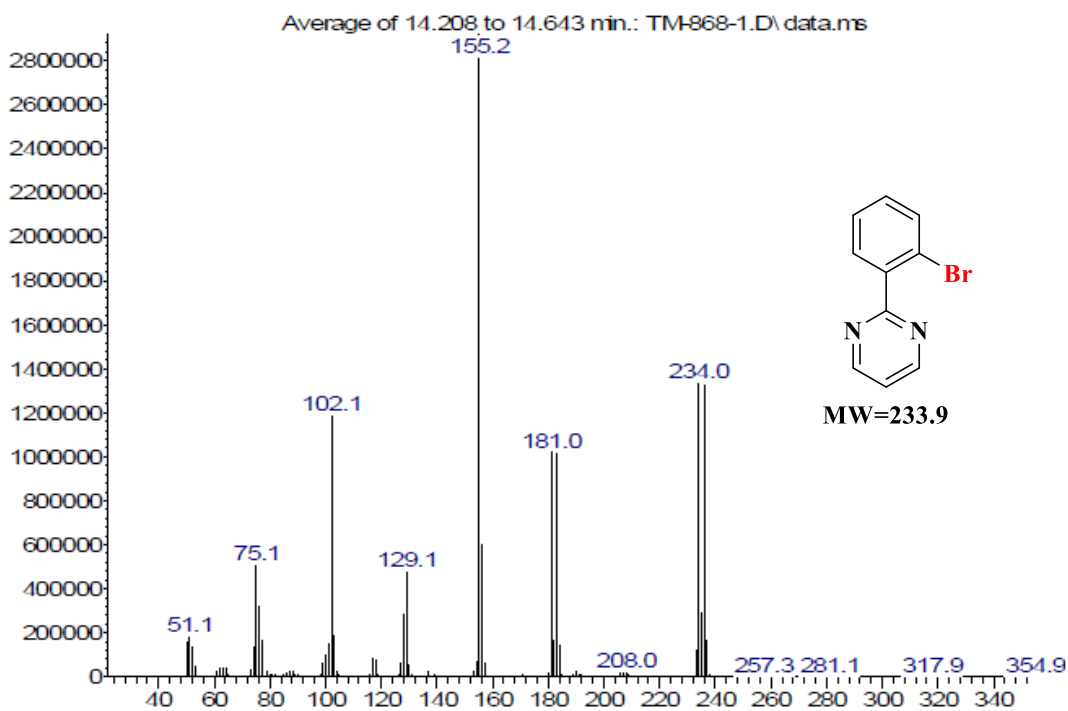


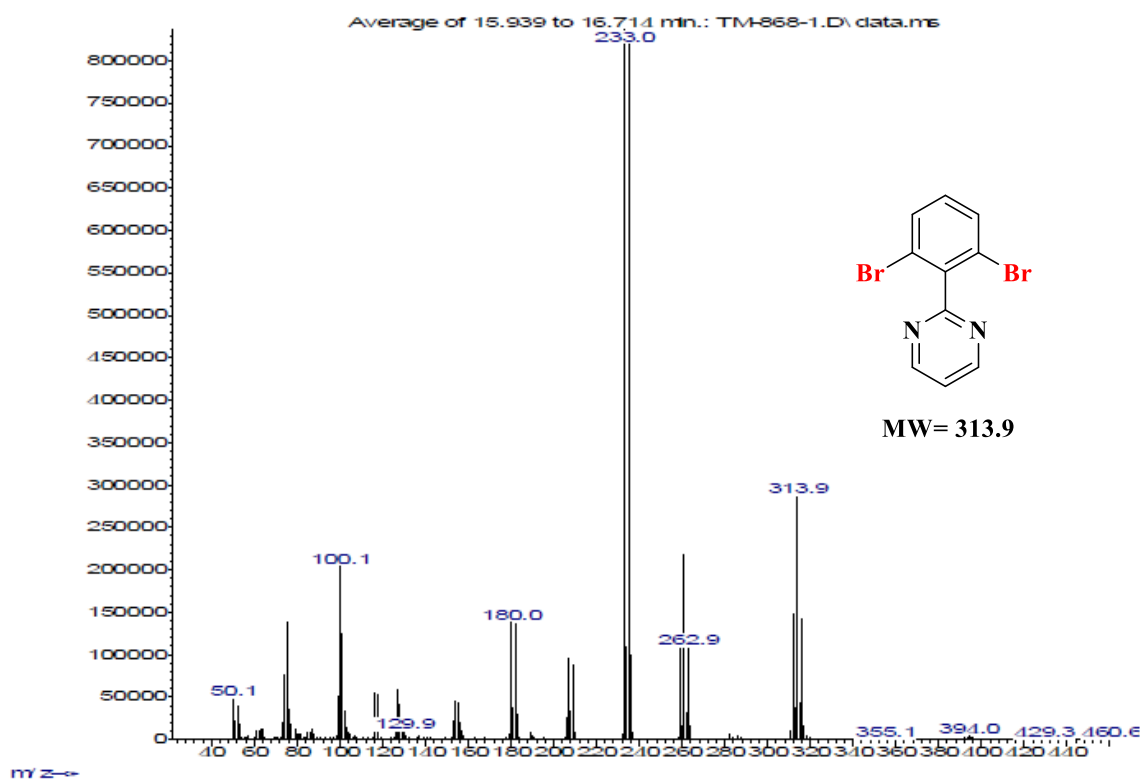
Figure S31. GCMS profile for the bromination of 2-phenylthiophene.



m/z →  
Abundance



m/z →

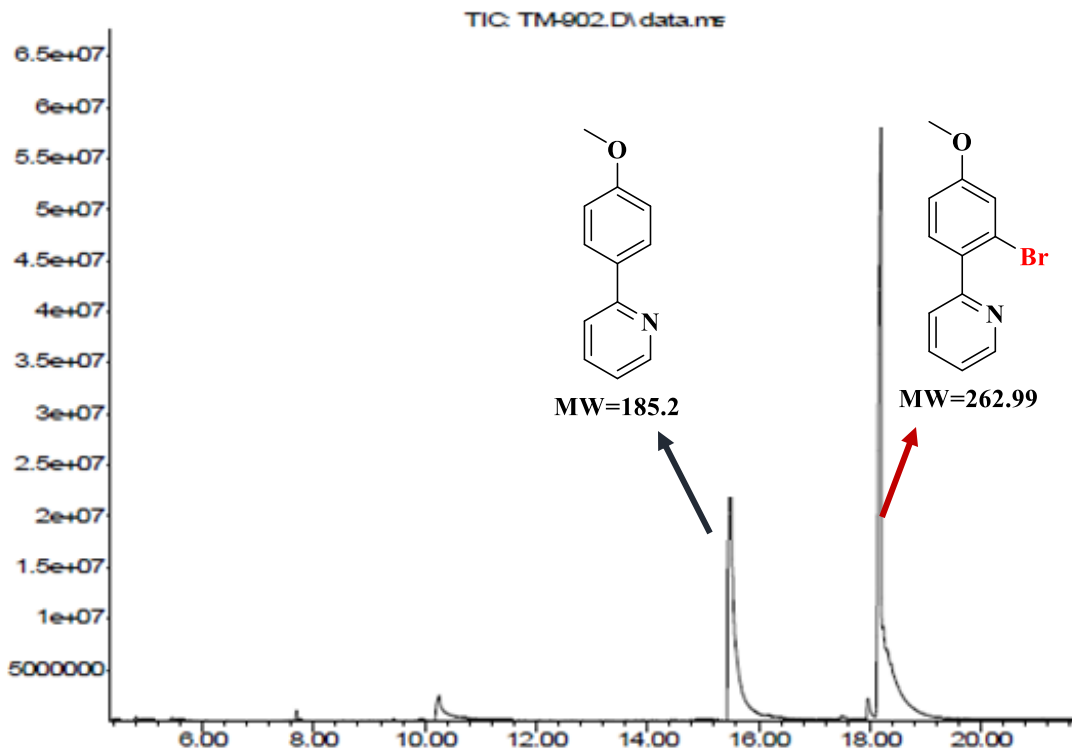


m/z →

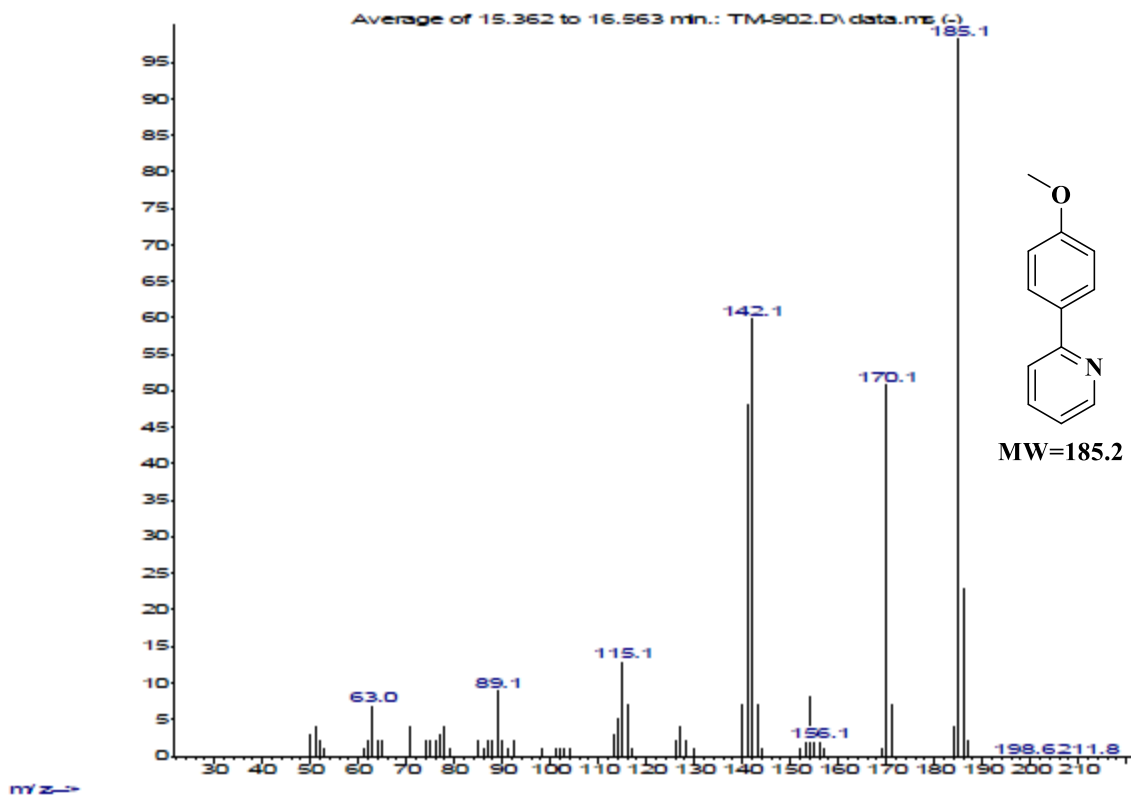
Figure S32. GCMS profile for the bromination of 2-phenylpyrimidine.



Abundance



Time→



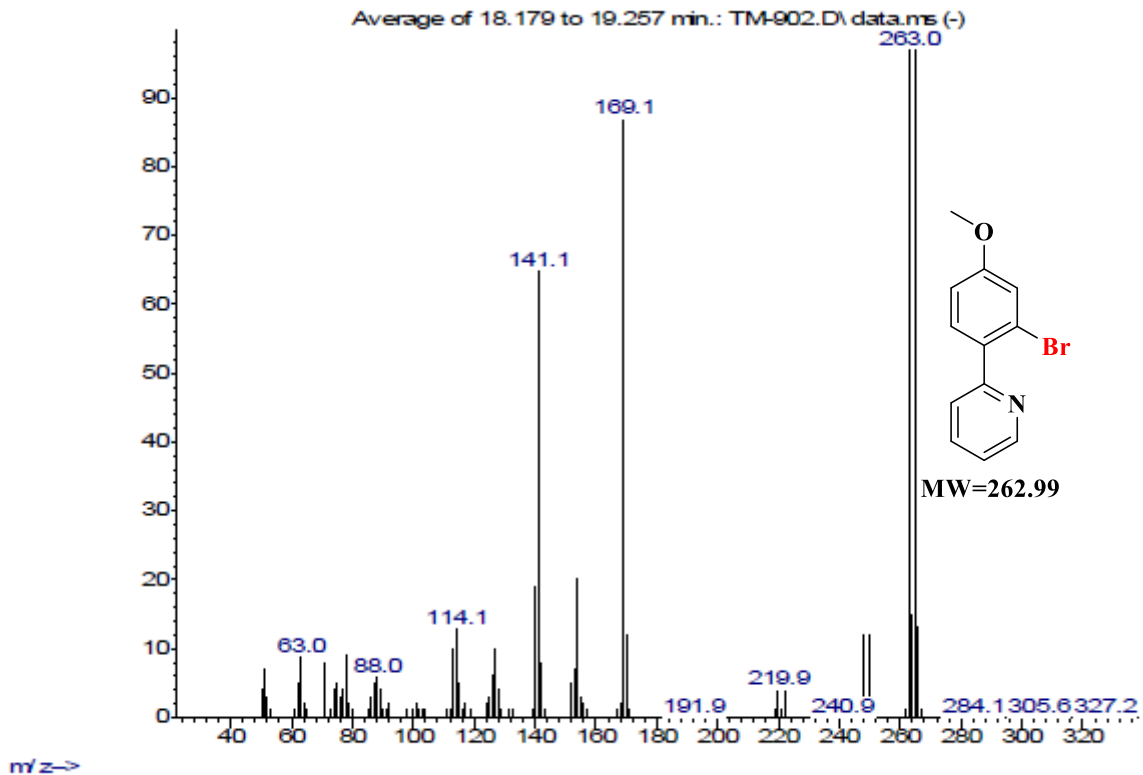
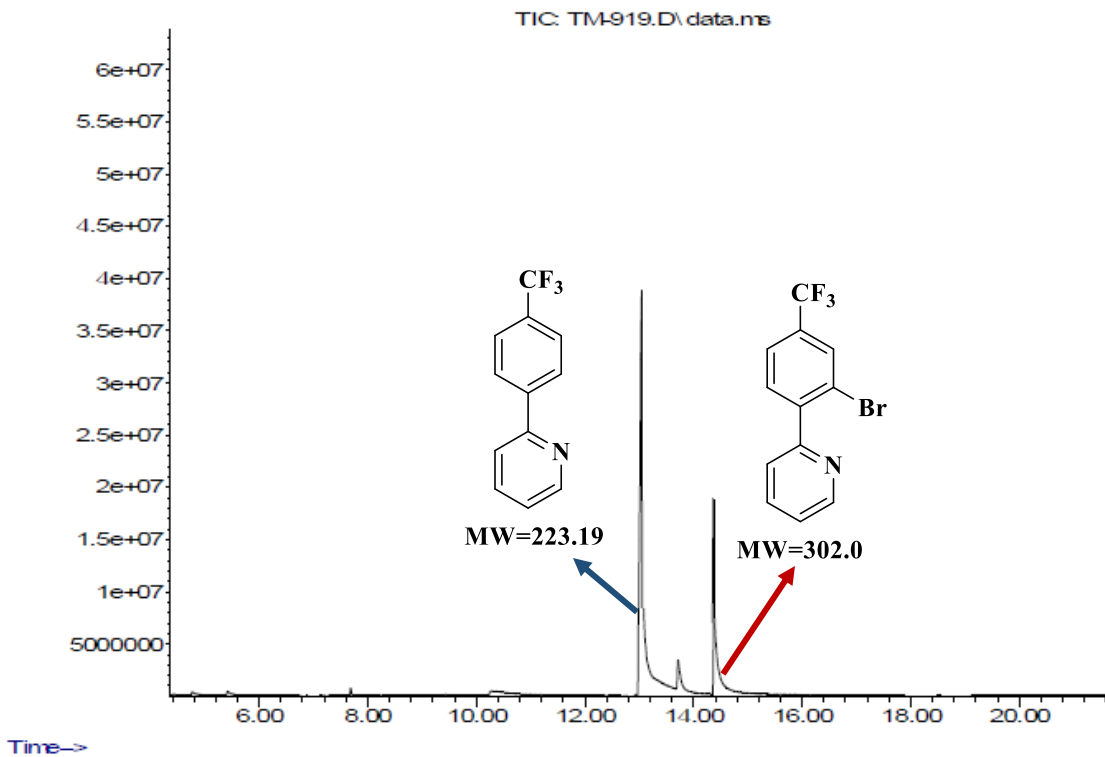


Figure S33. GCMS profile for the bromination of 2-(4-methoxyphenyl) pyridine.



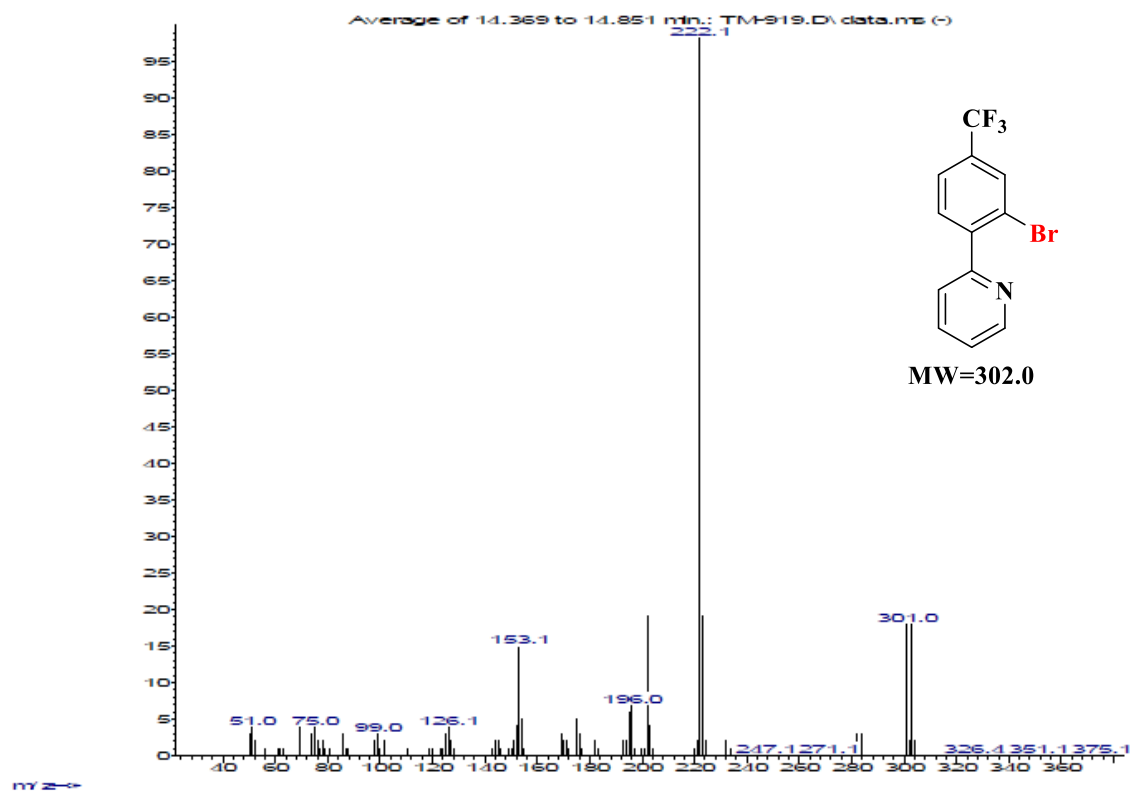
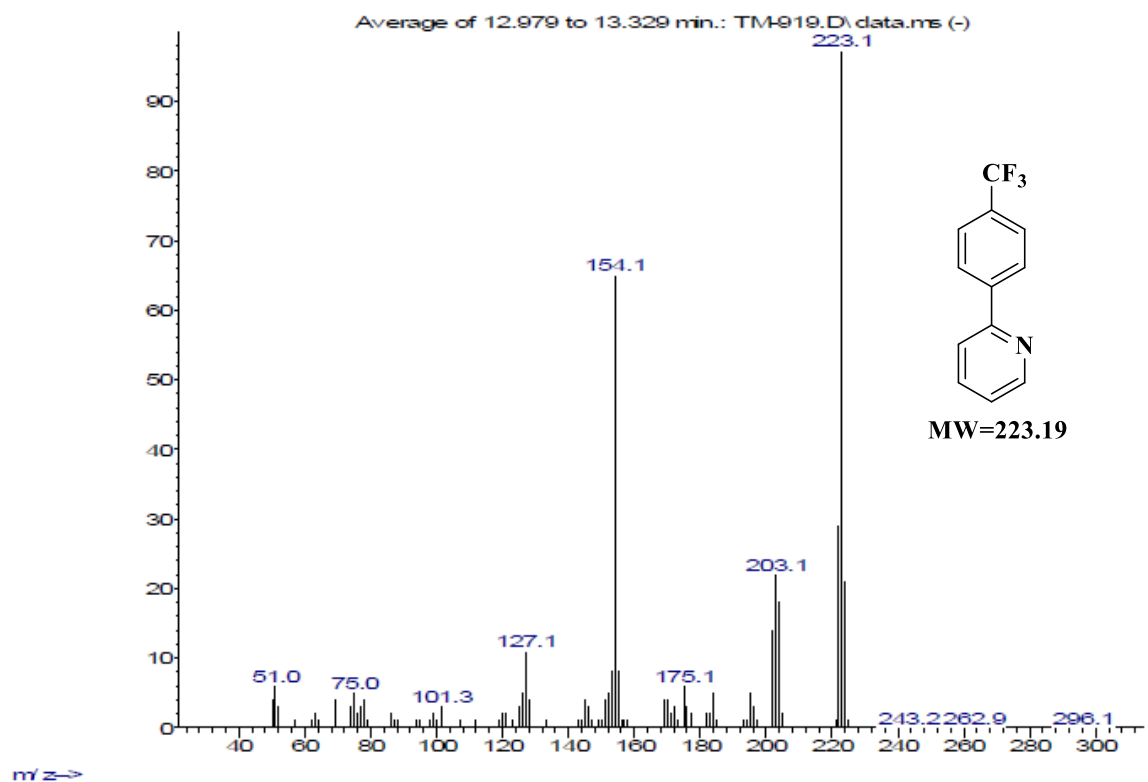
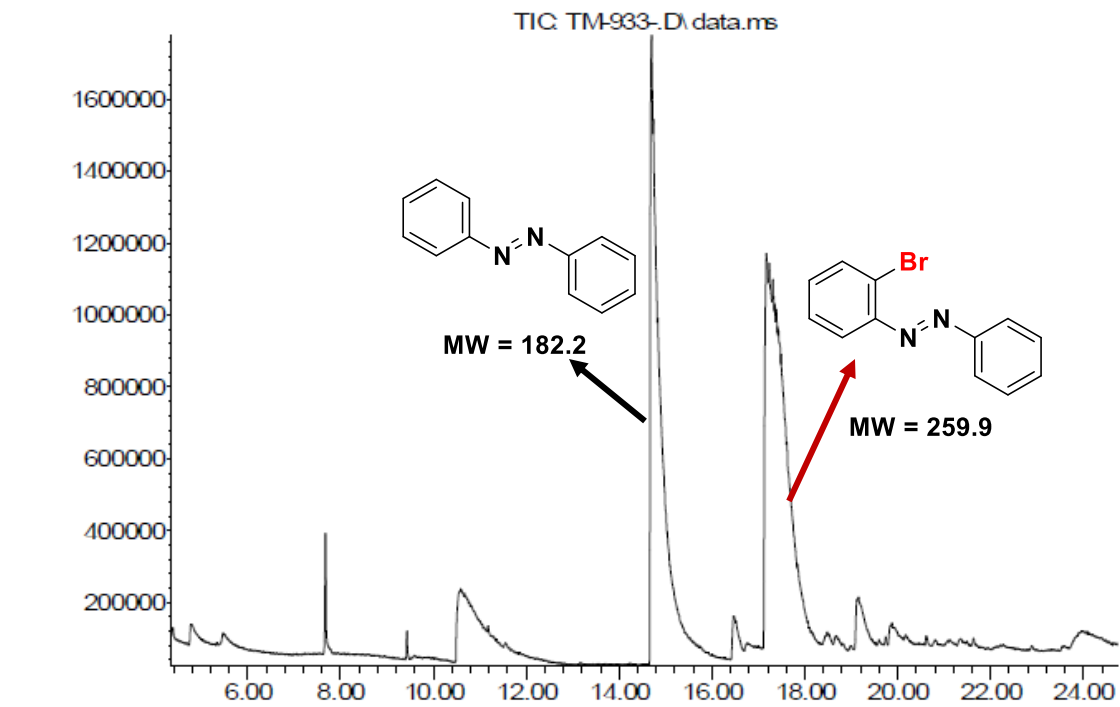
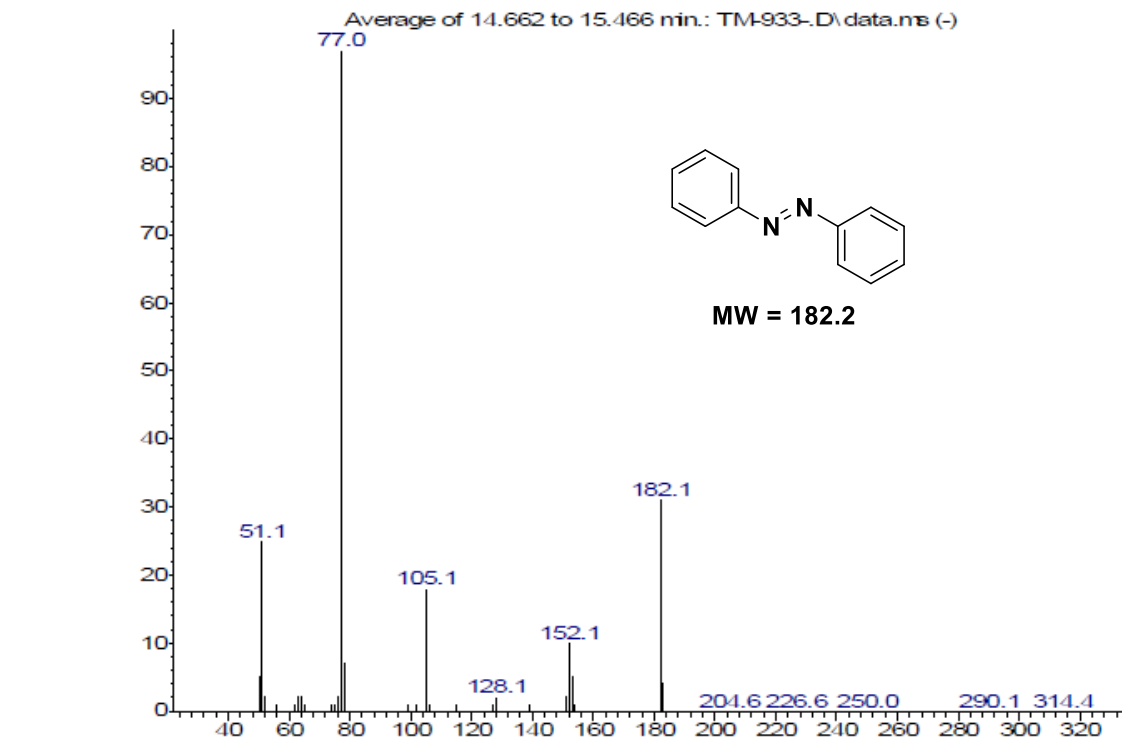


Figure S34. GCMS profile for the bromination of 2-(4-(trifluoromethyl)phenyl)pyridine.



Time→

Abundance



m/z→

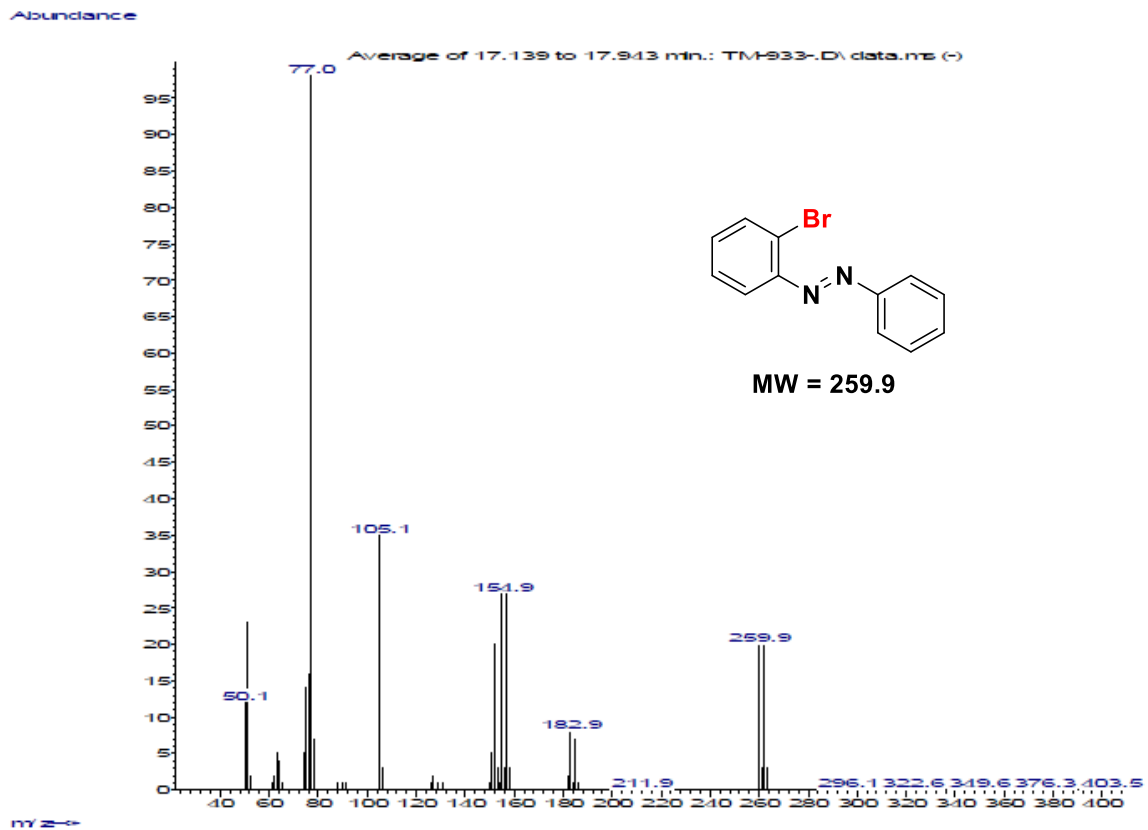
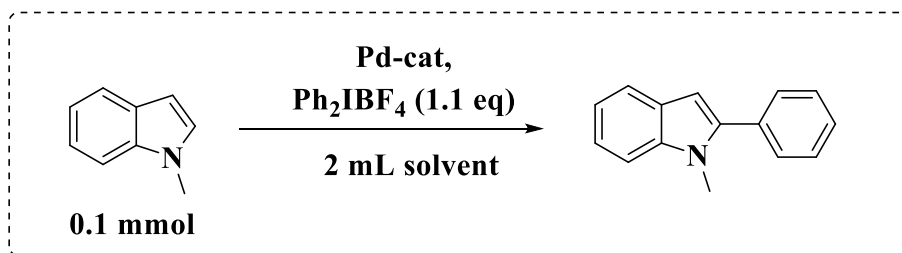


Figure S35. GCMS profile for the bromination of (E)-1,2-diphenyldiazene.

## XIV. Catalytic arylation:

### A. Heterogeneous C-H arylation of heteroarenes:



**Scheme S7:** Reaction optimization for arylation reaction using 1-methylindole as model substrate.

For C–H arylation of the heterocyclic compound, heteroarene (0.1 mmol) was placed in a pressure tube. Then diphenyliodonium tetrafluoroborate (0.11 mmol, 41.1 mg) was added. 5 mol % Pd catalyst was added to this. At last, 2 mL solvent was added and the pressure tube was capped tightly. The resulting solution was stirred at different temperatures for selected time intervals. After that, the reaction mixture was cooled and PhCl was added as an internal standard. Then 0.250 mL reaction mixture was taken, diluted with ethyl acetate, and injected into GC for yield calculation. The products were further verified by GCMS analysis. When the reaction was completed, it was allowed to cool to room temperature. Catalysts were separated and products were purified by column chromatography. <sup>1</sup>H NMR spectra were recorded for the compounds.

### Reaction optimization:

Entry	Solvent	Temperature (°C)	Time (h)	Yield (%)	Reactant Conversion (%)	Side product formation (%)
1	EtOH	100	12	65 %	100 %	10 %
2	THF	100	12	90 %	100 %	4 %
3	H <sub>2</sub> O	100	12	80 %	90 %	1 %
4	THF	65	6	60 %	75 %	4 %
5	H <sub>2</sub> O	65	6	45 %	50 %	1 %
6	DCE	65	6	75 %	85 %	4 %
7	ACN	65	6	15 %	25 %	10 %
8	TOLUENE	65	6	30 %	40 %	6 %

<sup>1</sup>H NMR data of the arylated products of heteroarenes:

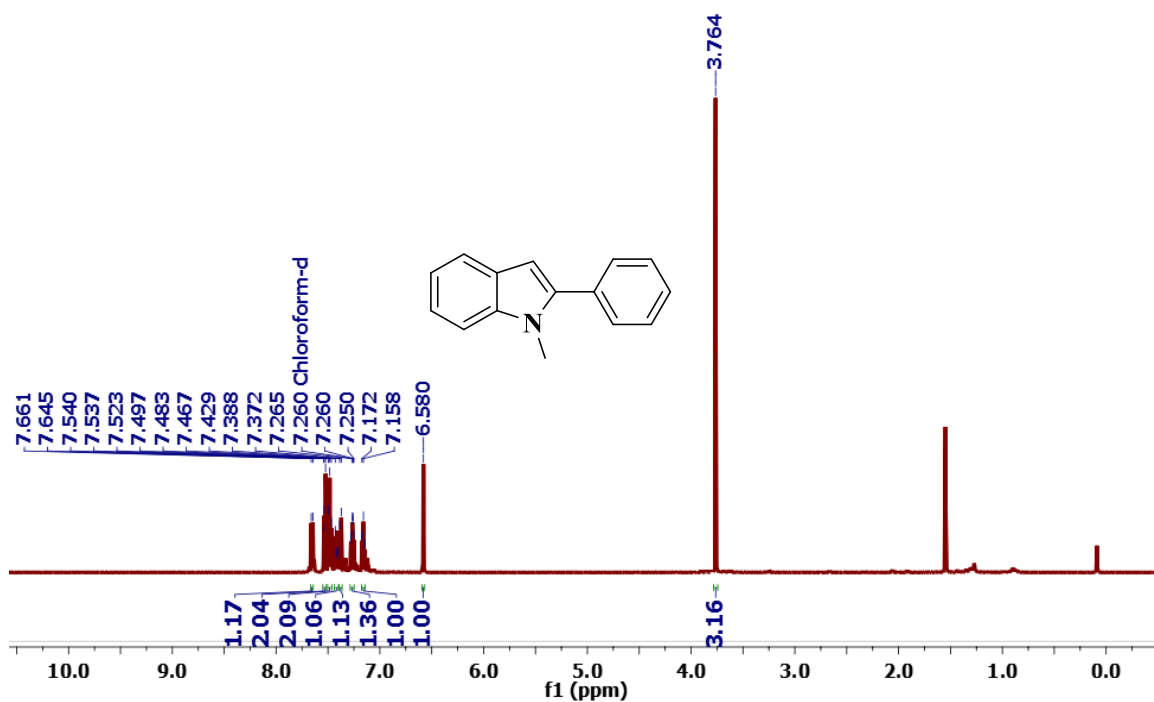


Figure S36. <sup>1</sup>H NMR spectra of 1-methyl-2-phenyl-1H-indole (500 MHz, CDCl<sub>3</sub>).

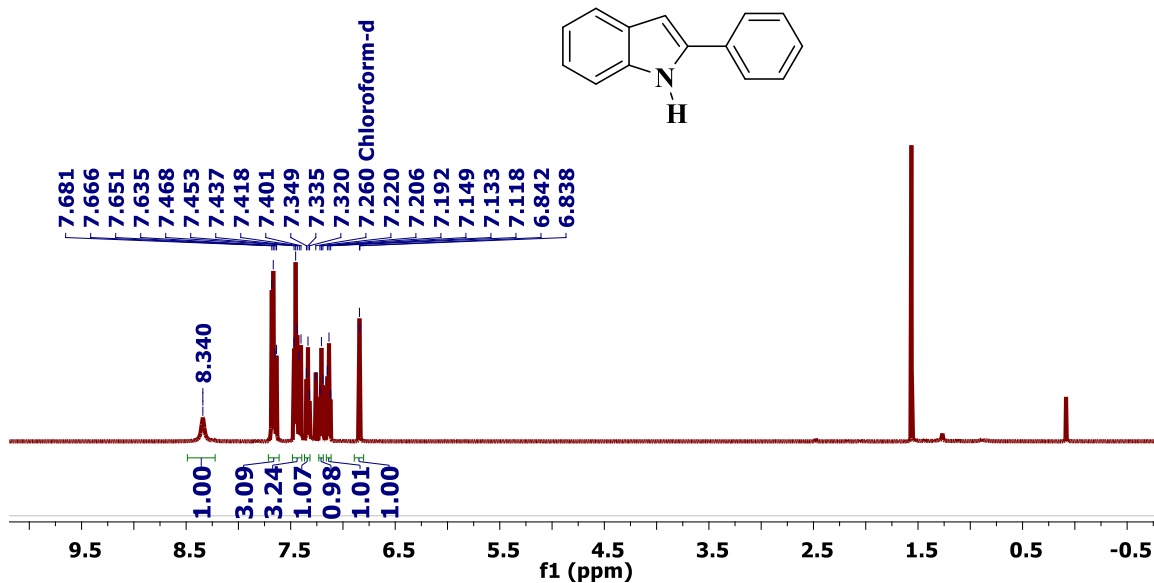


Figure S37. <sup>1</sup>H NMR spectra of 2-phenyl-1H-indole (500 MHz, CDCl<sub>3</sub>).

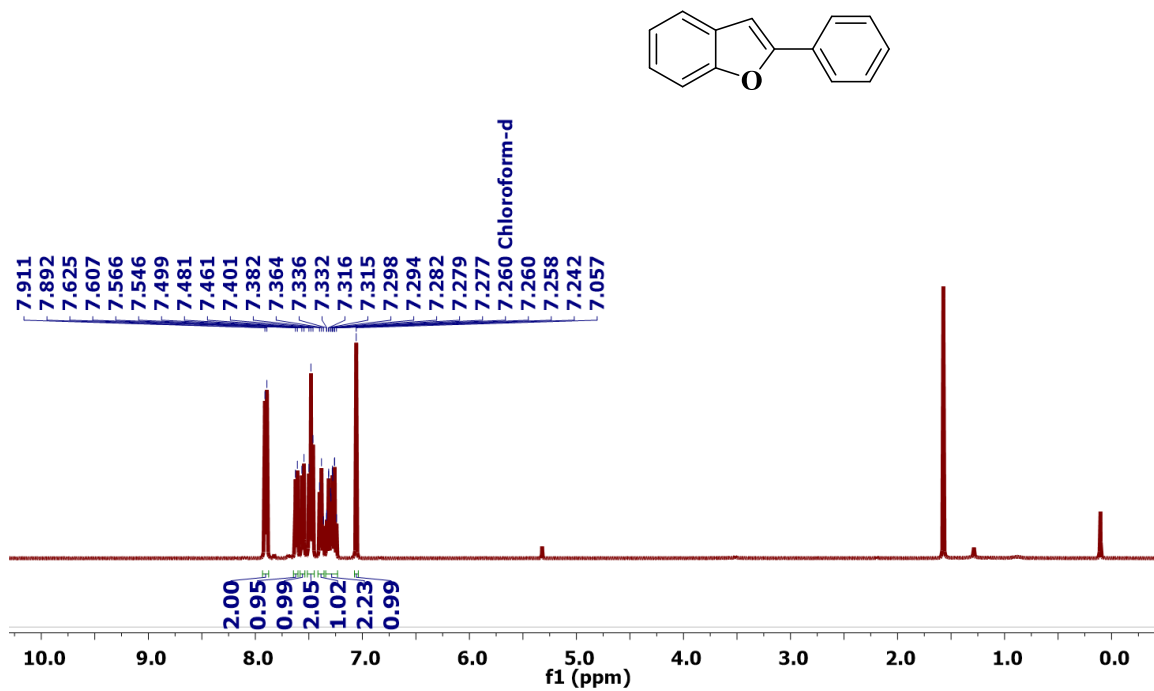


Figure S38.  $^1\text{H}$  NMR spectra of 2-phenylbenzofuran (500 MHz,  $\text{CDCl}_3$ ).

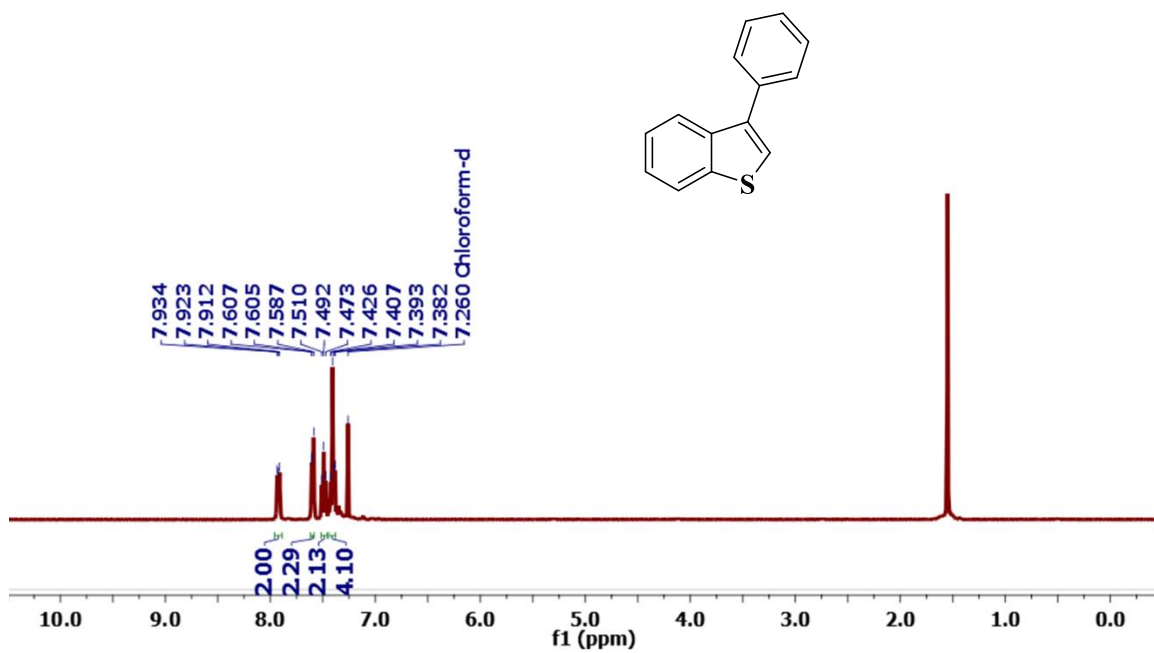


Figure S39.  $^1\text{H}$  NMR spectra of 3-phenylbenzo[b]thiophene (500 MHz,  $\text{CDCl}_3$ ).



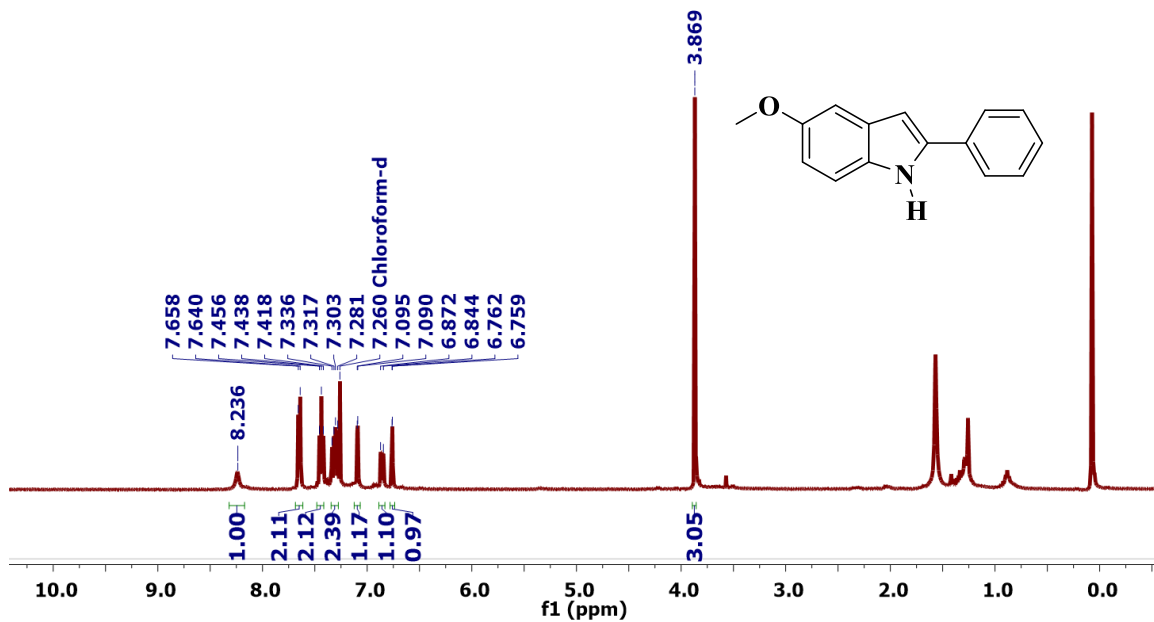


Figure S40. <sup>1</sup>H NMR spectra of 5-methoxy-2-phenyl-1H-indole (500 MHz, CDCl<sub>3</sub>).

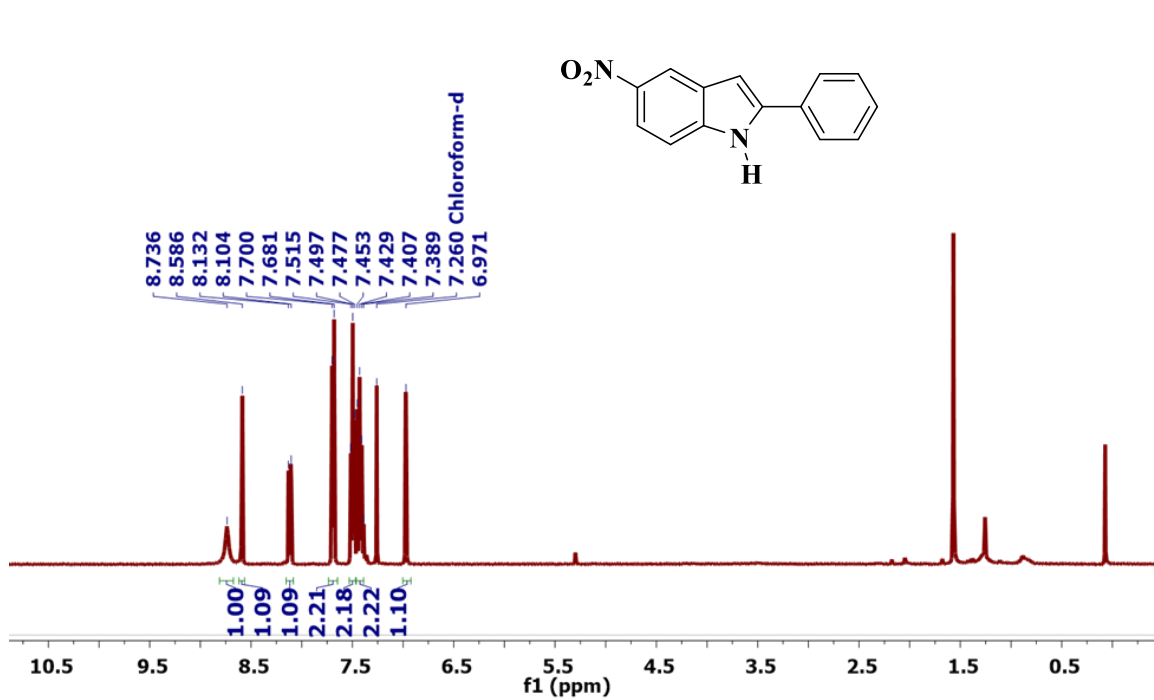


Figure S41. <sup>1</sup>H NMR spectra of 5-nitro-2-phenyl-1H-indole (500 MHz, CDCl<sub>3</sub>).

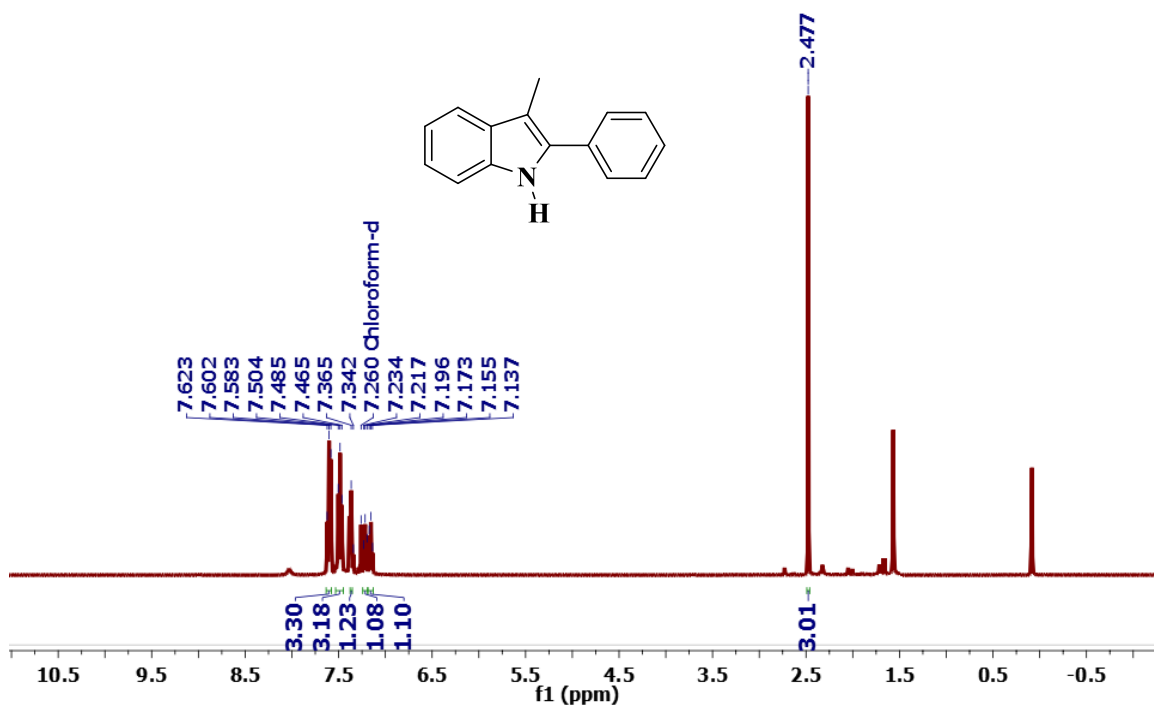


Figure S42. <sup>1</sup>H NMR spectra of 3-methyl-2-phenyl-1H-indole (500 MHz, CDCl<sub>3</sub>).

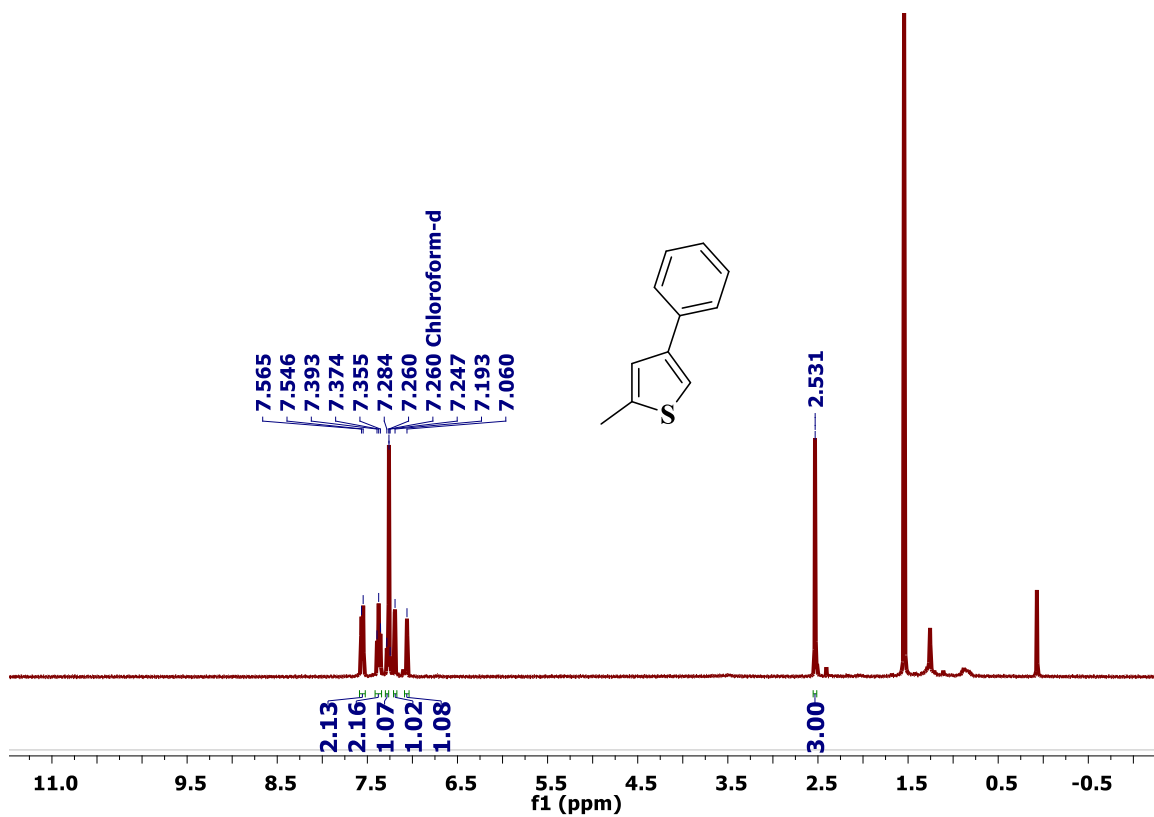
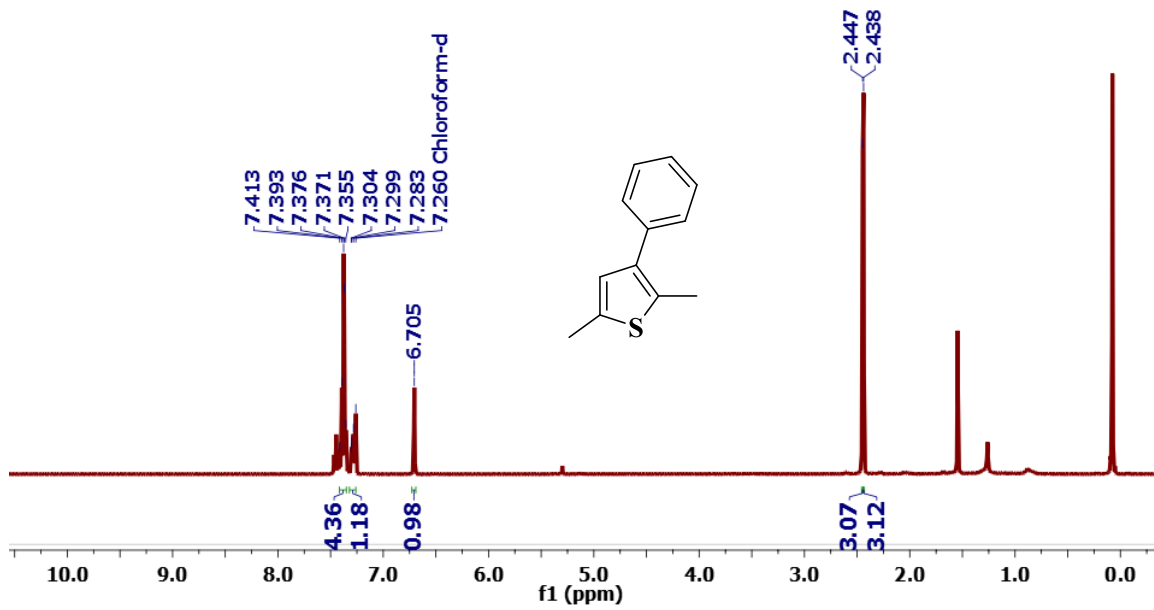


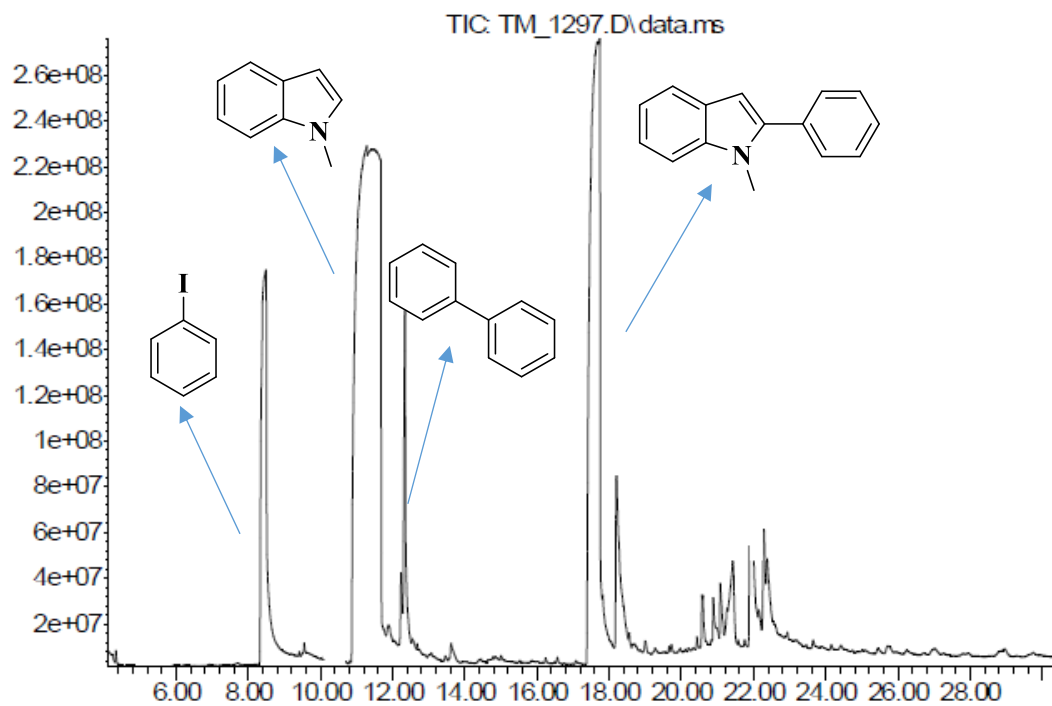
Figure S43. <sup>1</sup>H NMR spectra of 2-methyl-4-phenylthiophene (500 MHz, CDCl<sub>3</sub>).



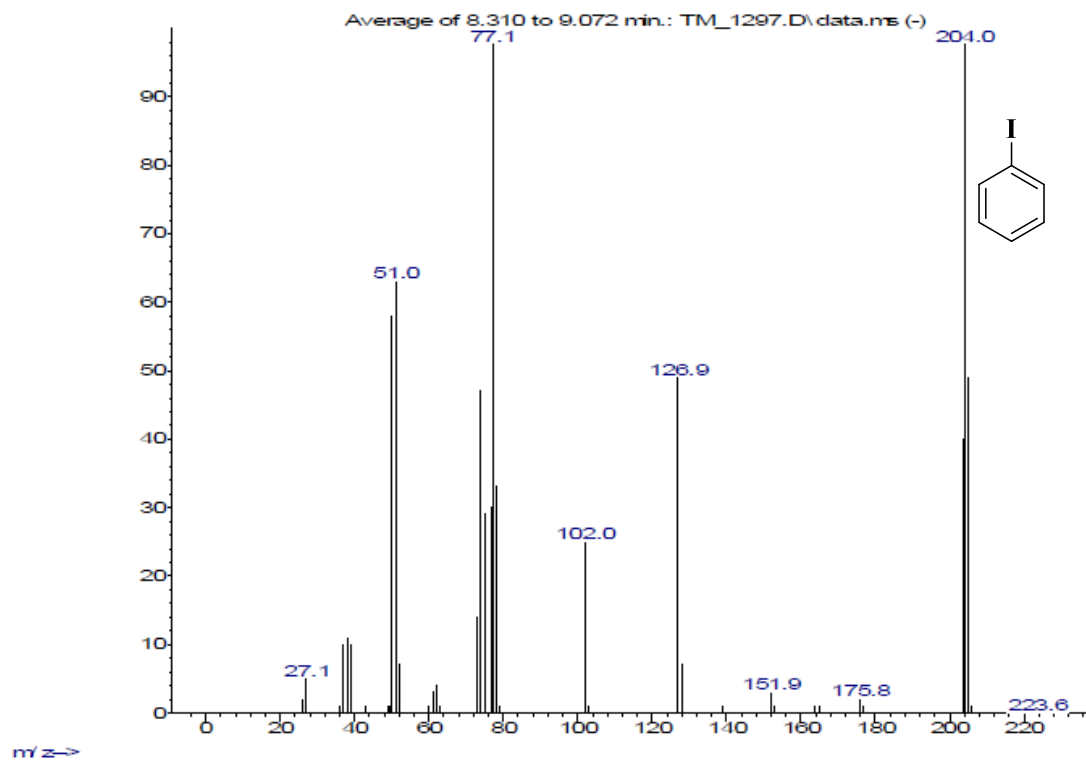
**Figure S44.**  $^1\text{H}$  NMR spectra of 2,5-dimethyl-3-phenylthiophene (500 MHz,  $\text{CDCl}_3$ ).

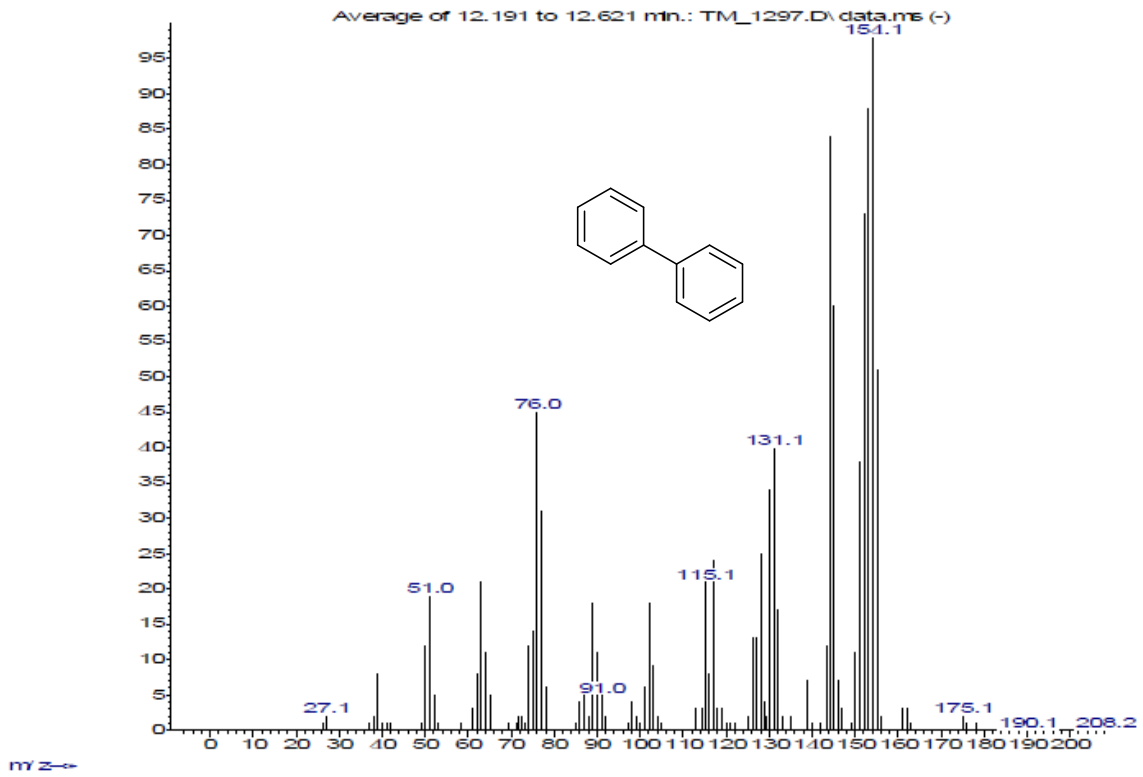
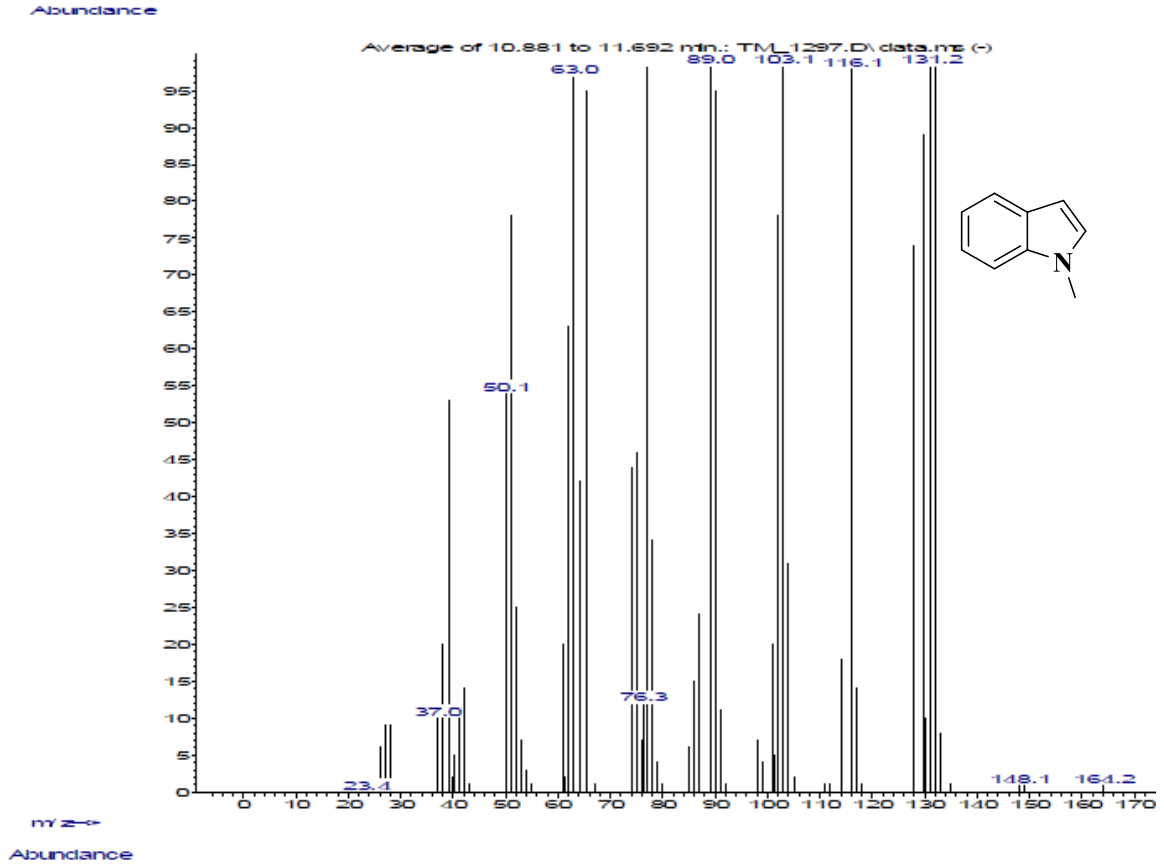
- GC-MS profile for the arylation reaction of heteroarenes:

Abundance



Time >





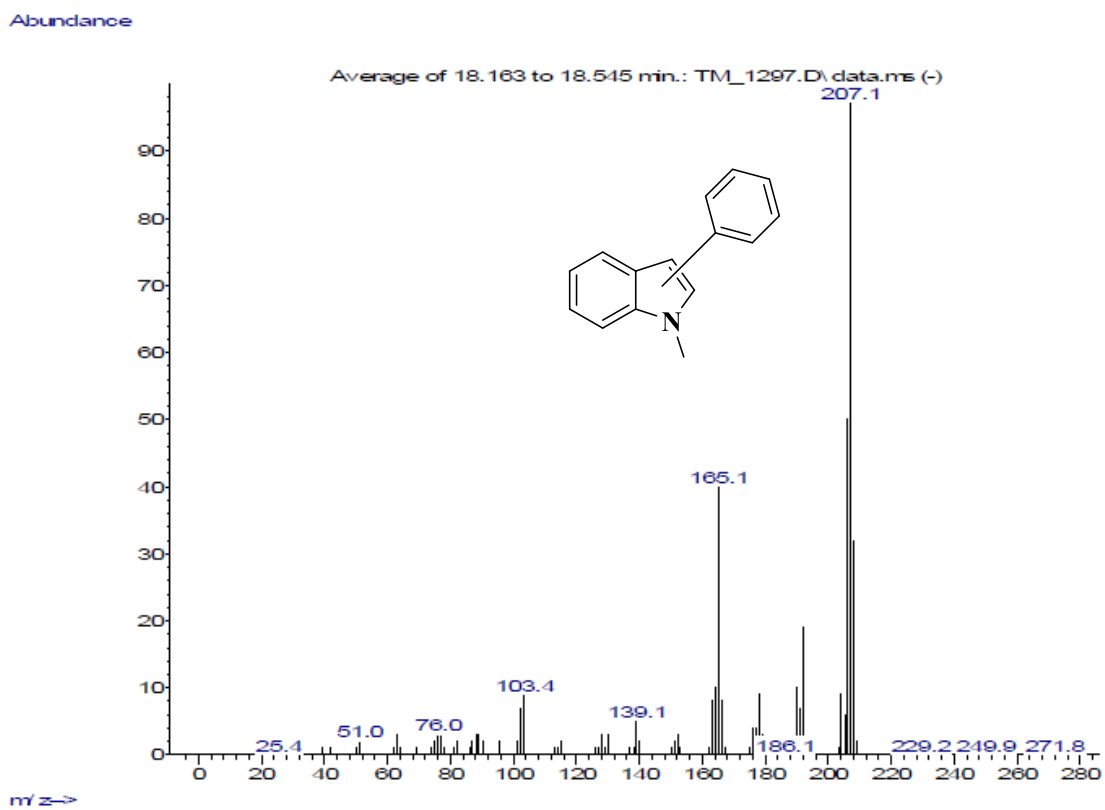
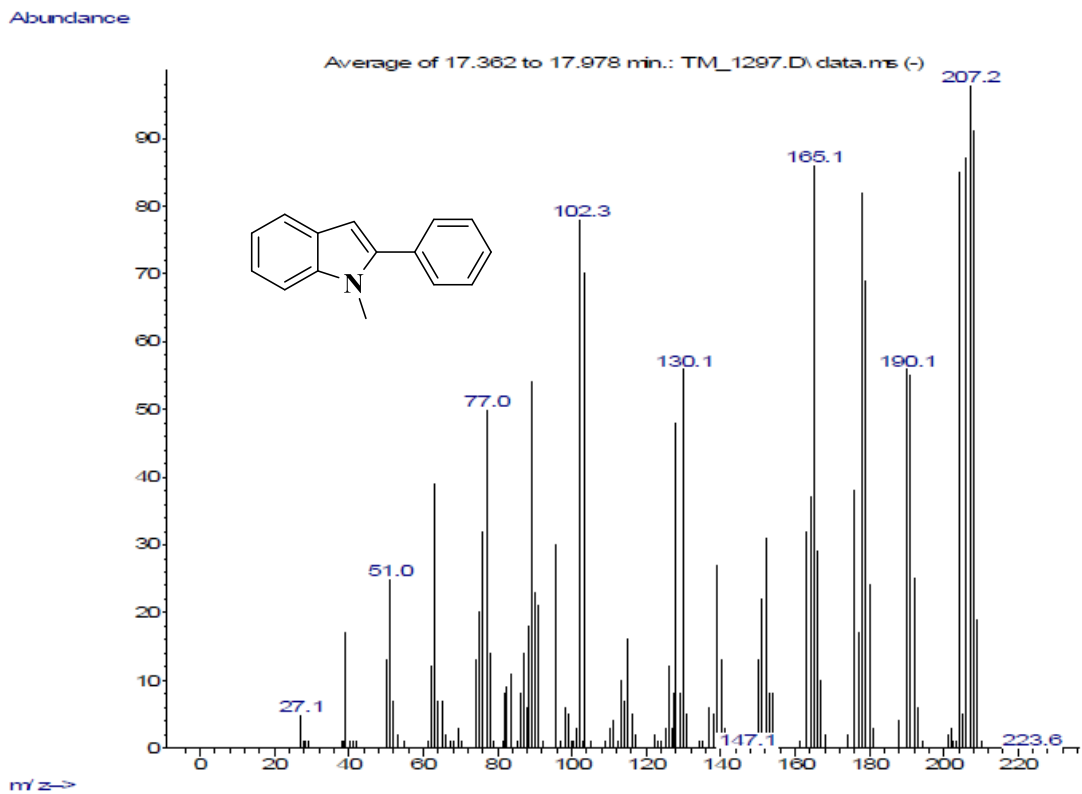
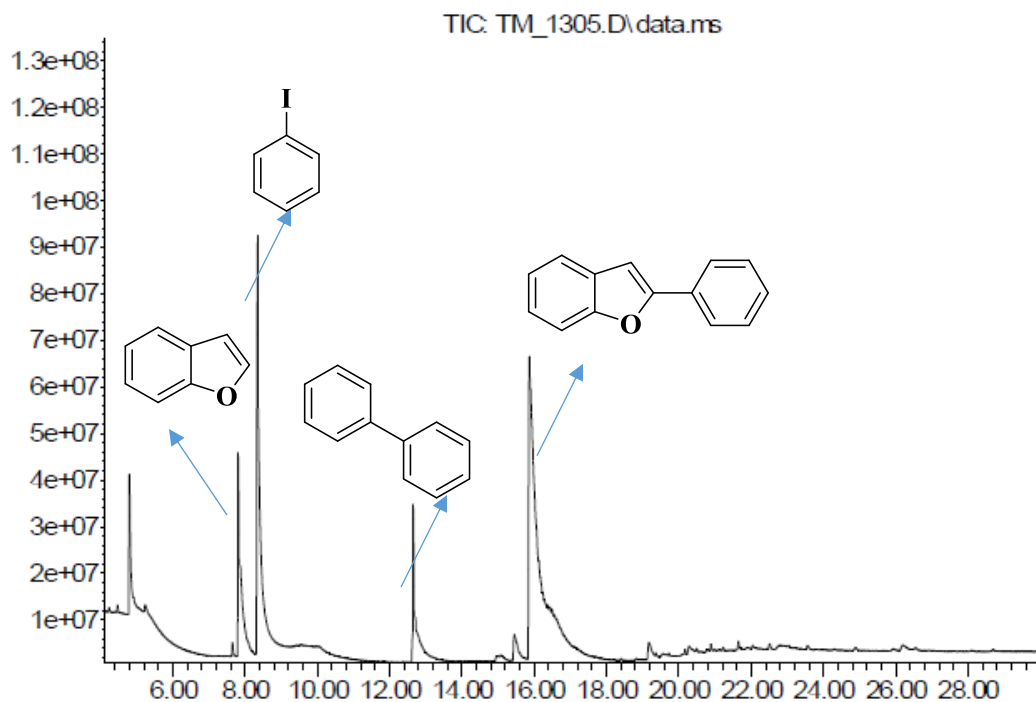
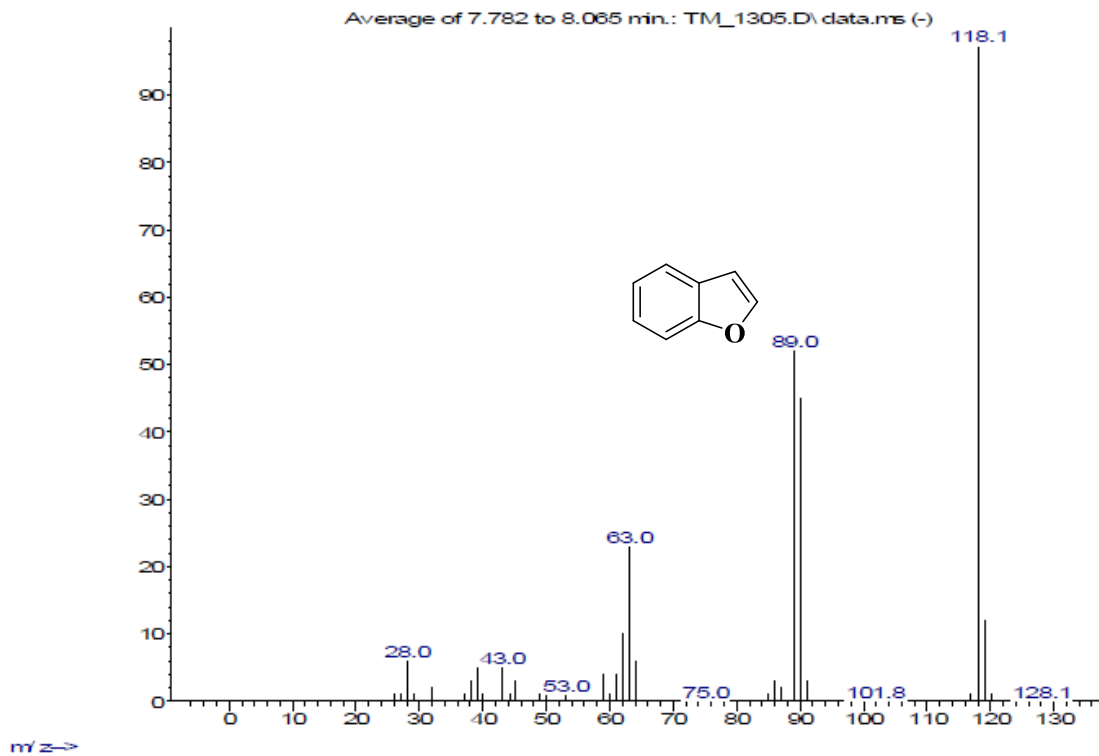


Figure S45. GCMS profile for the arylation of N methyl indole.

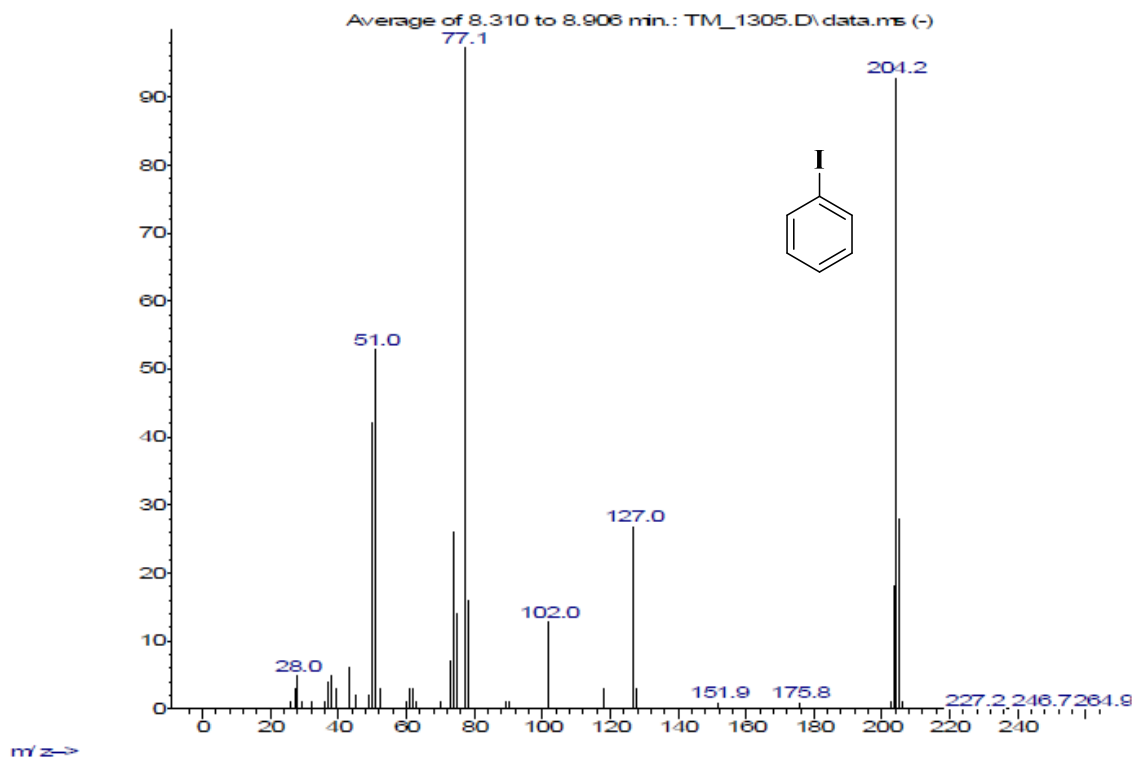
Abundance



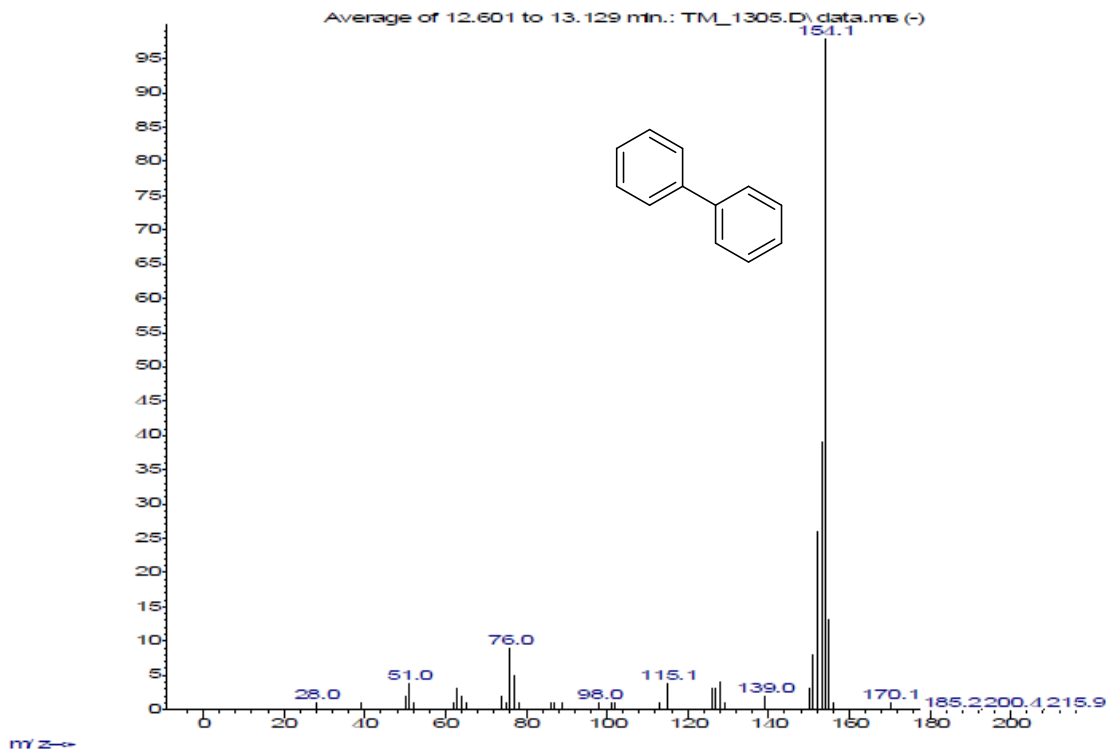
Abundance



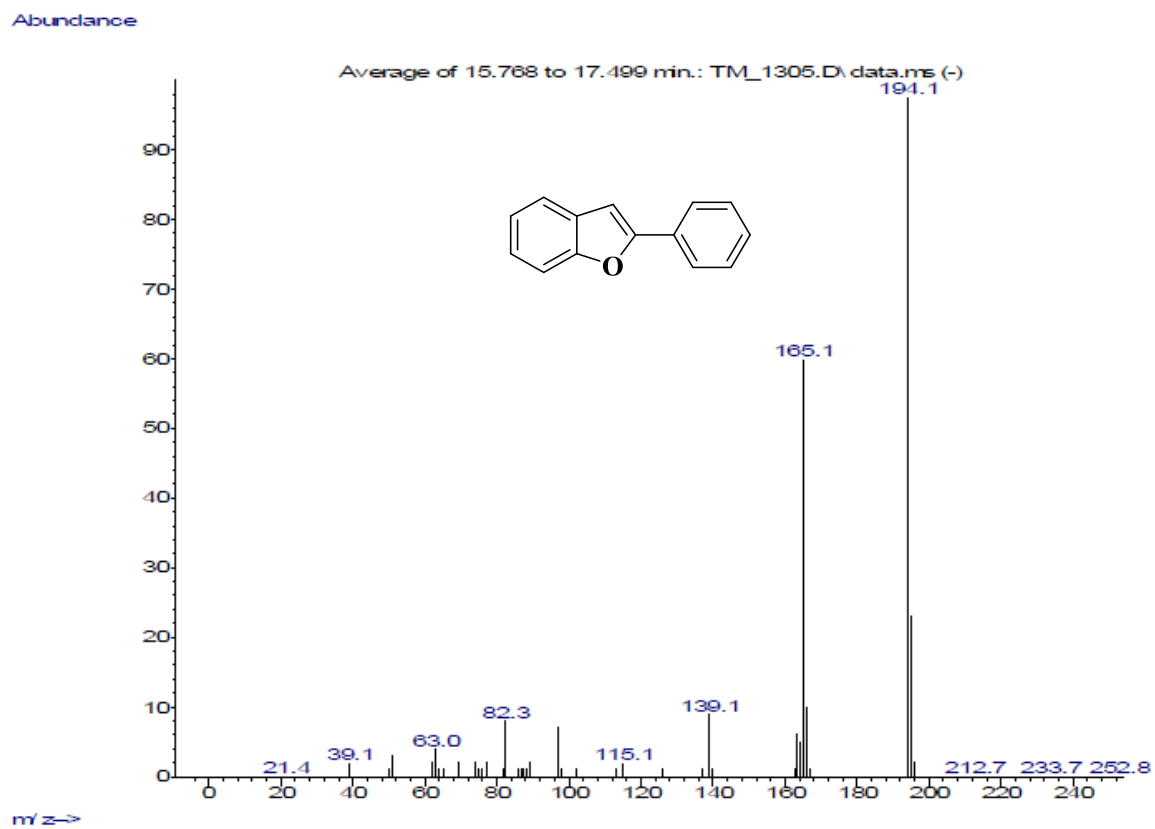
Abundance



Abundance

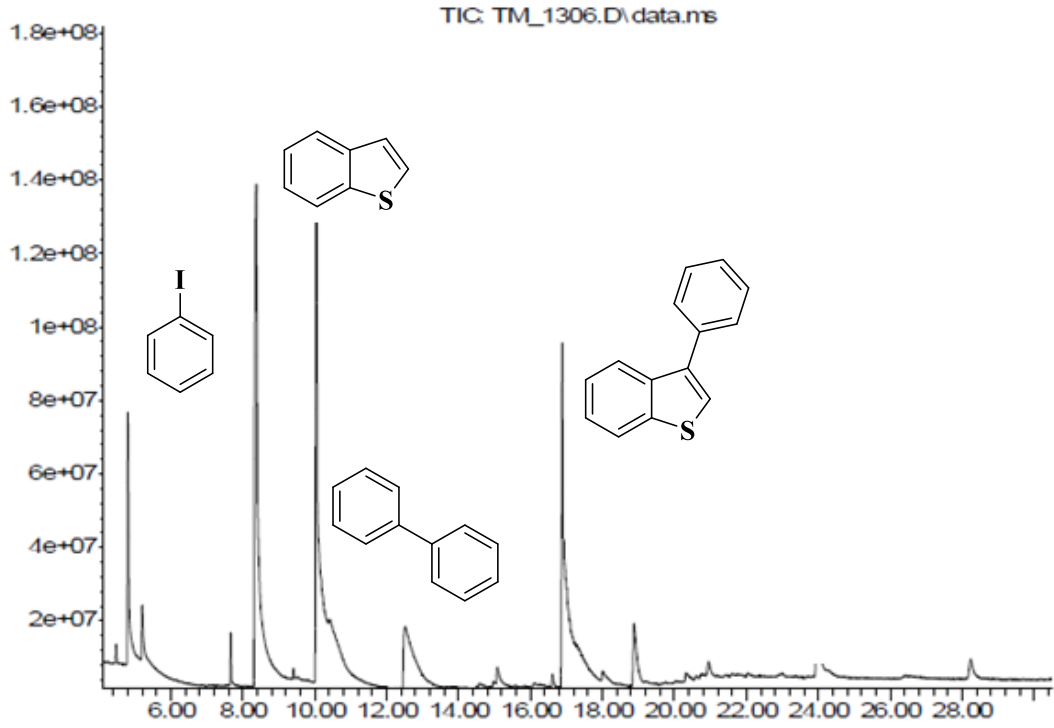




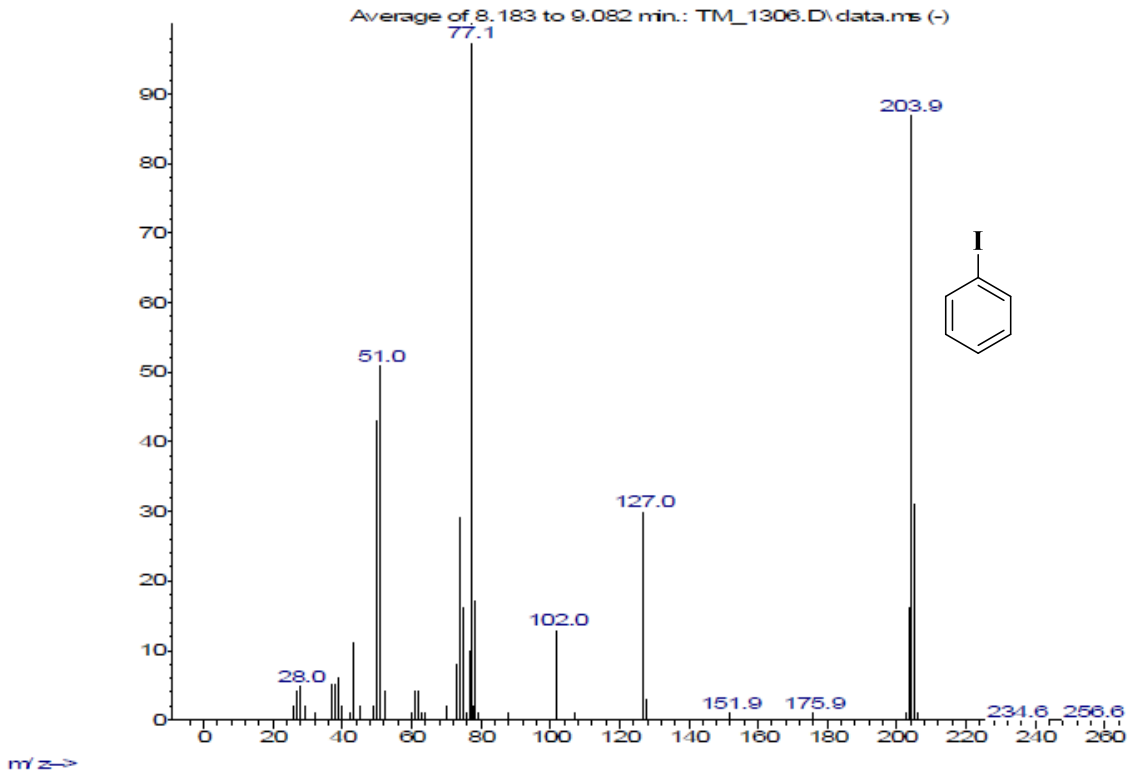


**Figure S46.** GCMS profile for the arylation of benzofuran.

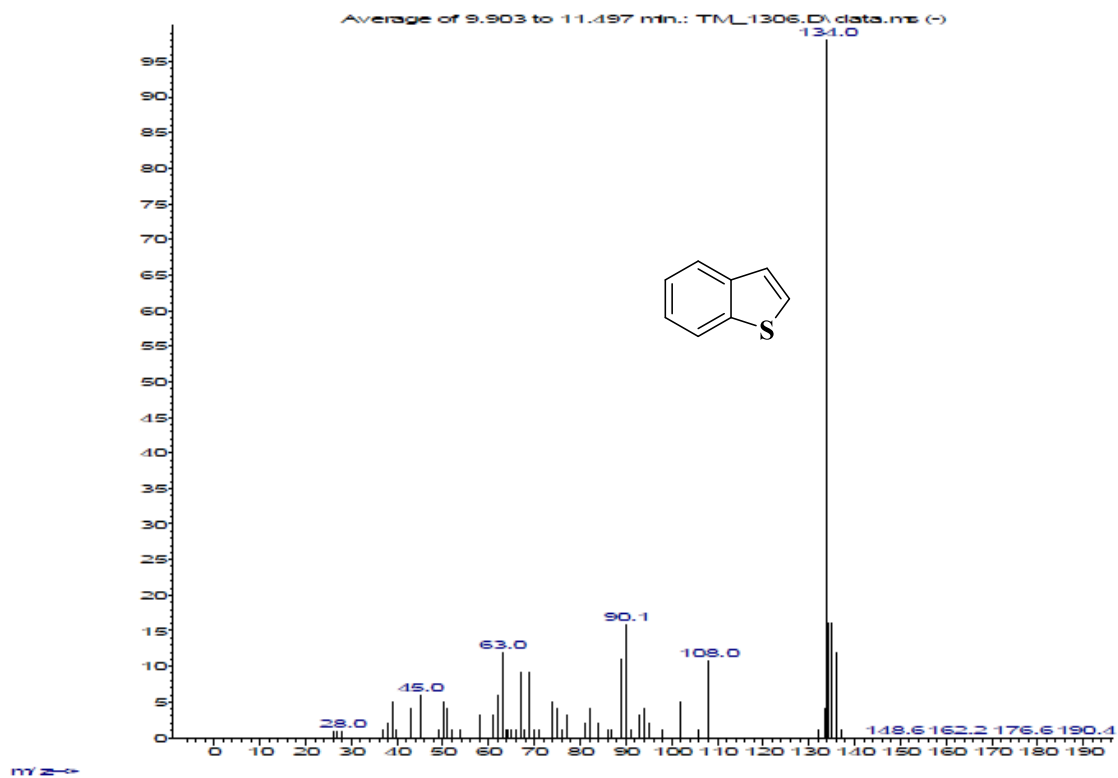
Abundance



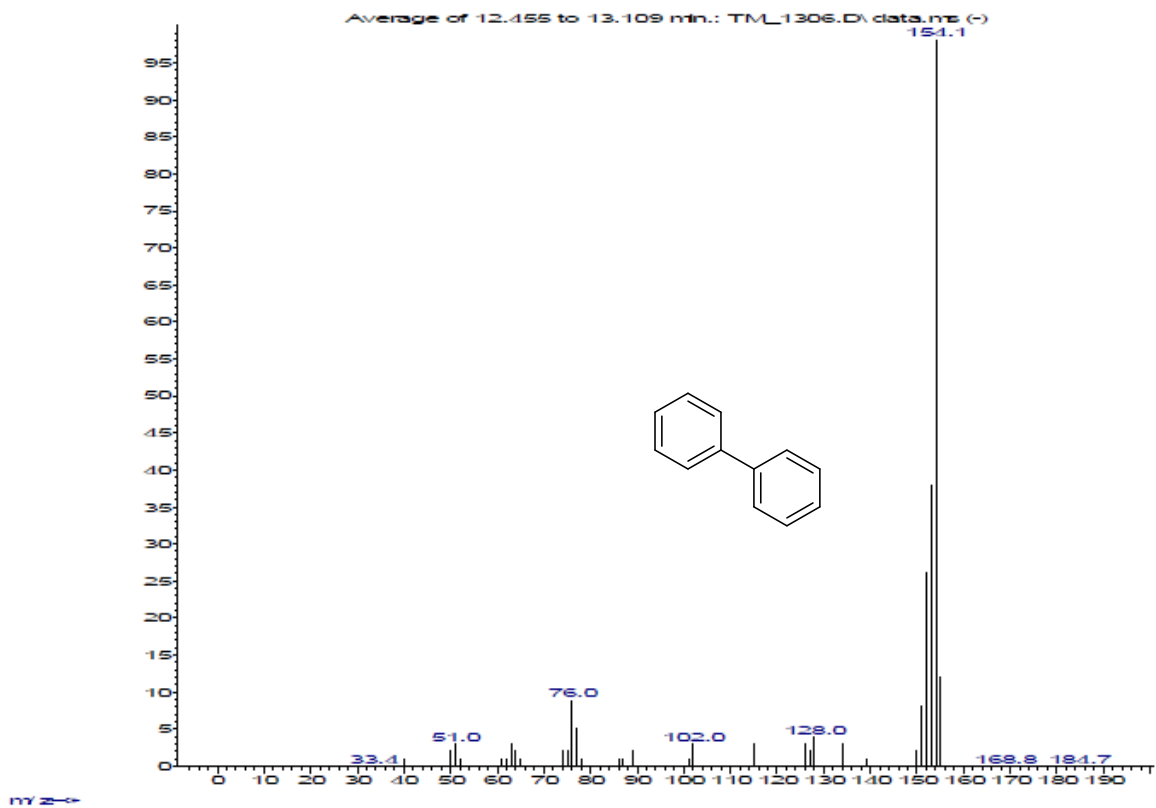
Abundance



Abundance



Abundance



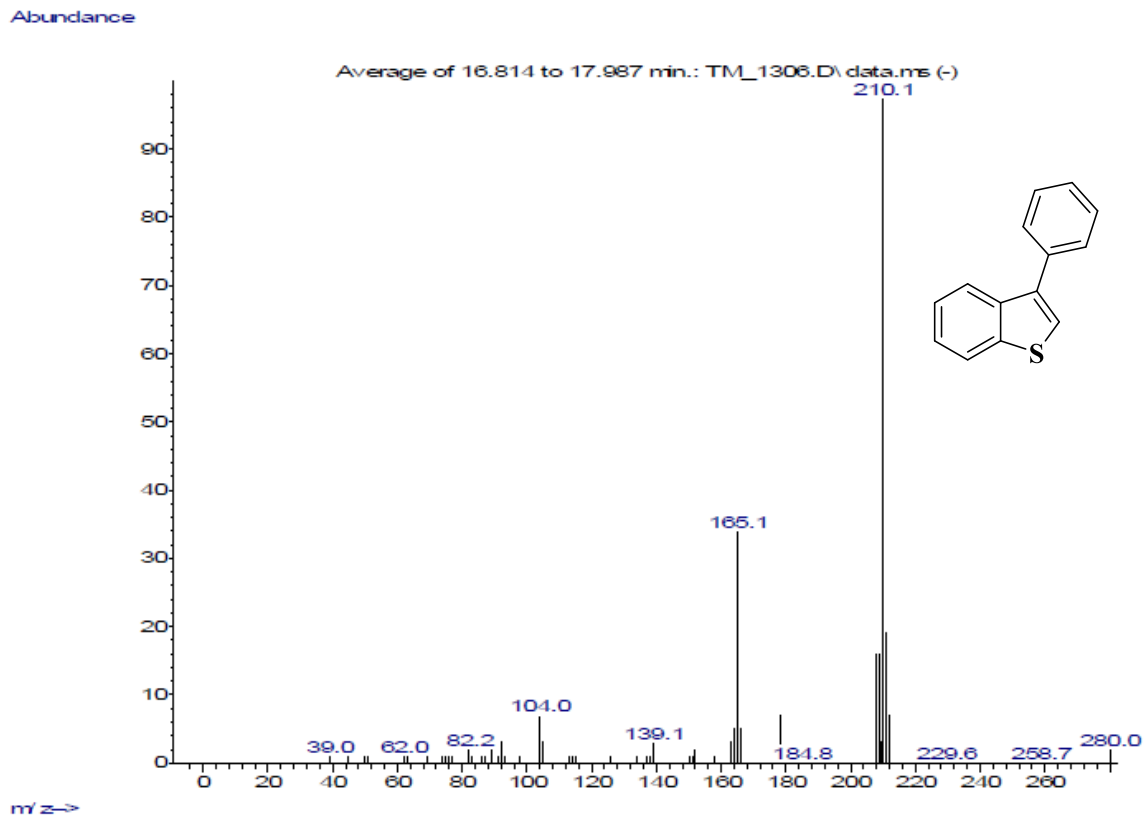
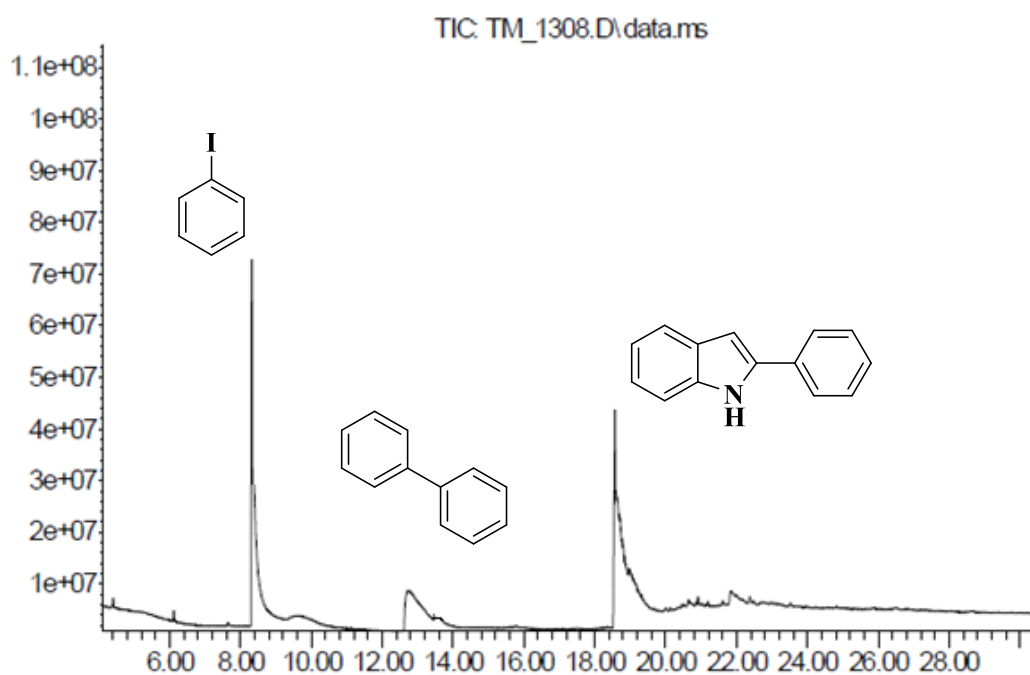
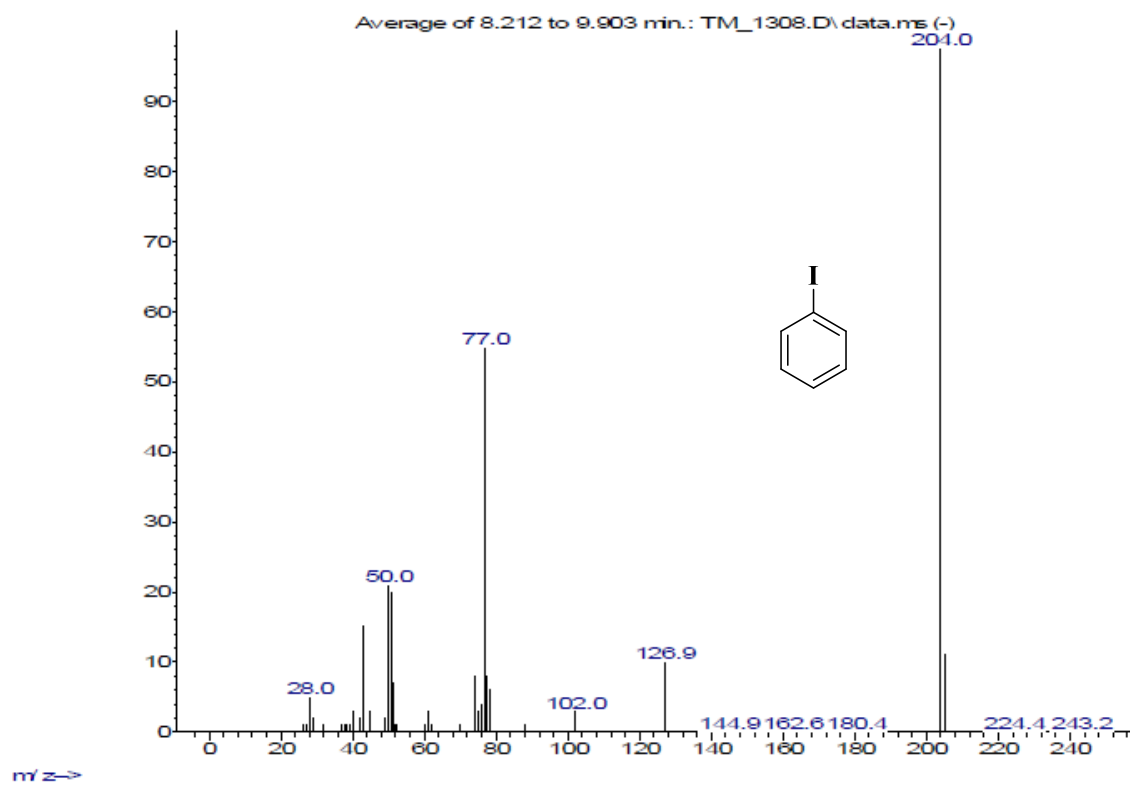


Figure S47. GCMS profile for the arylation of benzothiophene.

Abundance



Time→



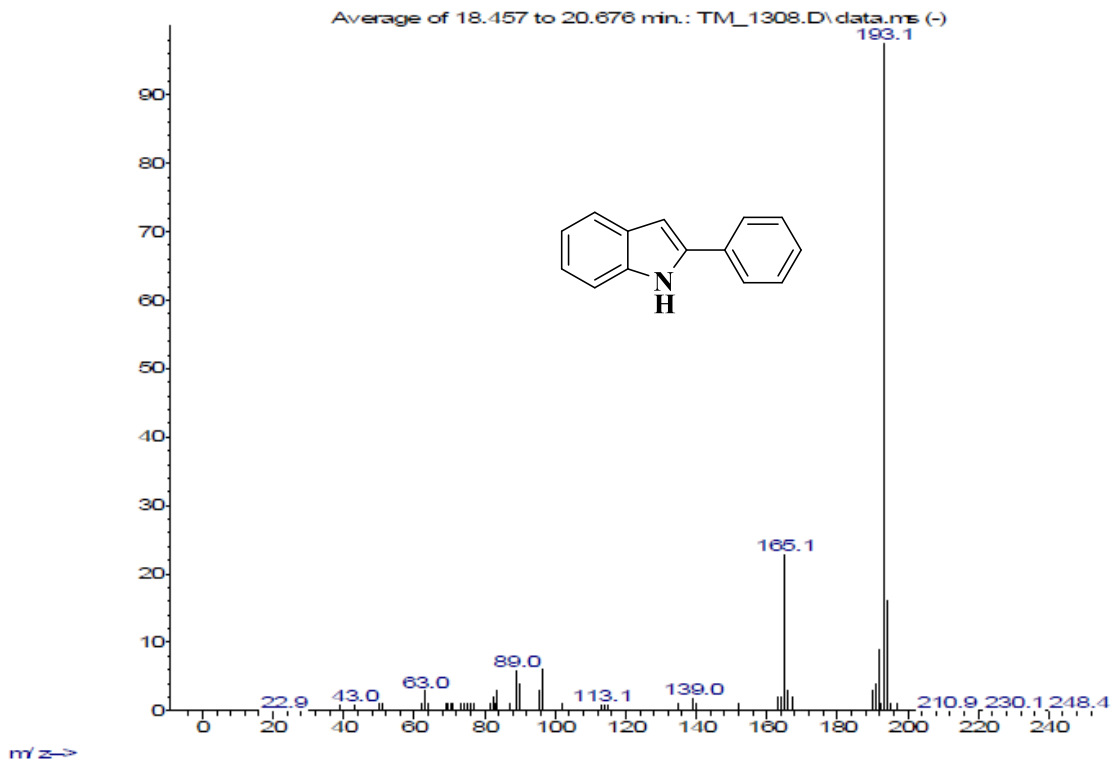
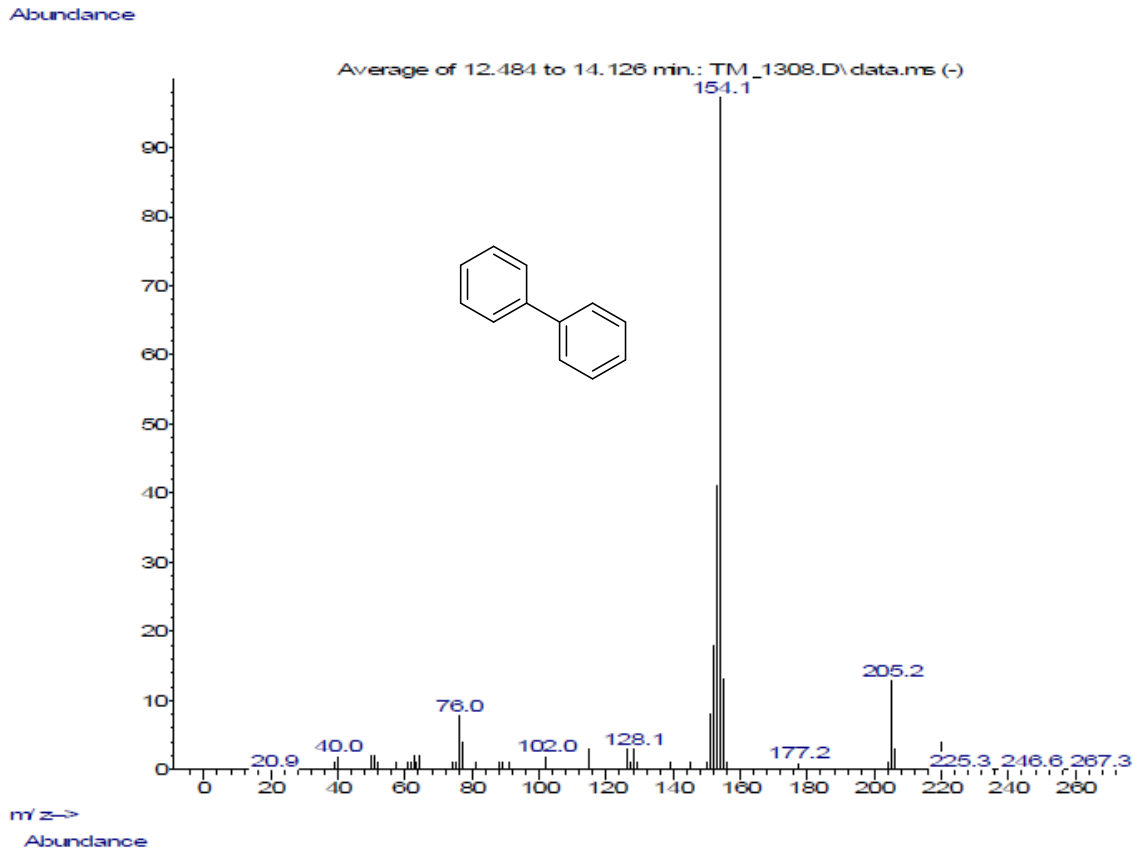
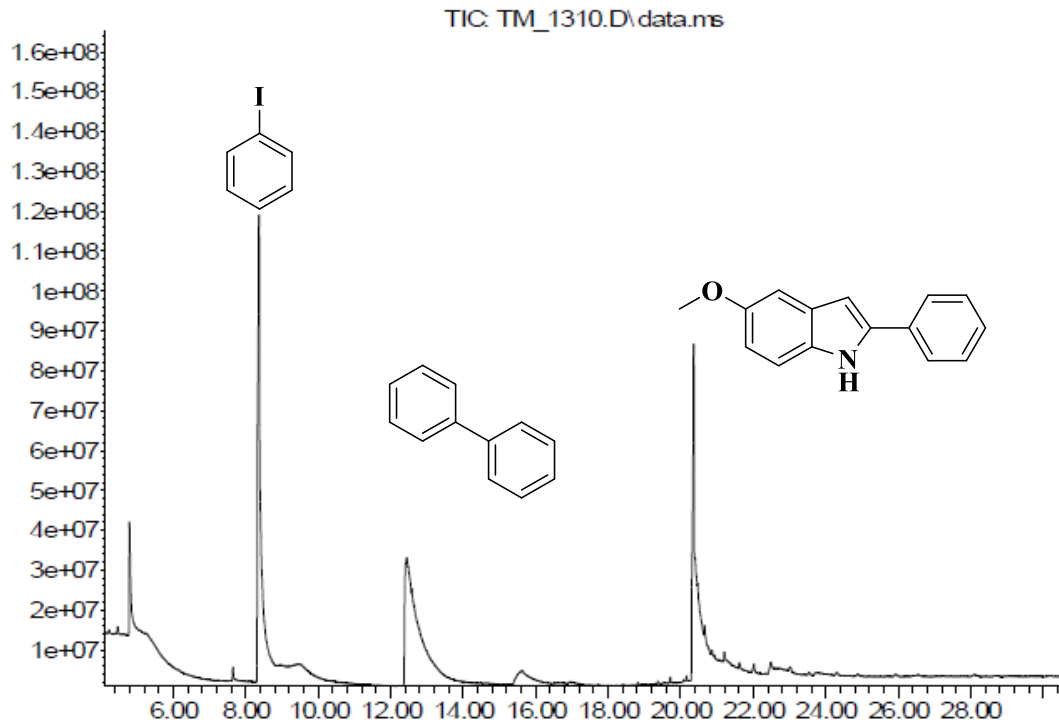
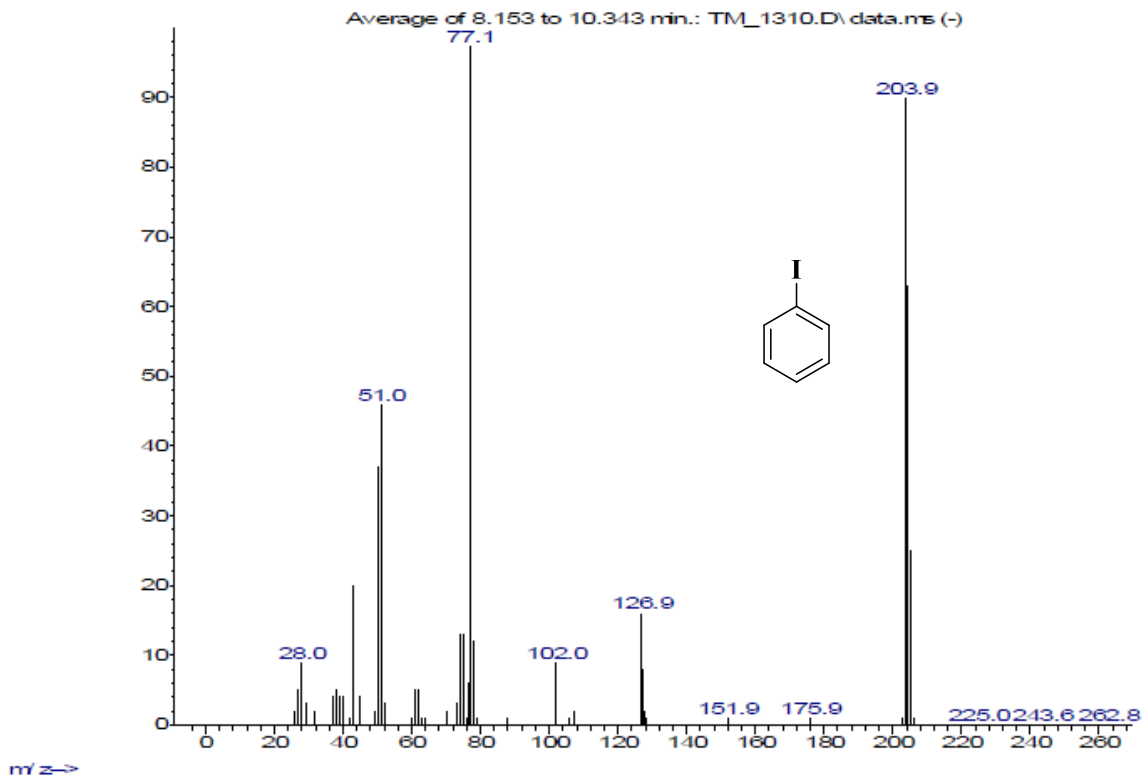


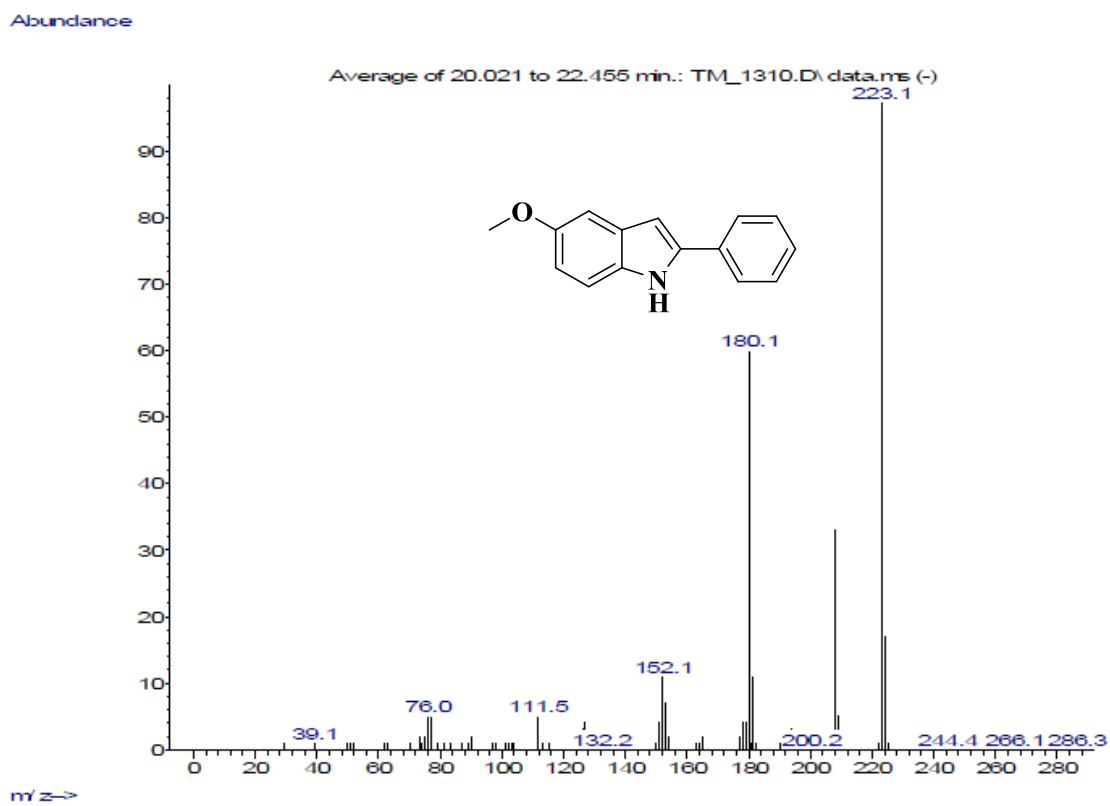
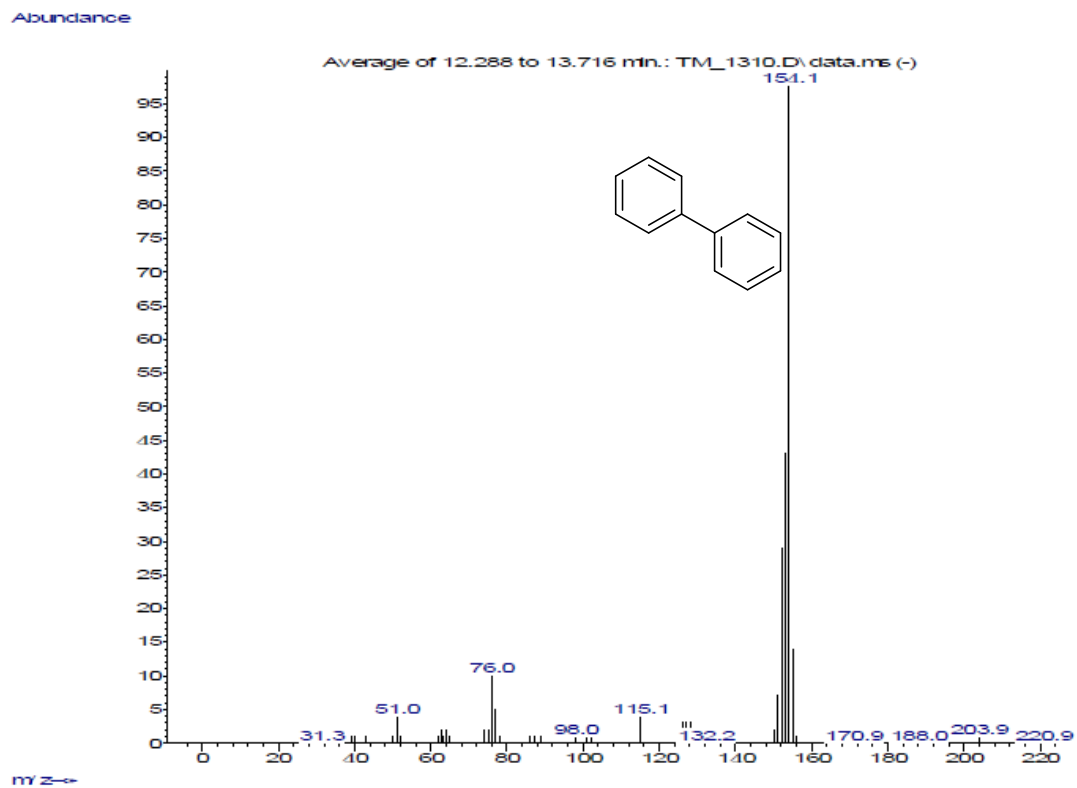
Figure S48. GCMS profile for the arylation of indole.

Abundance



Abundance

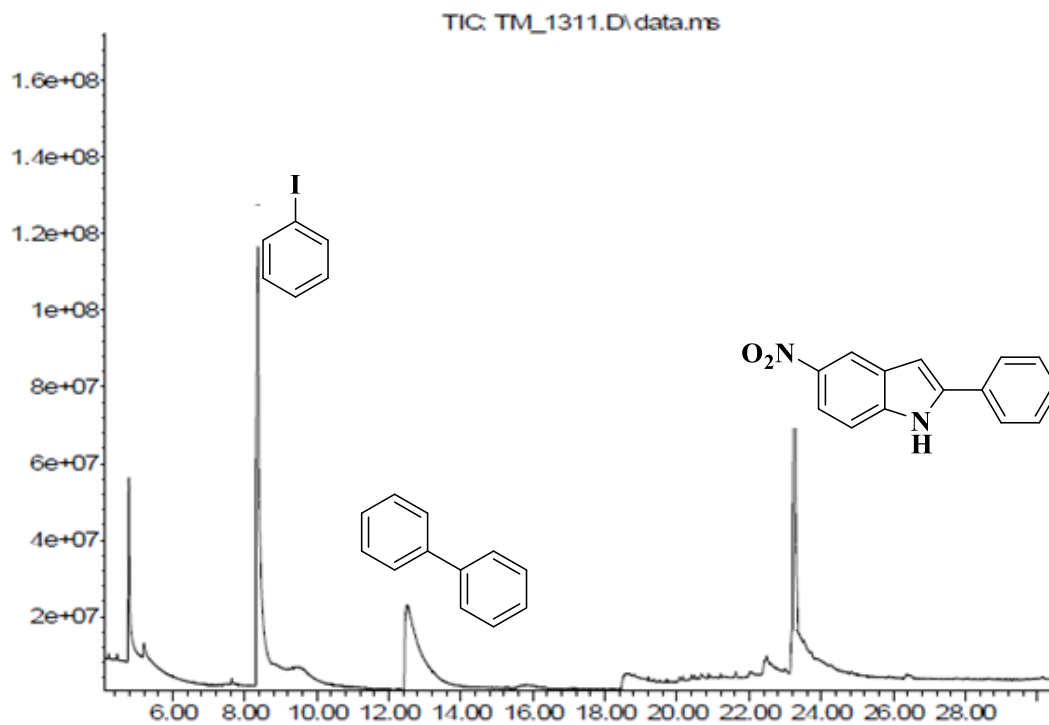




**Figure S49.** GCMS profile for the arylation of 5-methoxyindole.

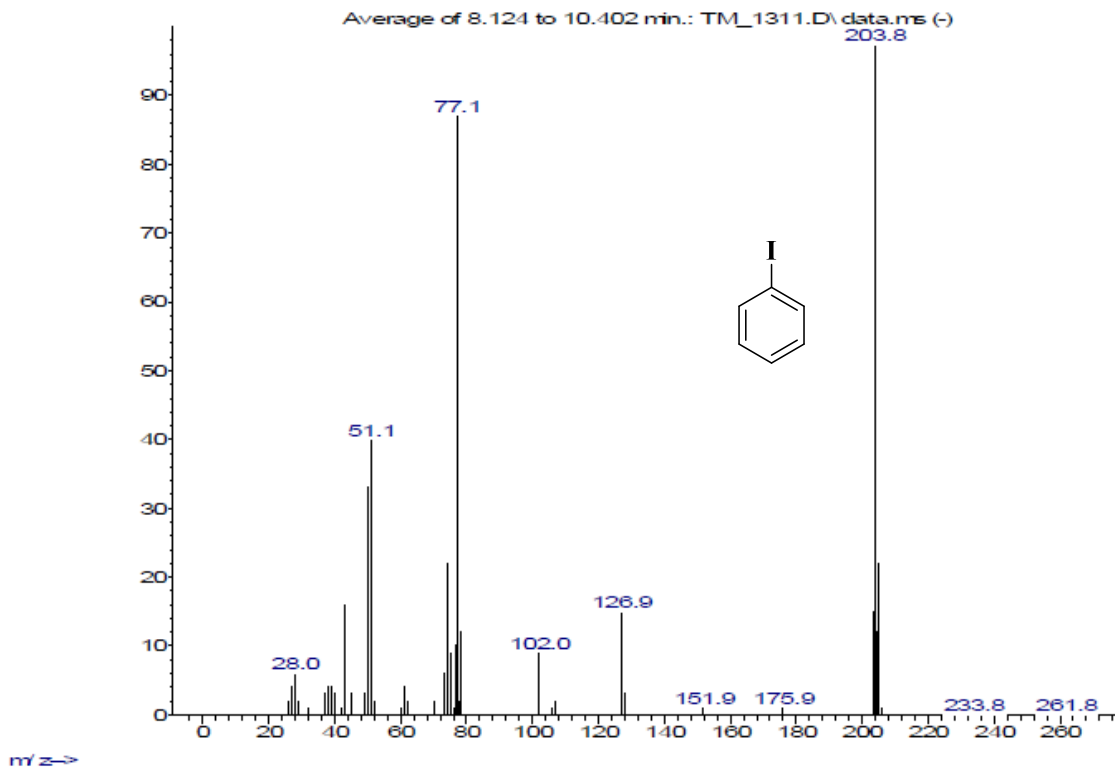


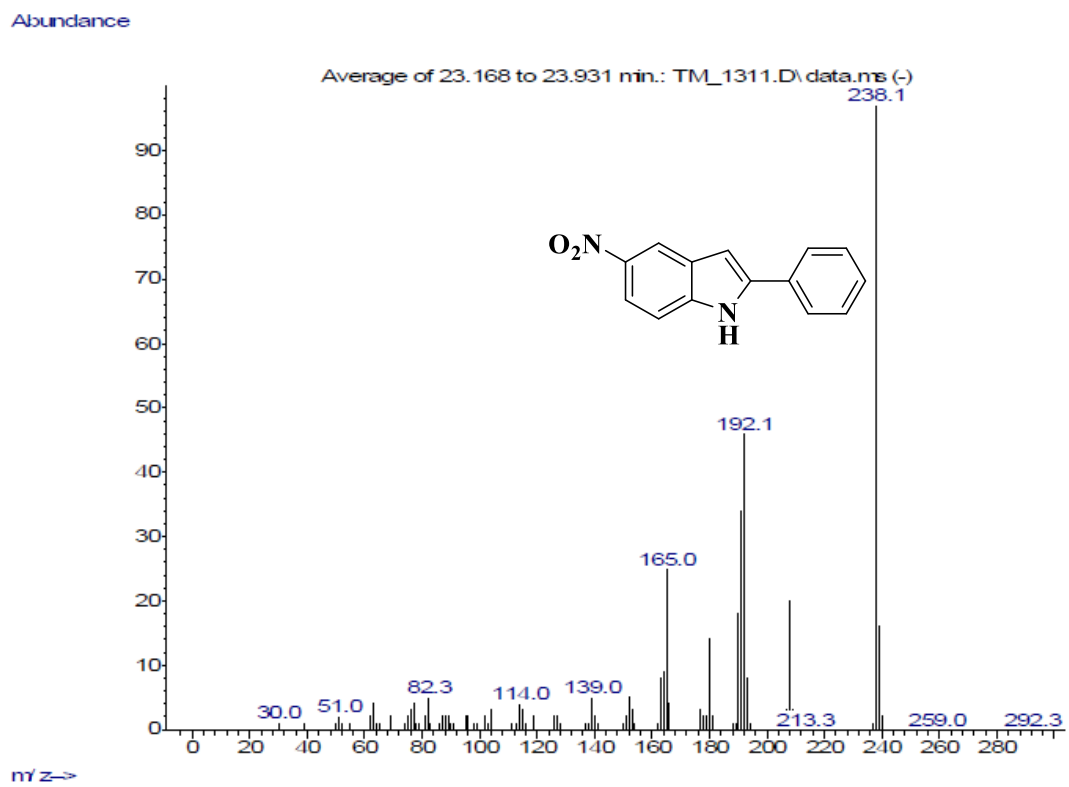
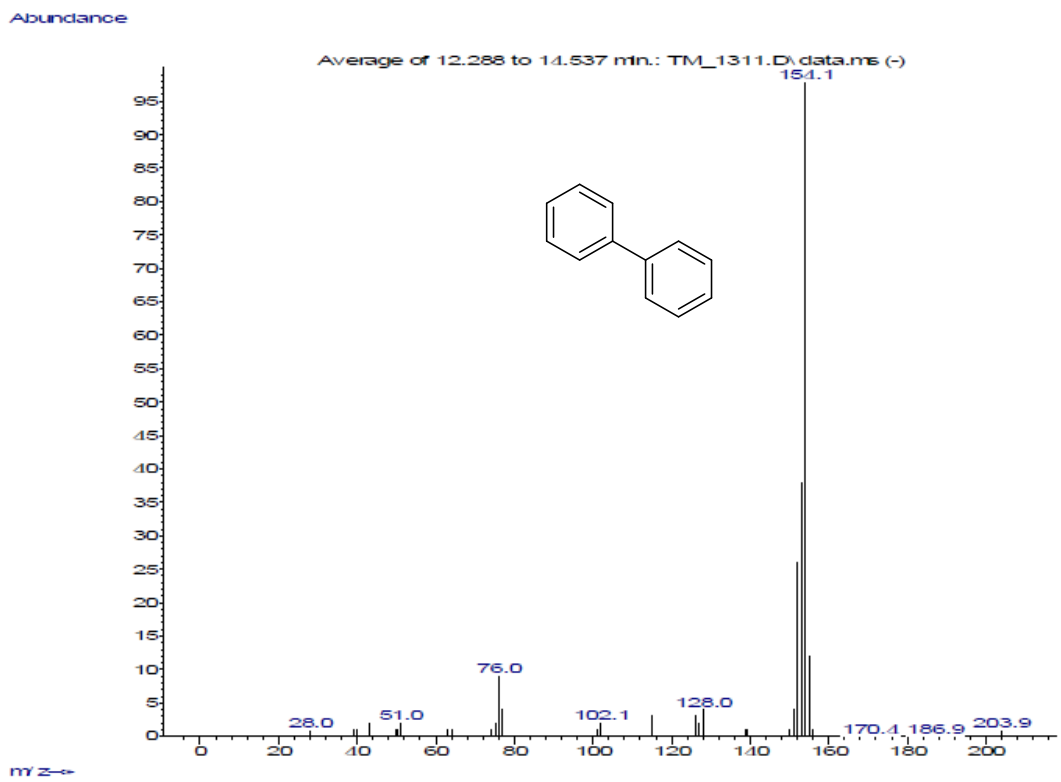
Abundance



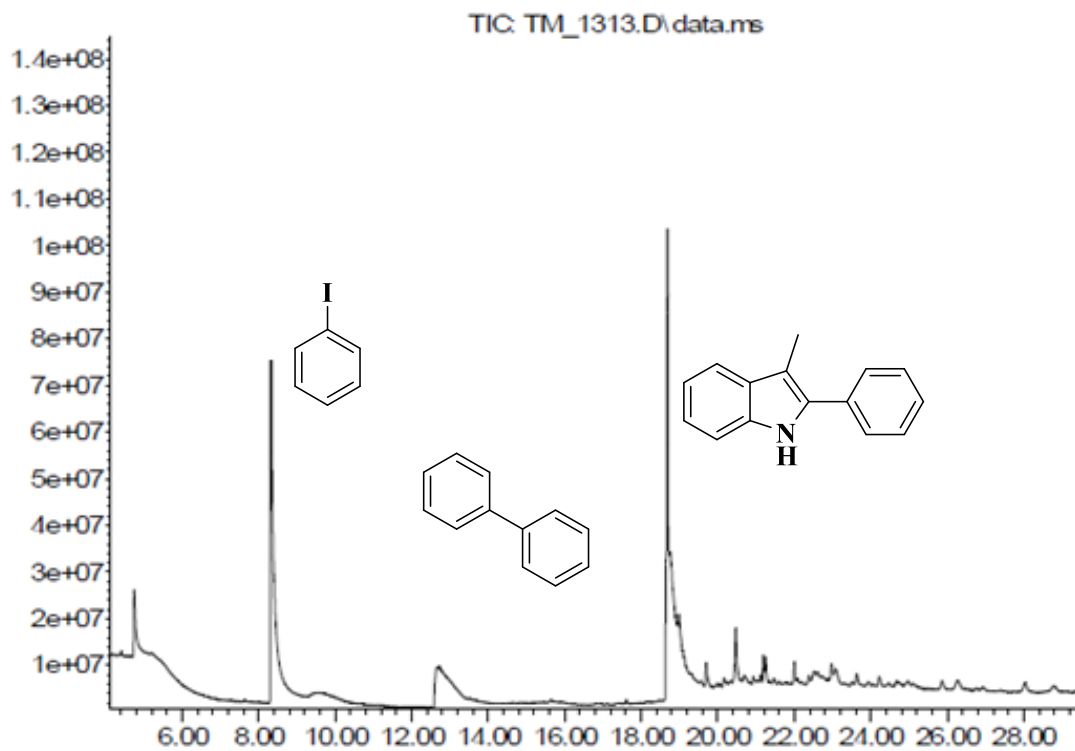
Time →

Abundance

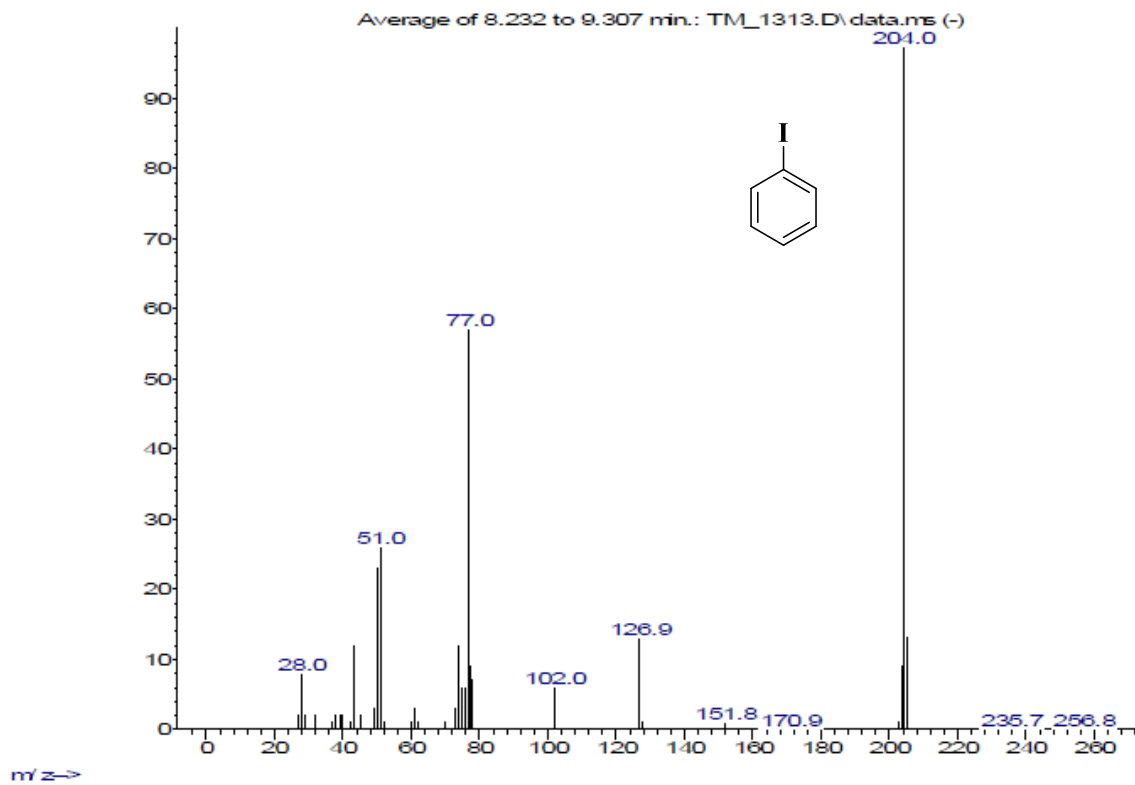




**Figure S50.** GCMS profile for the arylation of 5-nitroindole.



Time→



m/z→

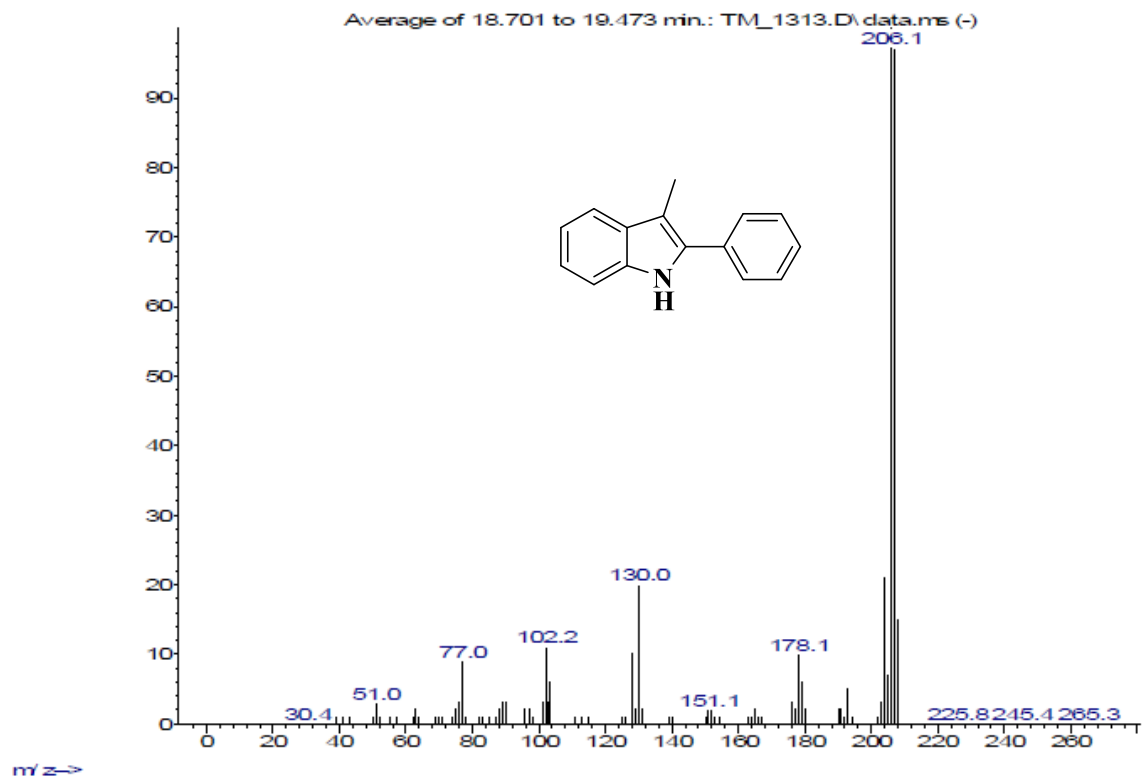
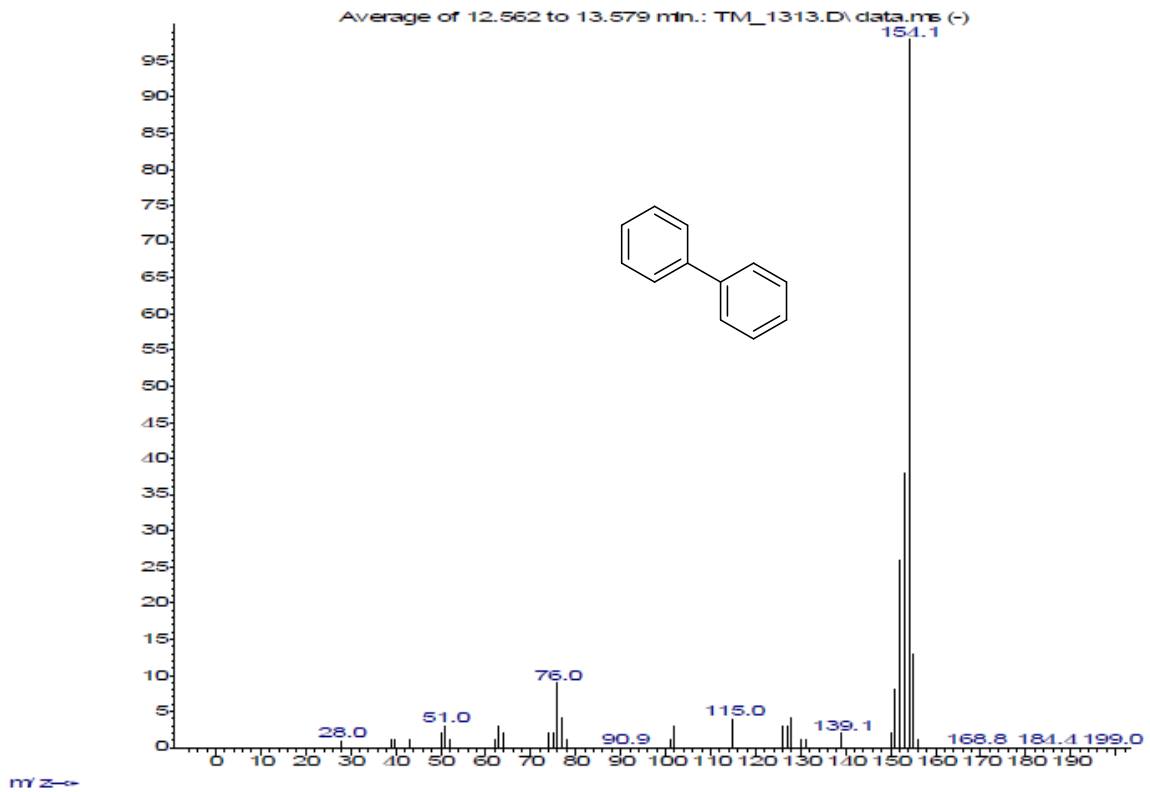
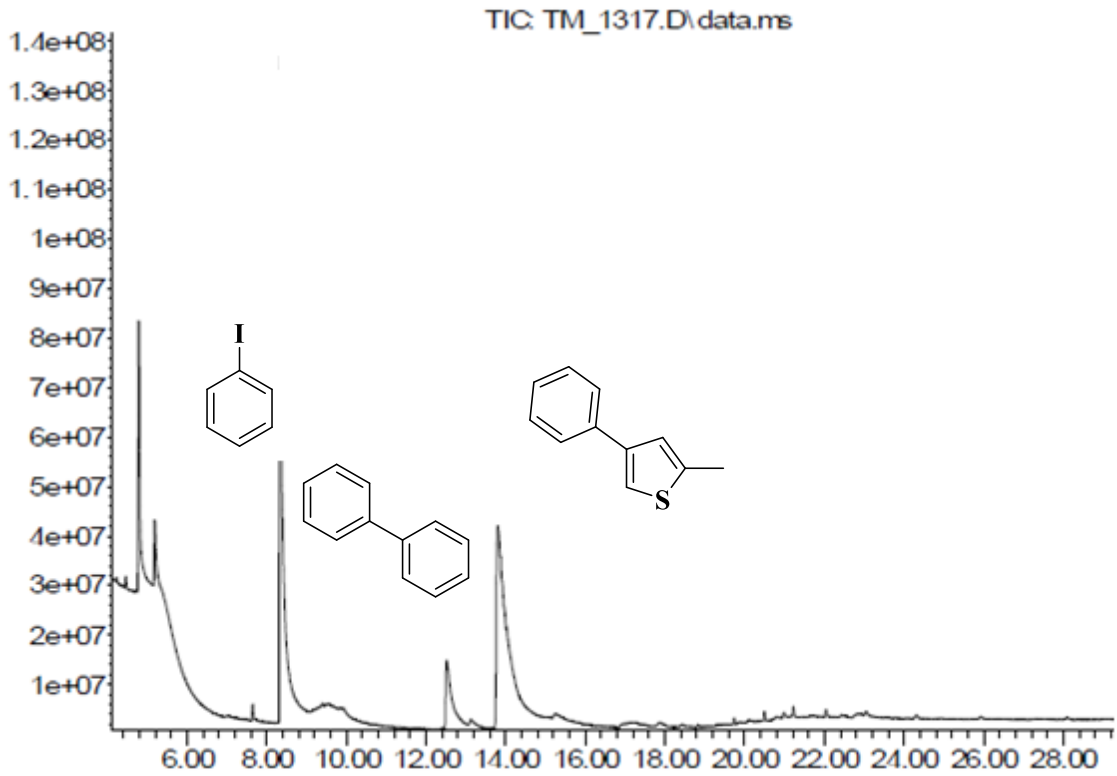
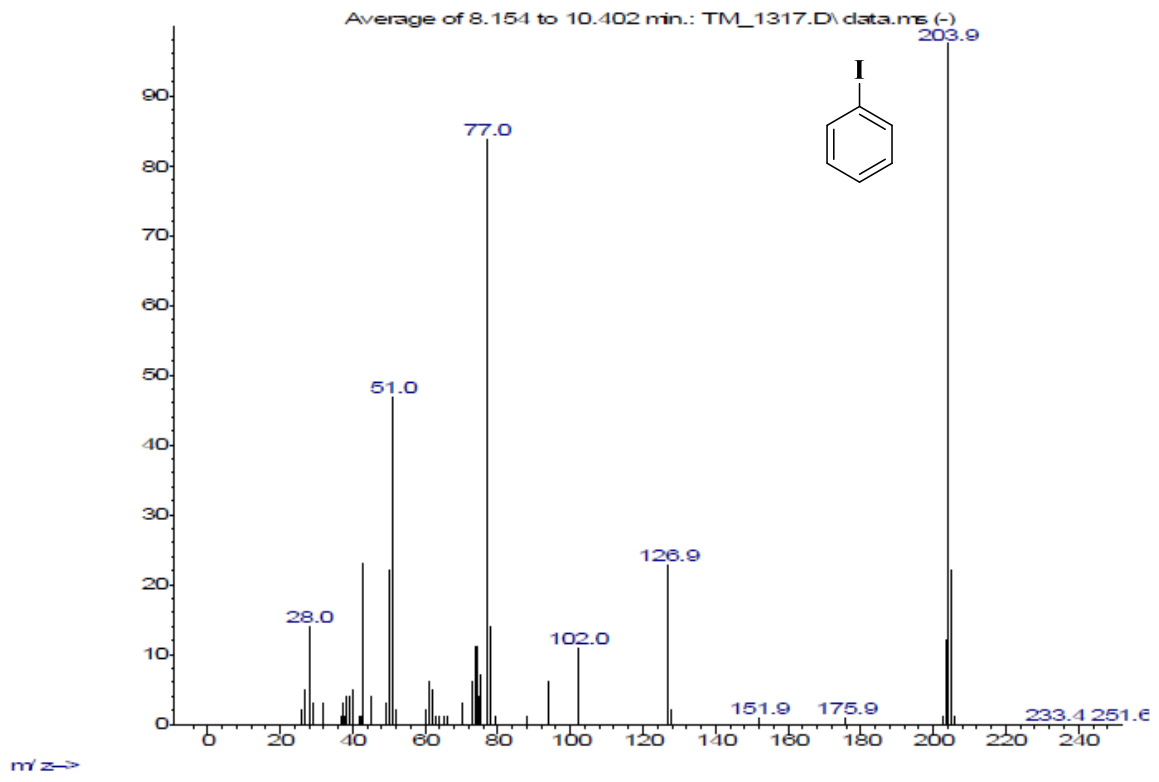
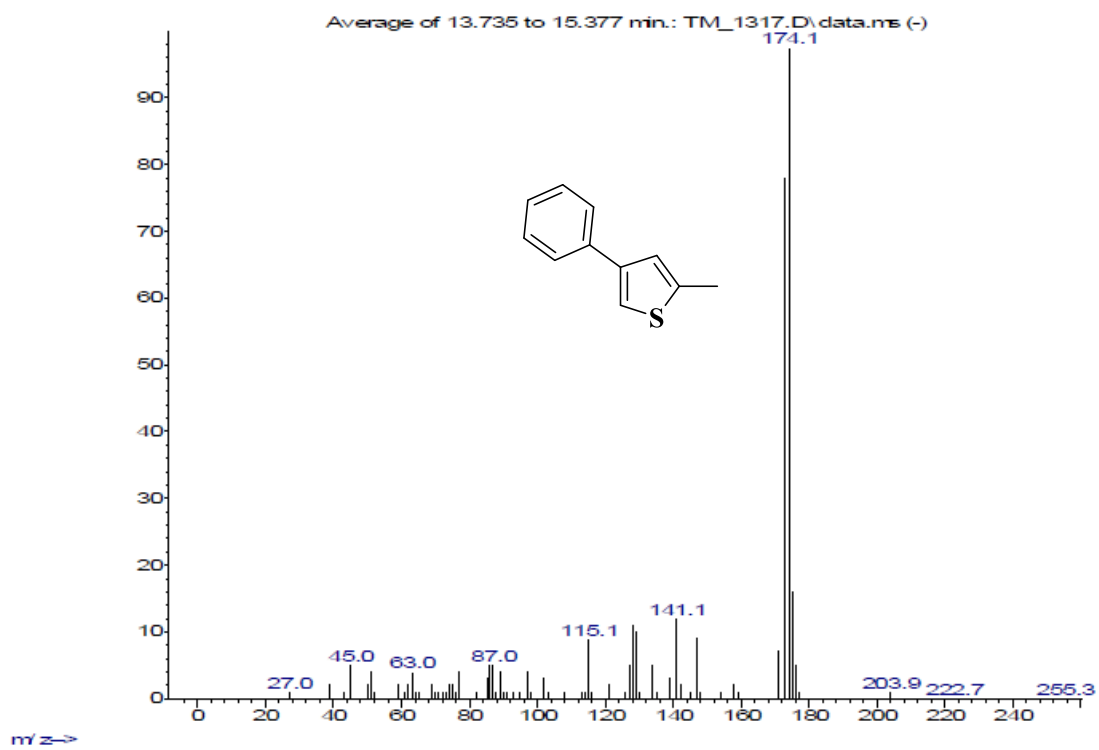
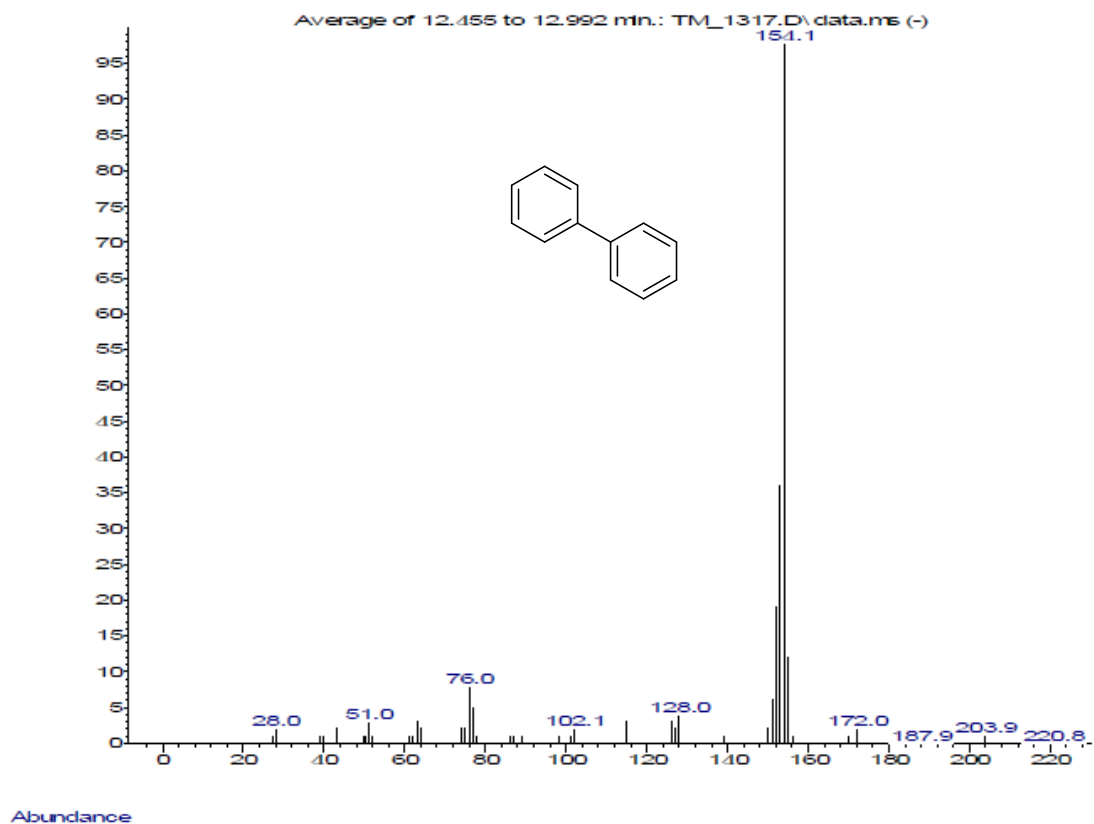


Figure S51. GCMS profile for the arylation of 3-methylindole.



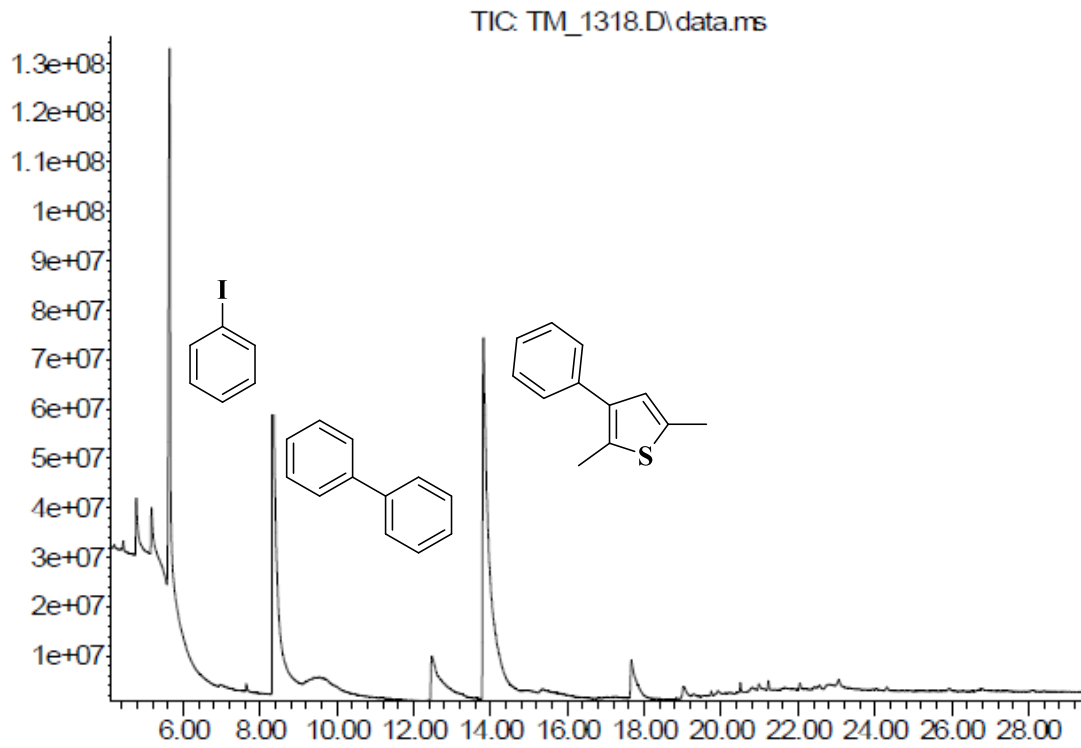
Abundance





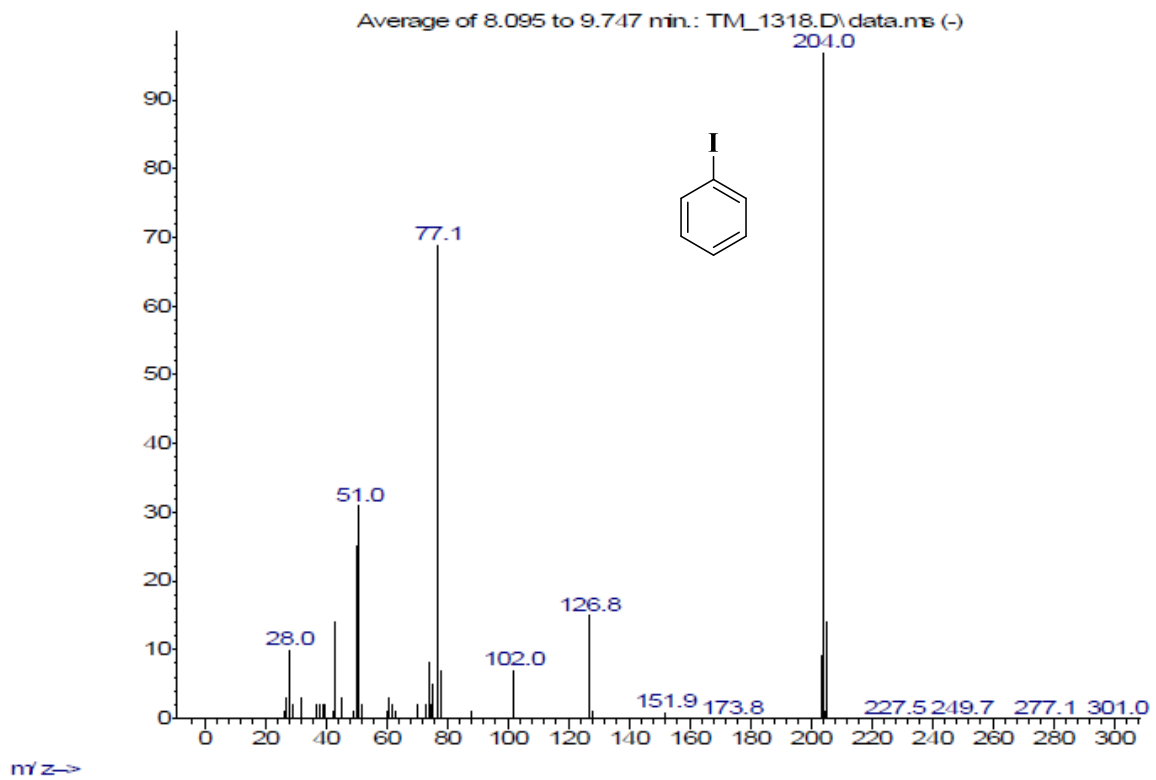
**Figure S52.** GCMS profile for the arylation of 2 methylthiophene.

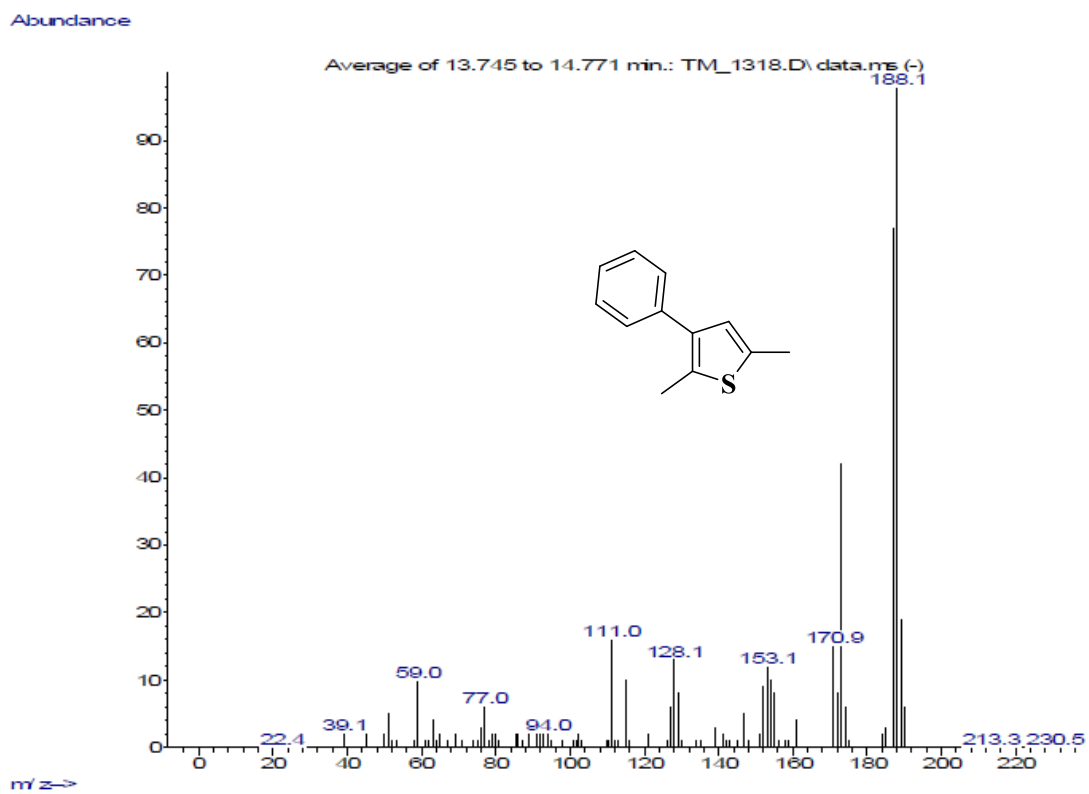
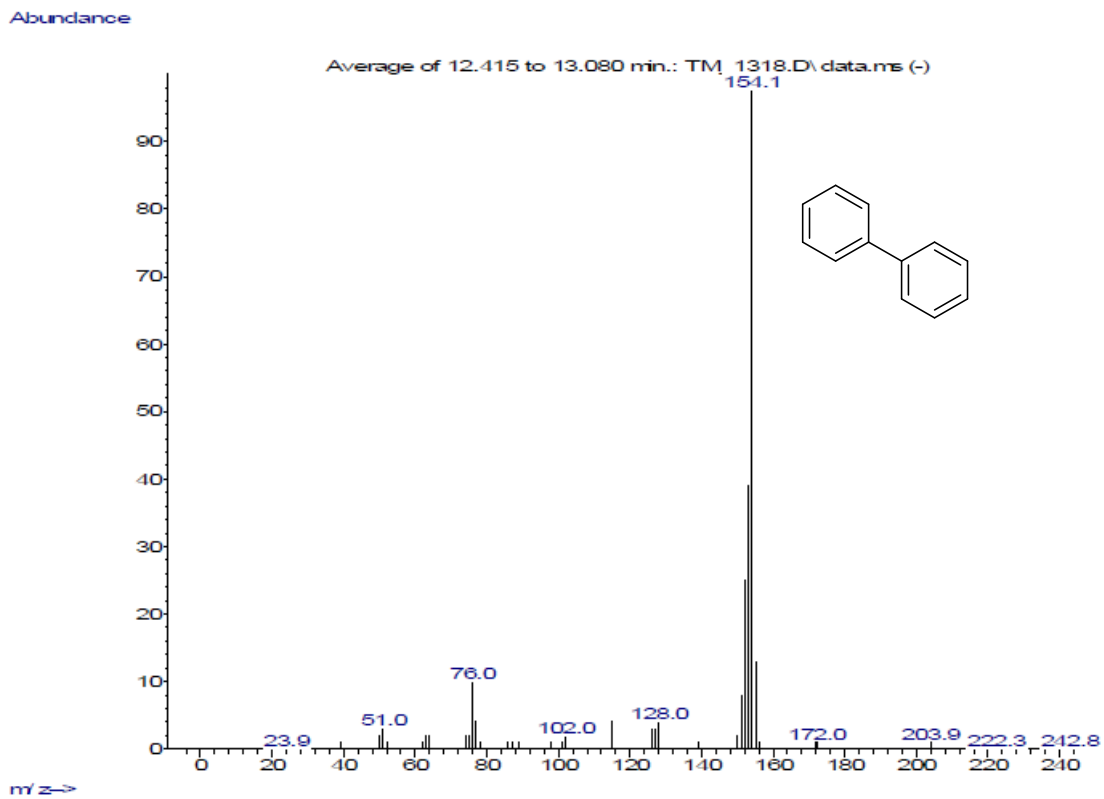
Abundance



Time

Abundance



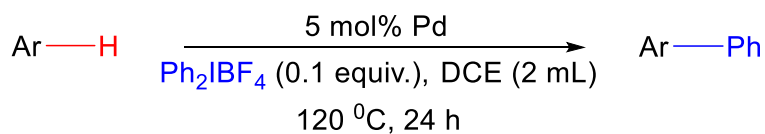


**Figure S53.** GCMS profile for the arylation of 2,5 dimethylthiophene.



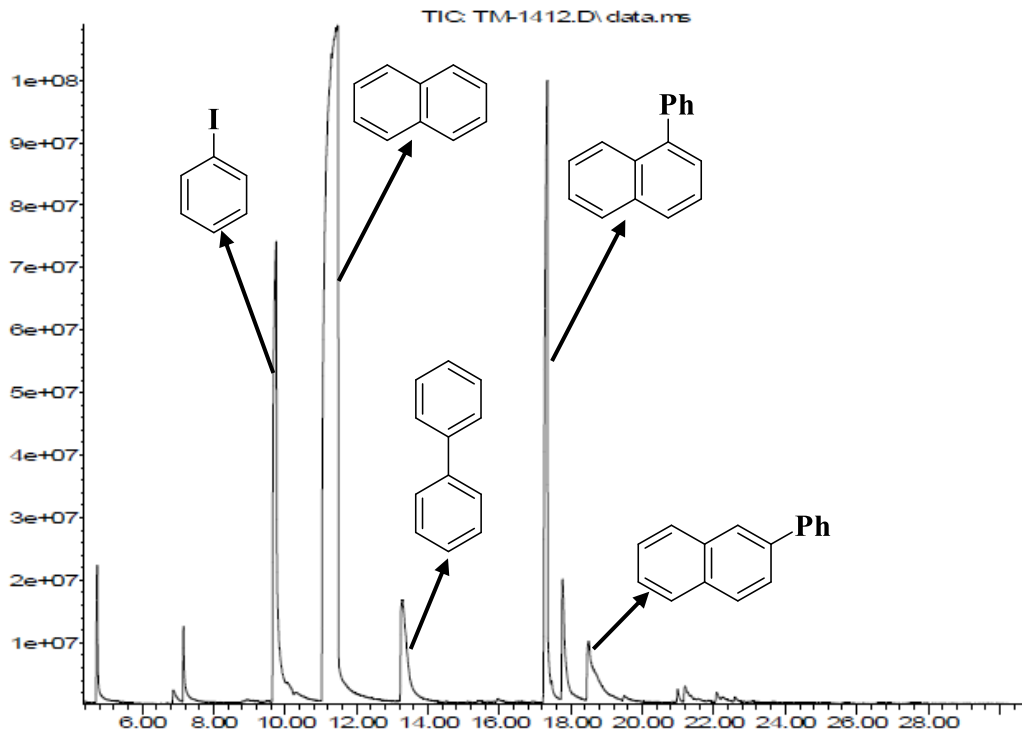
***B. Heterogeneous non directed C-H arylation of simple arenes:***

For arylation of simple arenes, arene (1.0 mmol) was placed in a pressure tube. Then diphenyliodonium tetrafluoroborate (0.1 mmol, 37.4 mg) was added. The Pd-catalyst (5.0 mol% Pd) was used. At last, 1.0 mL solvent was added and the pressure tube was capped tightly. The resulting solution was stirred at different temperatures for selected time intervals. After that, the reaction mixture was cooled and PhCl was added as an internal standard. Then 0.250 mL reaction mixture was taken, diluted with ethyl acetate, and injected into GC for yield calculation. The products were further verified by GCMS analysis. When the reaction was completed, it was allowed to cool to room temperature. Catalysts were separated and products were purified by column chromatography to record <sup>1</sup>H NMR spectra.

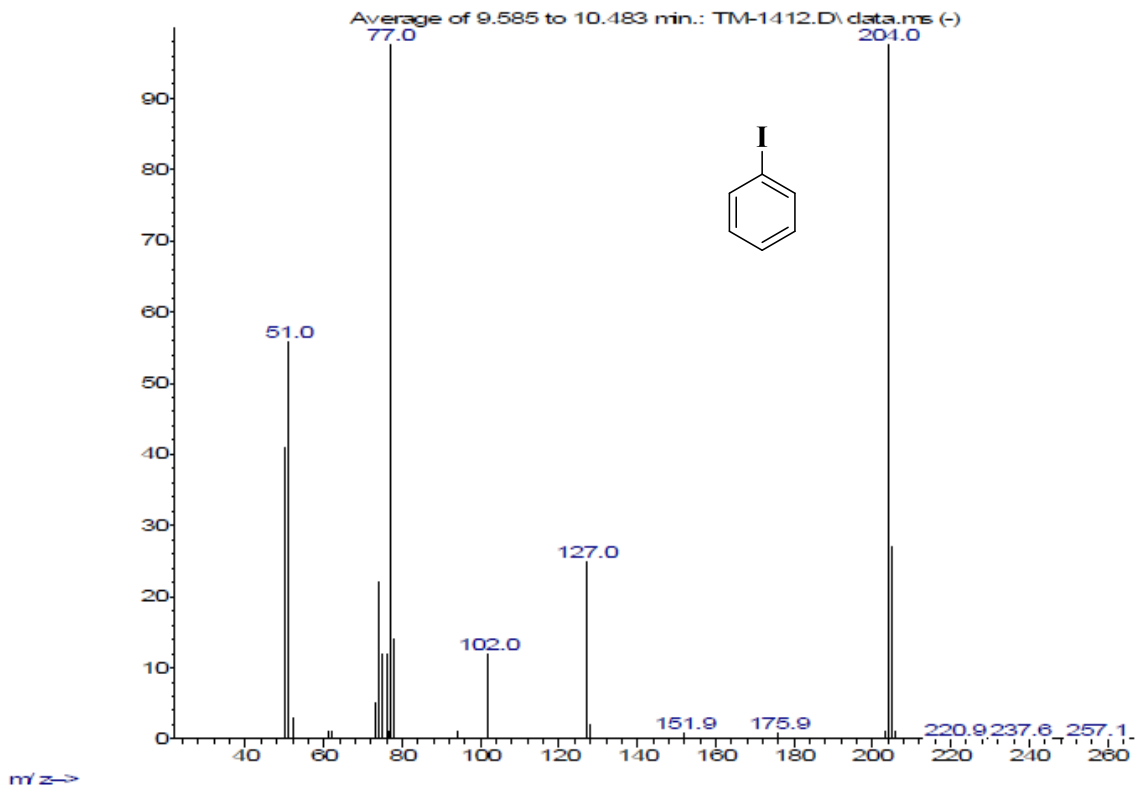


**Scheme S8:** Non-directed C–H arylation of simple arenes.

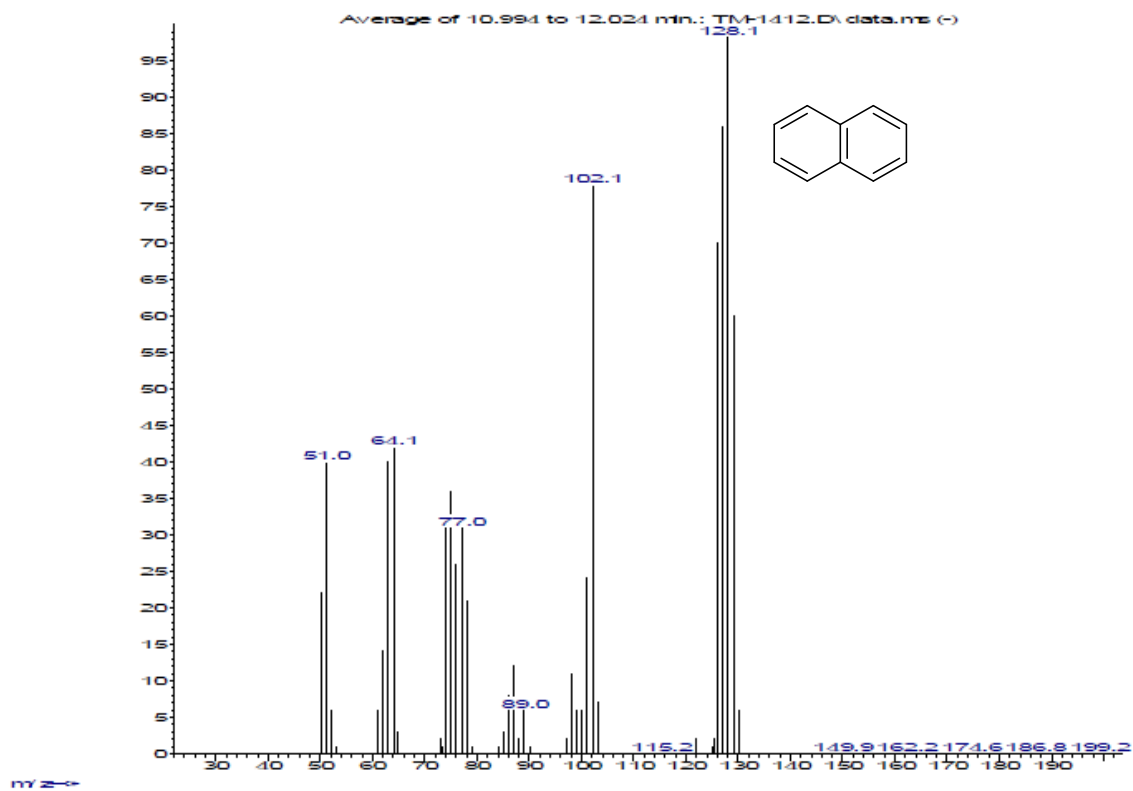
Abundance



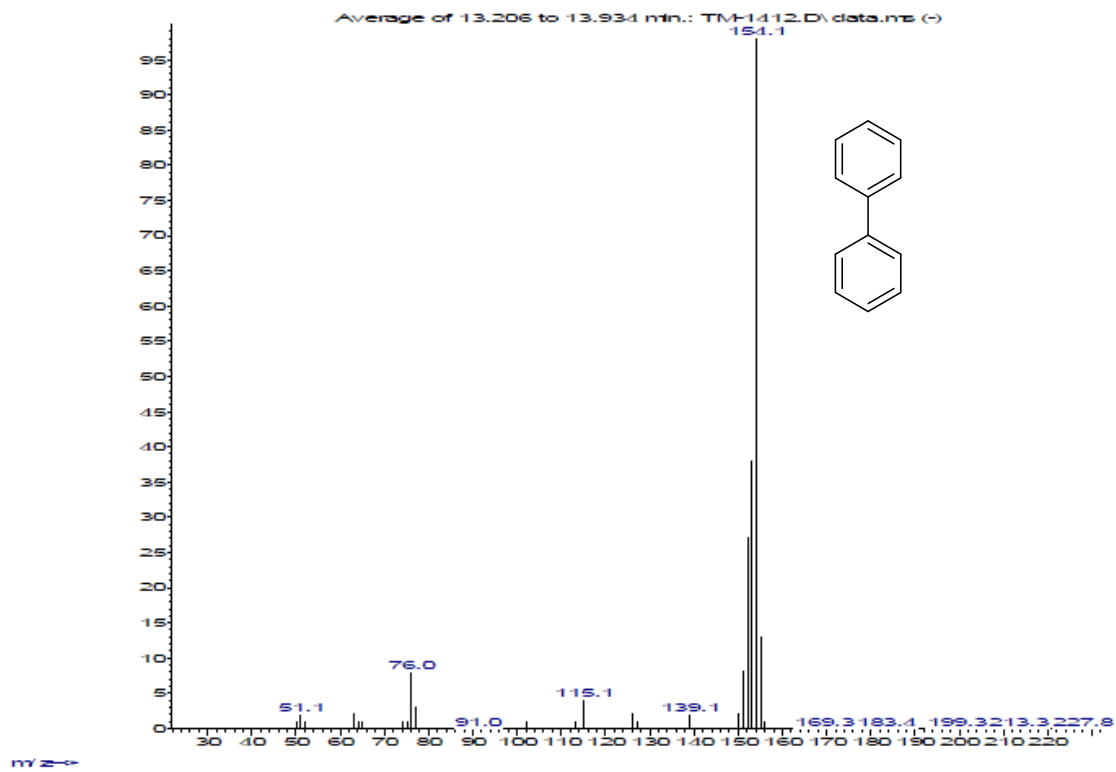
Abundance



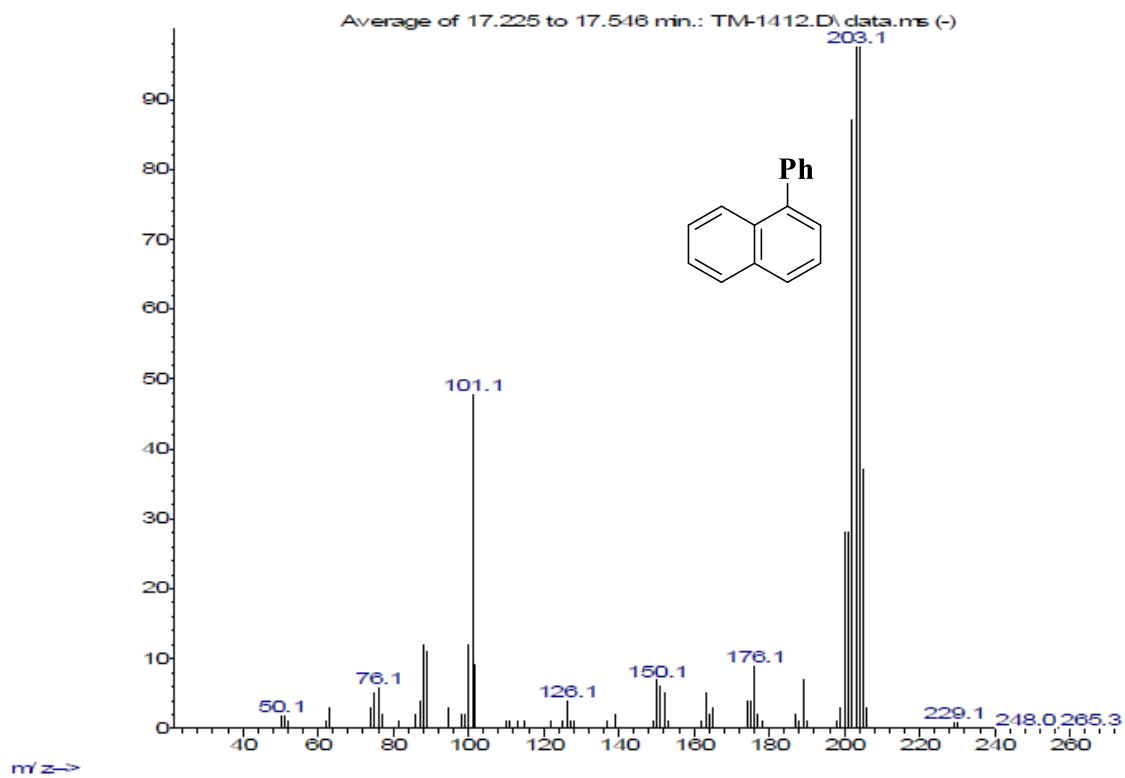
Abundance



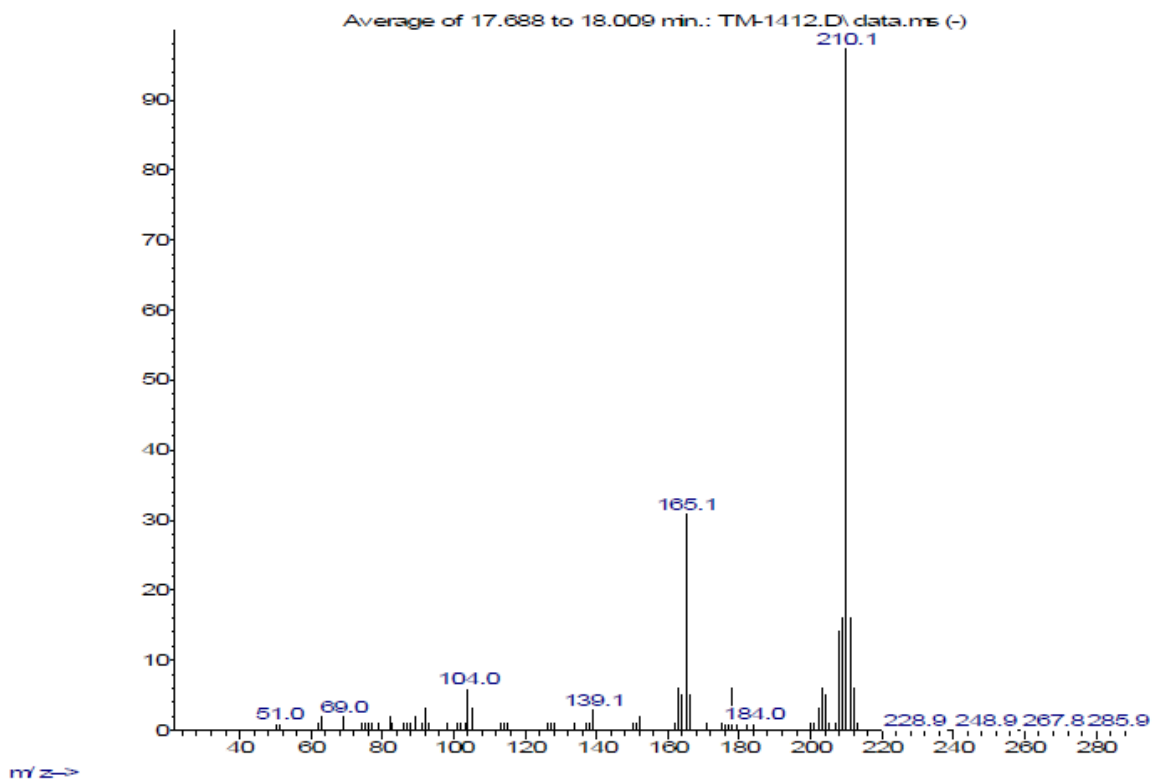
Abundance

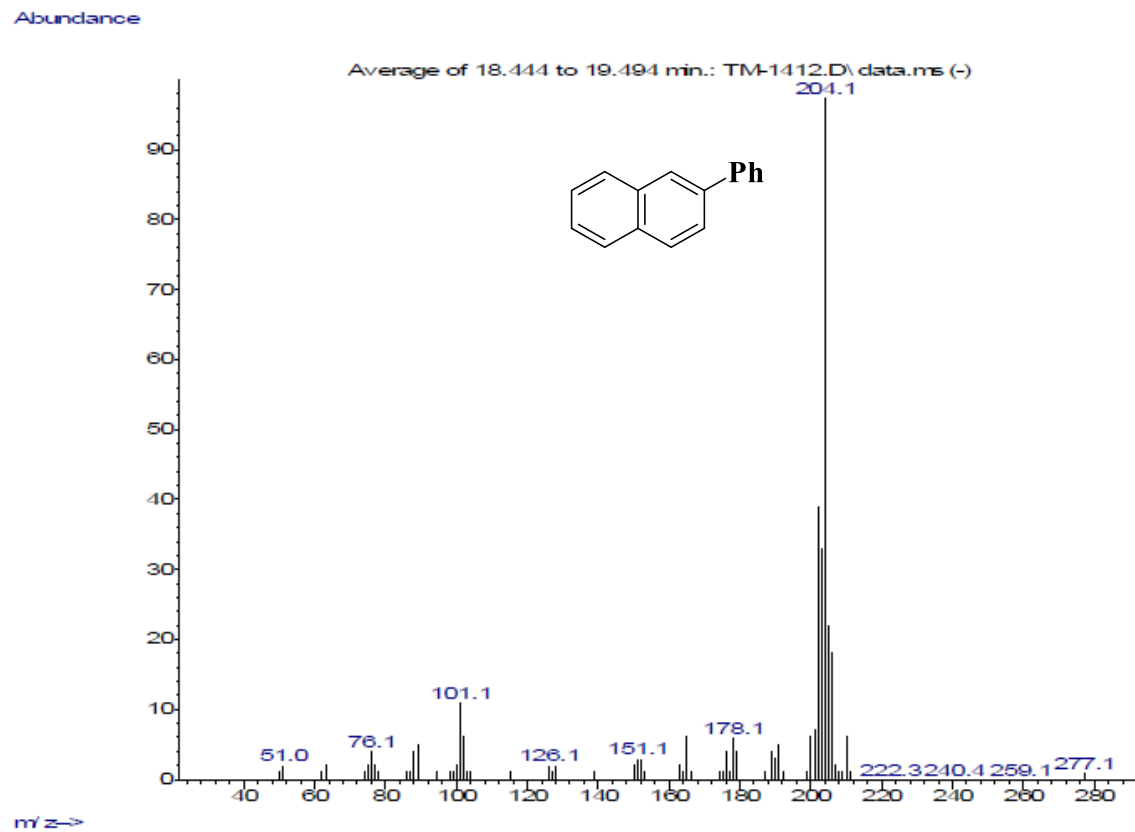


Abundance



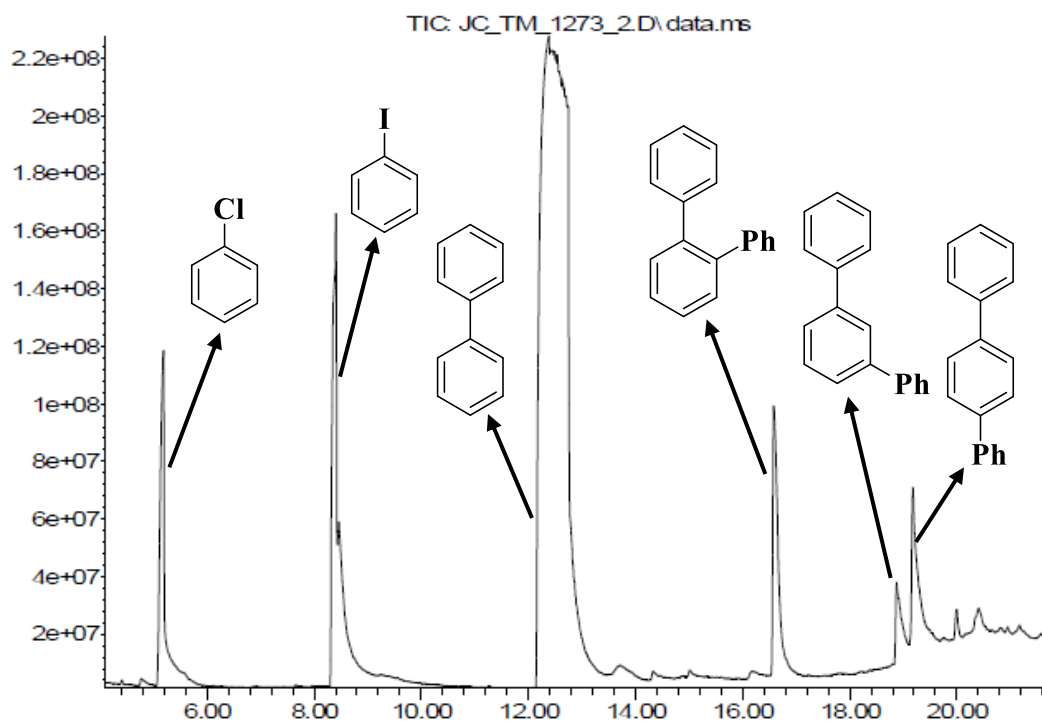
Abundance



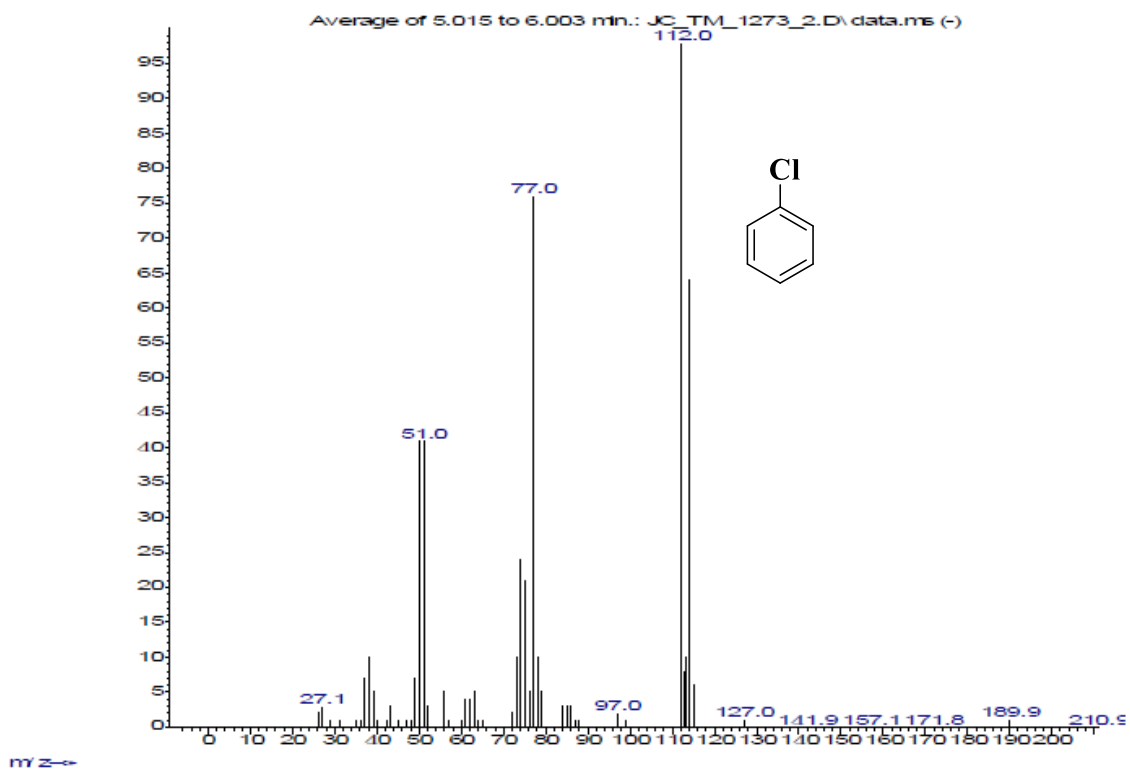


**Figure S54.** GCMS profile for the arylation naphthalene.

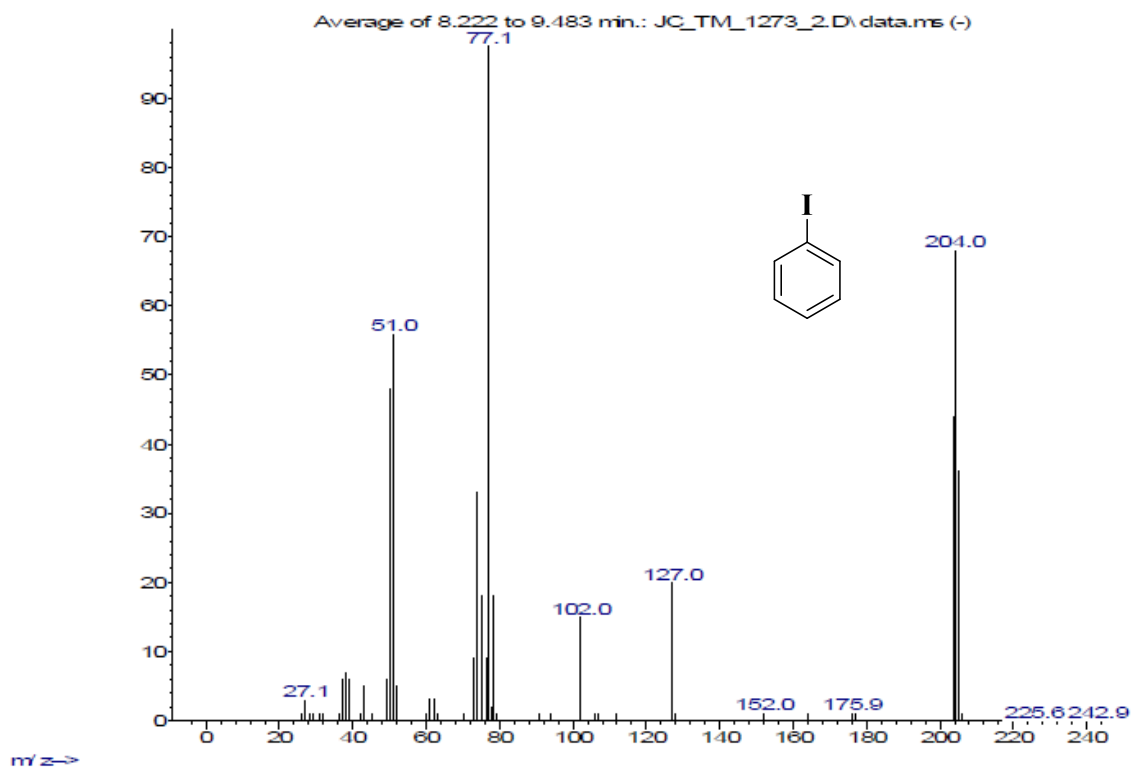
Abundance



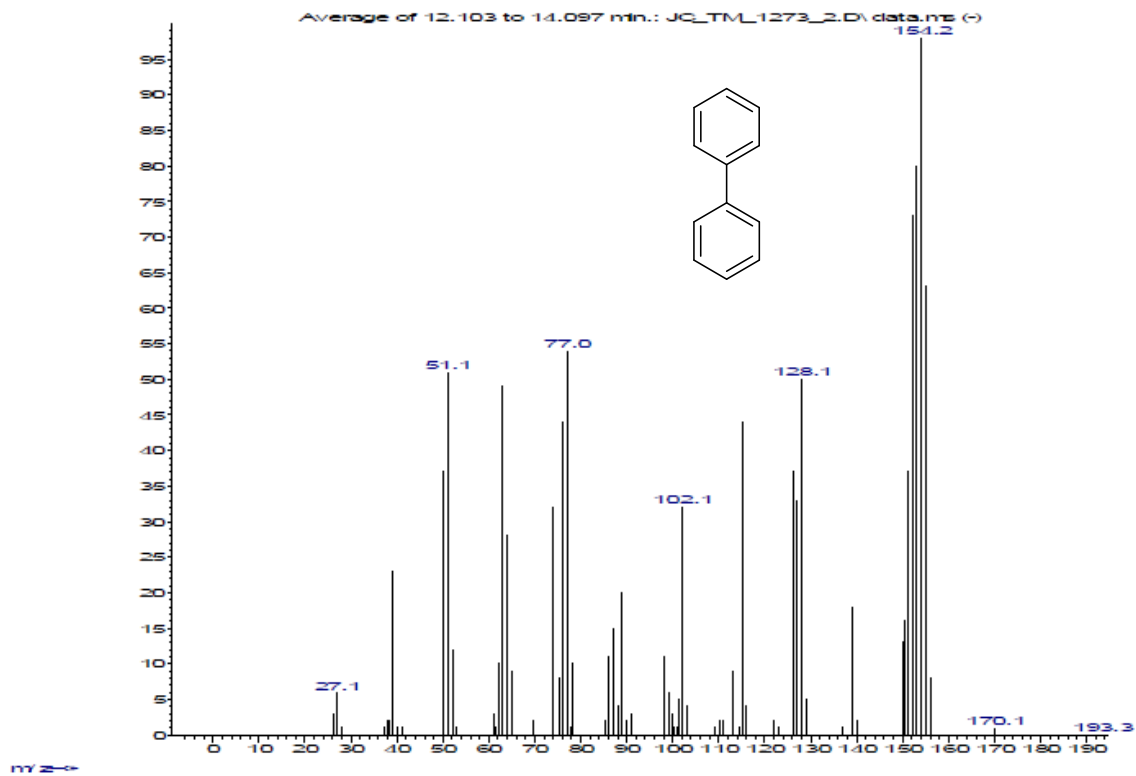
Abundance



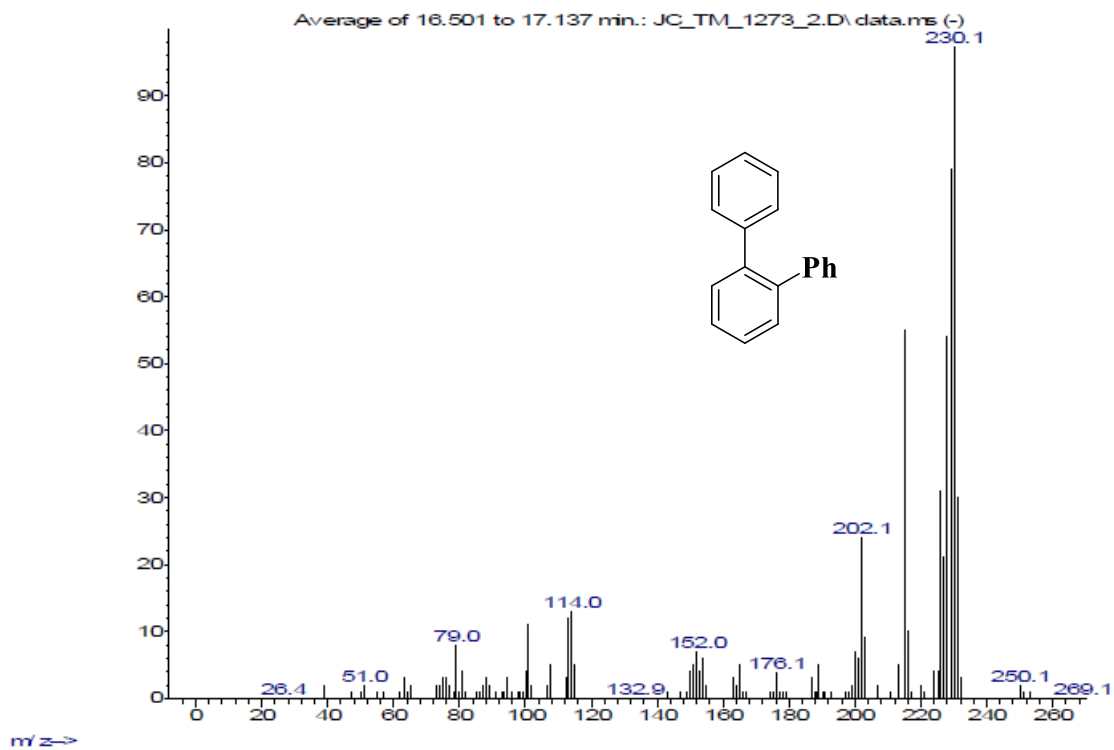
Abundance



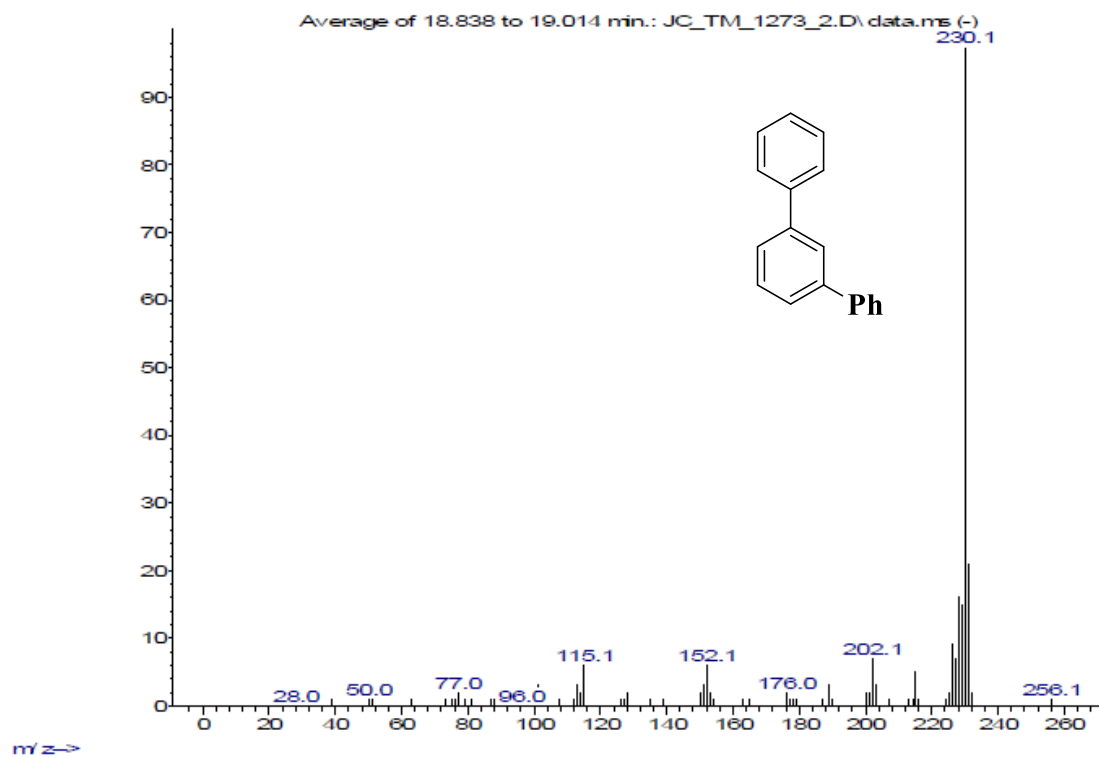
Abundance



Abundance



Abundance





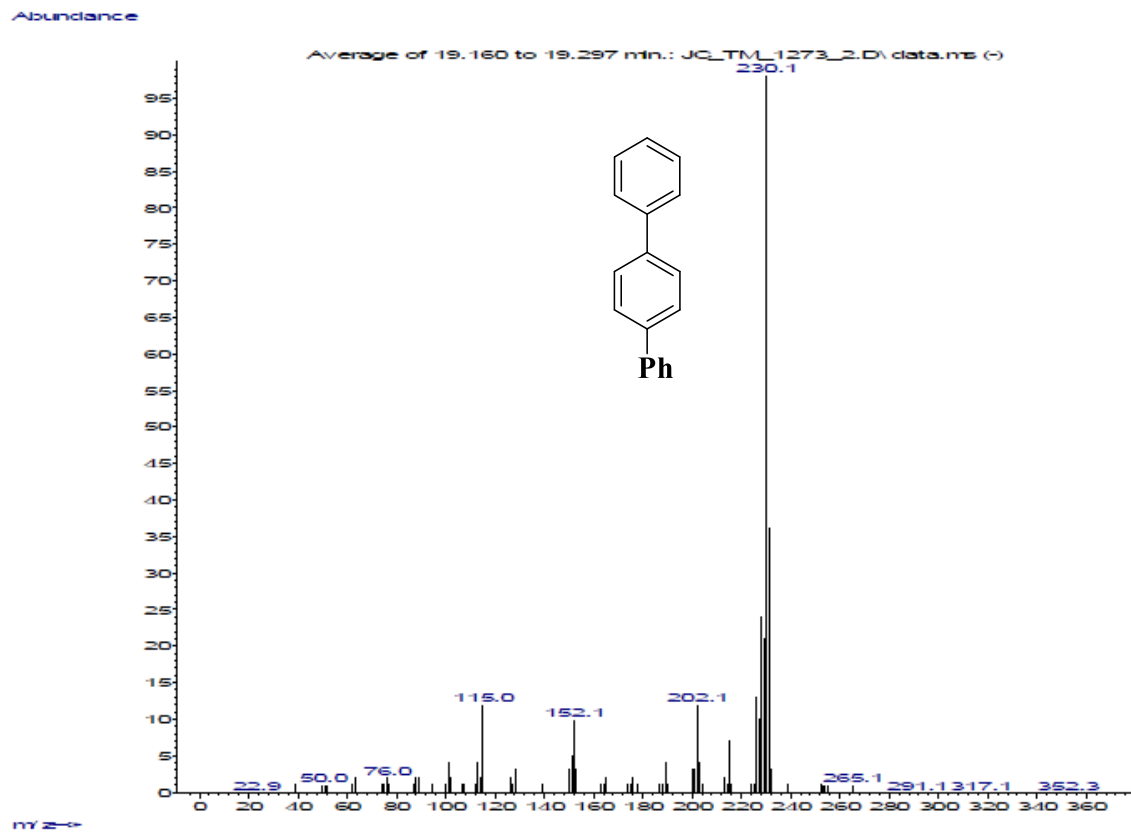
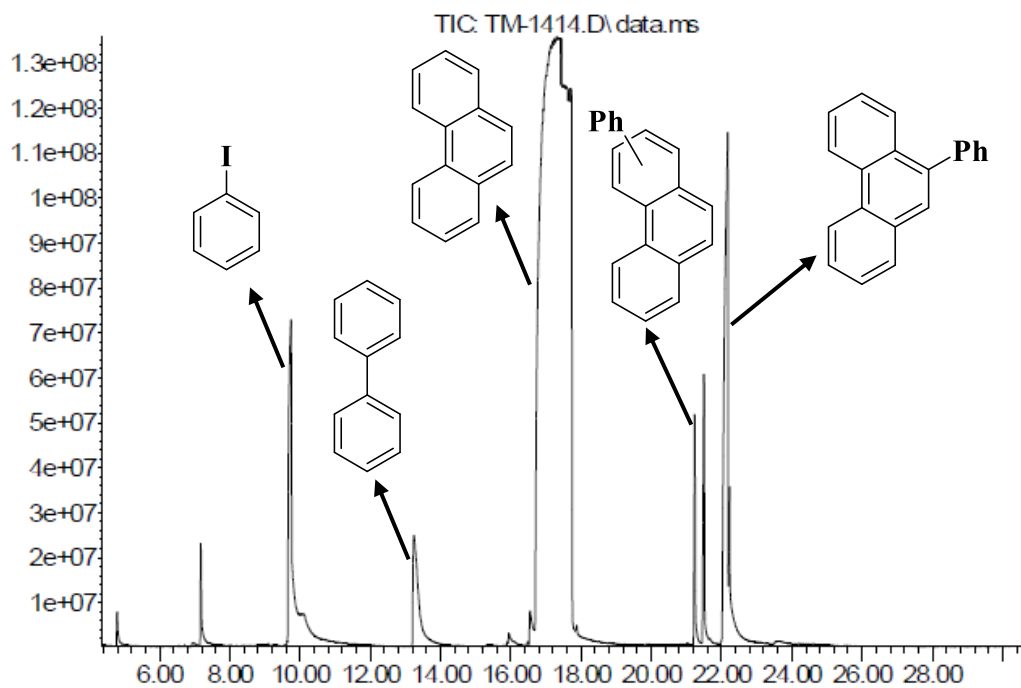


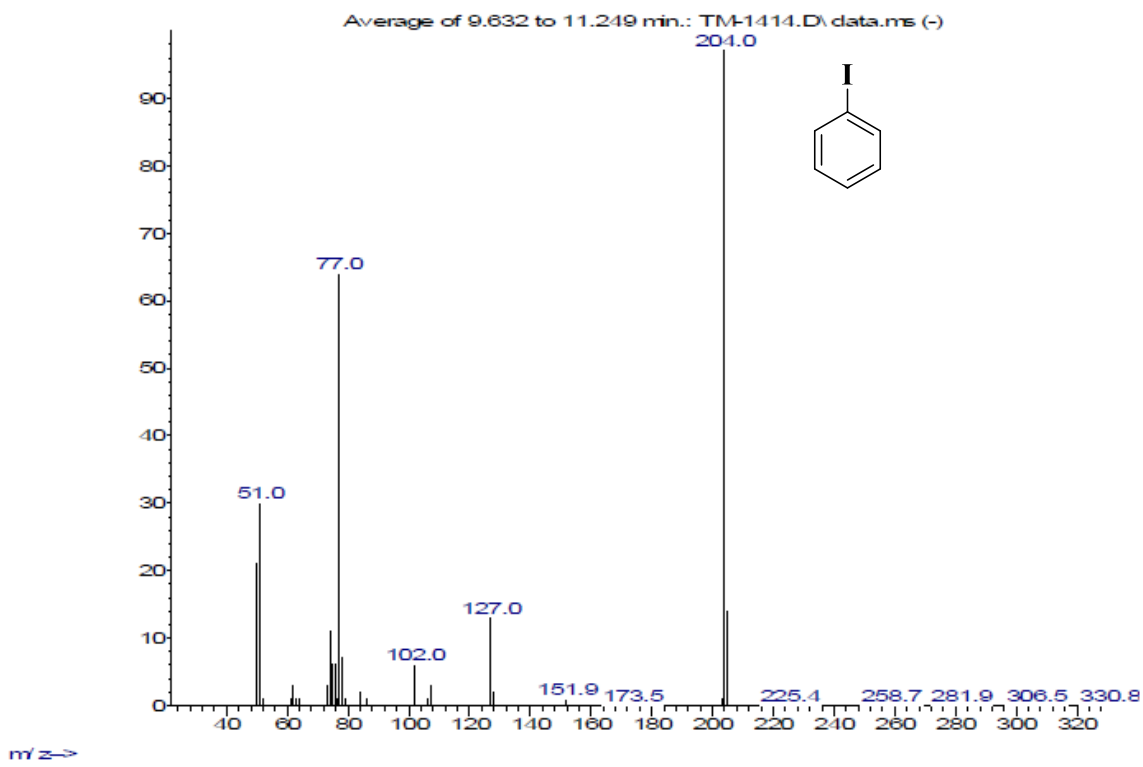
Figure S55. GCMS profile for the arylation of biphenyl.

Abundance

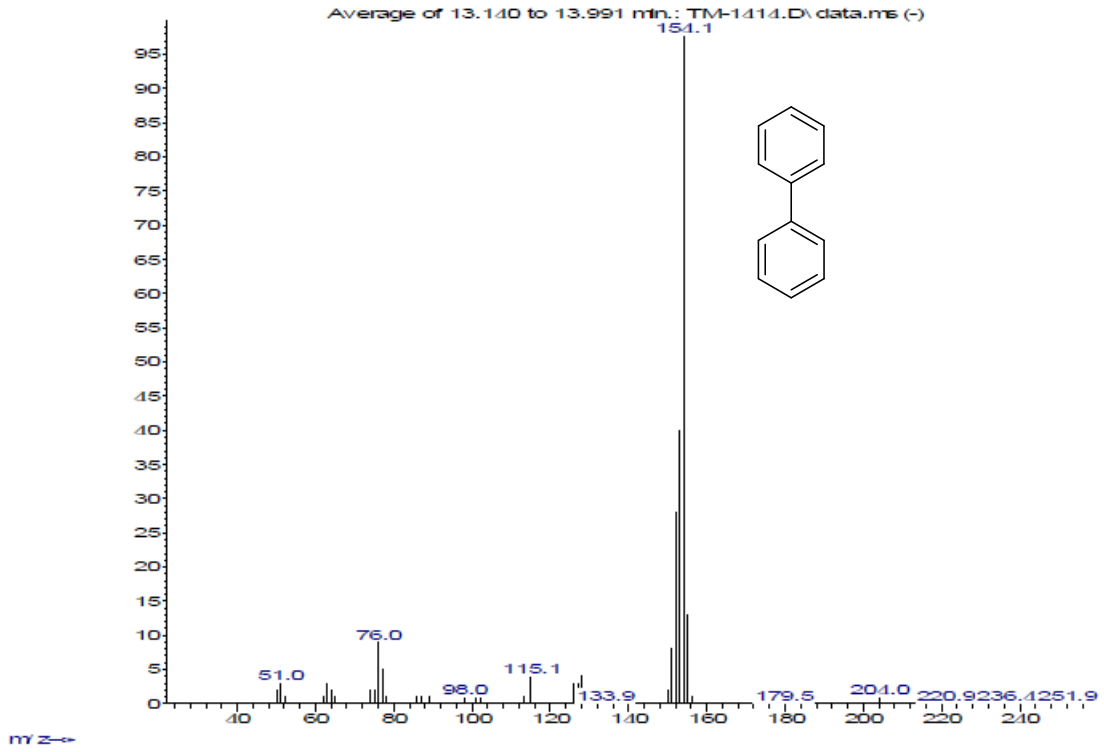


Time→

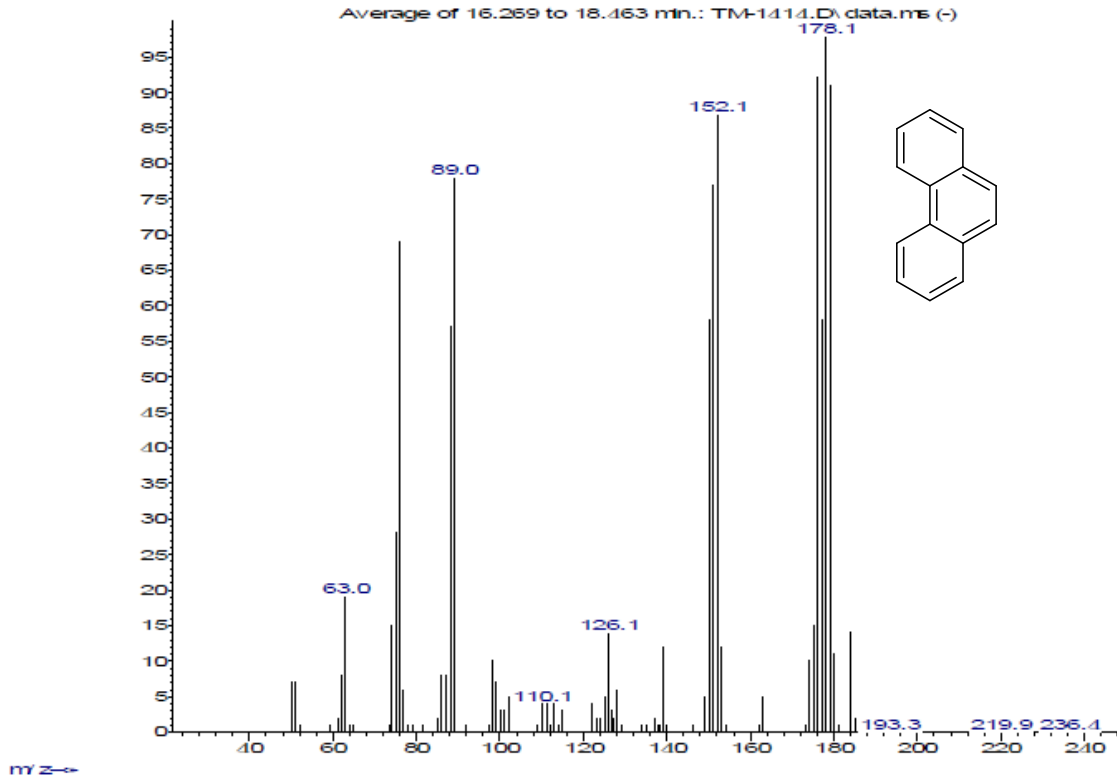
Abundance



Abundance



Abundance



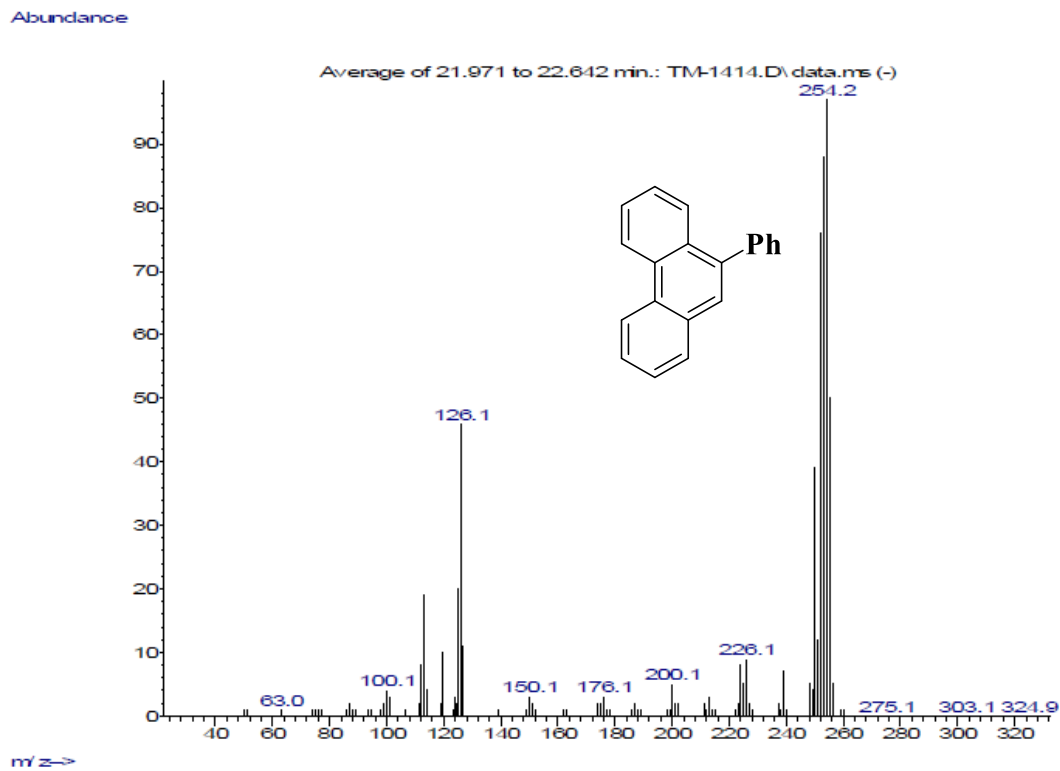
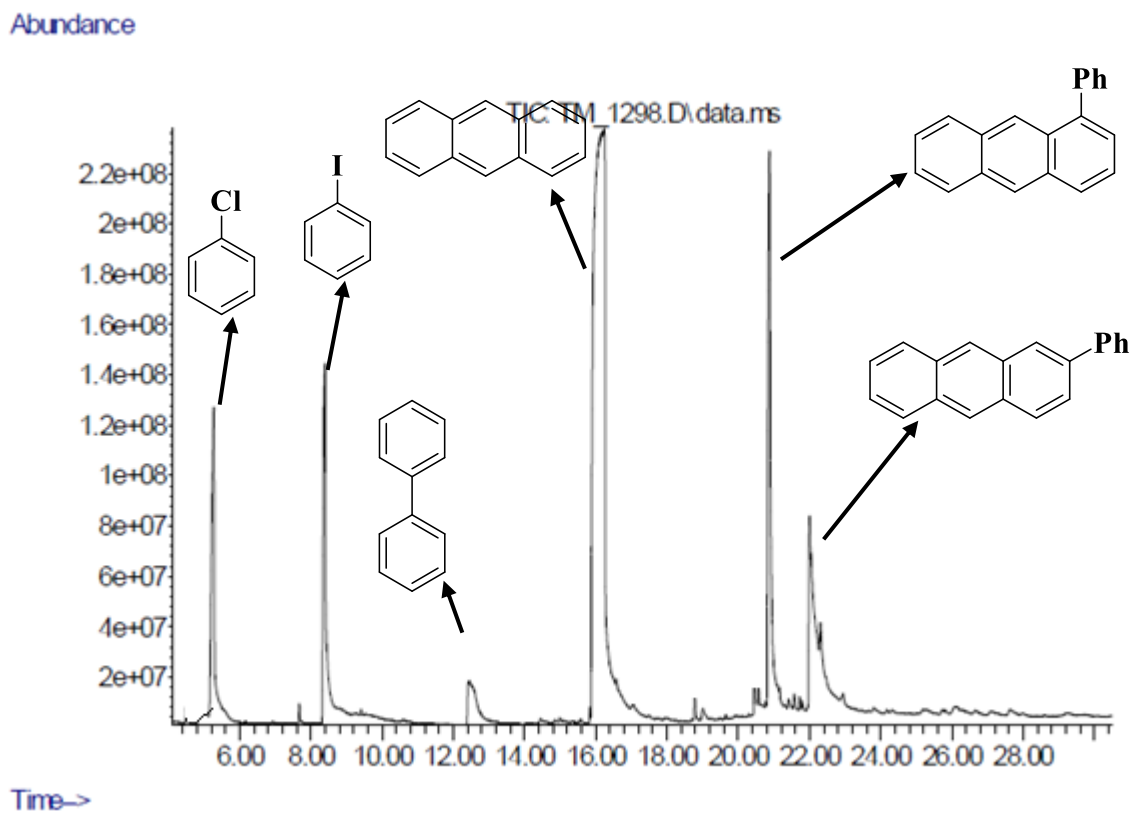
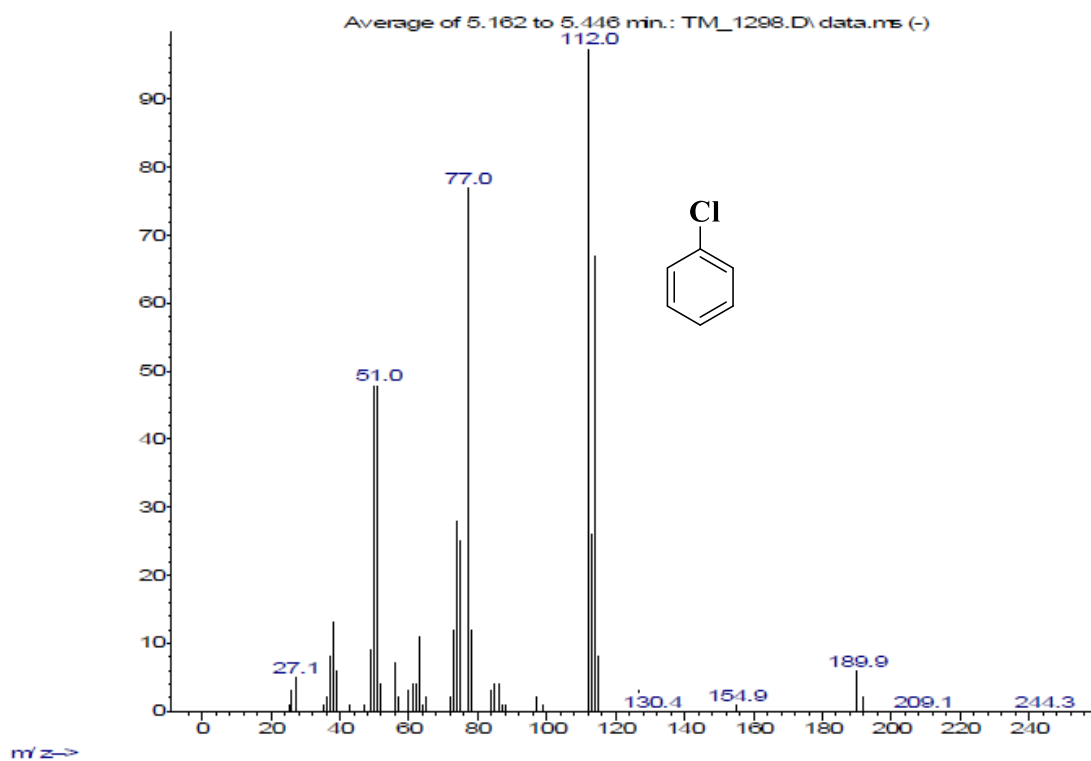


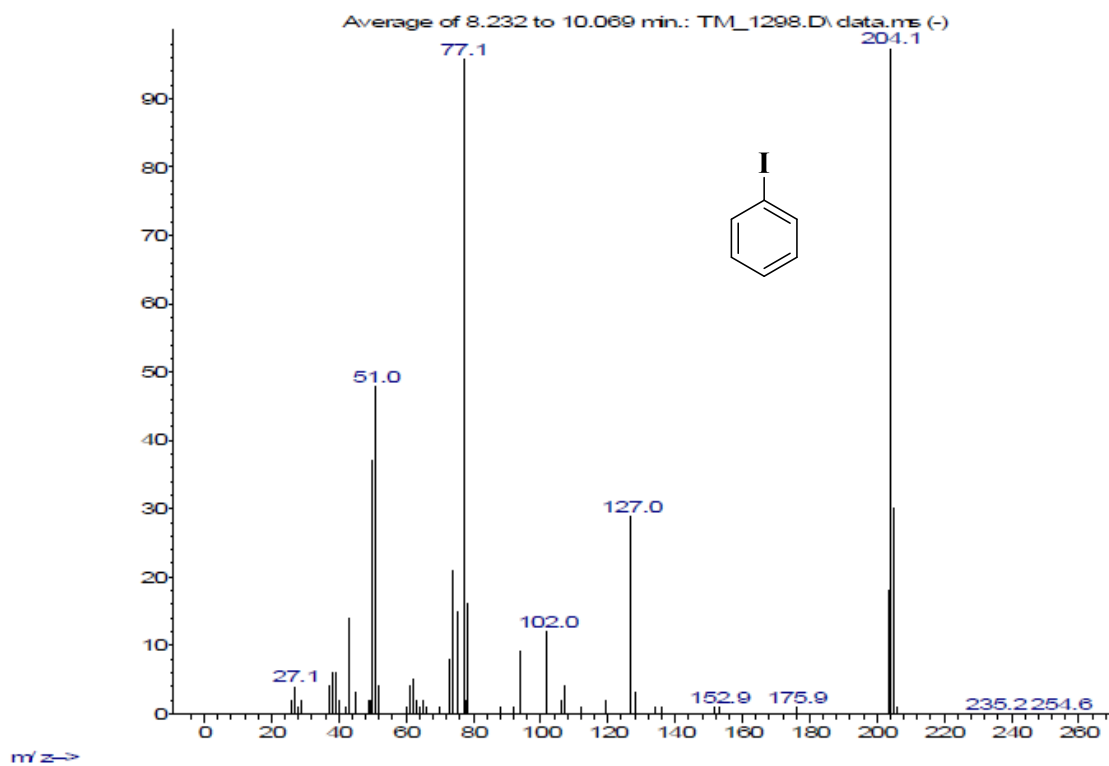
Figure S56. GCMS profile for the arylation of phenanthrene.



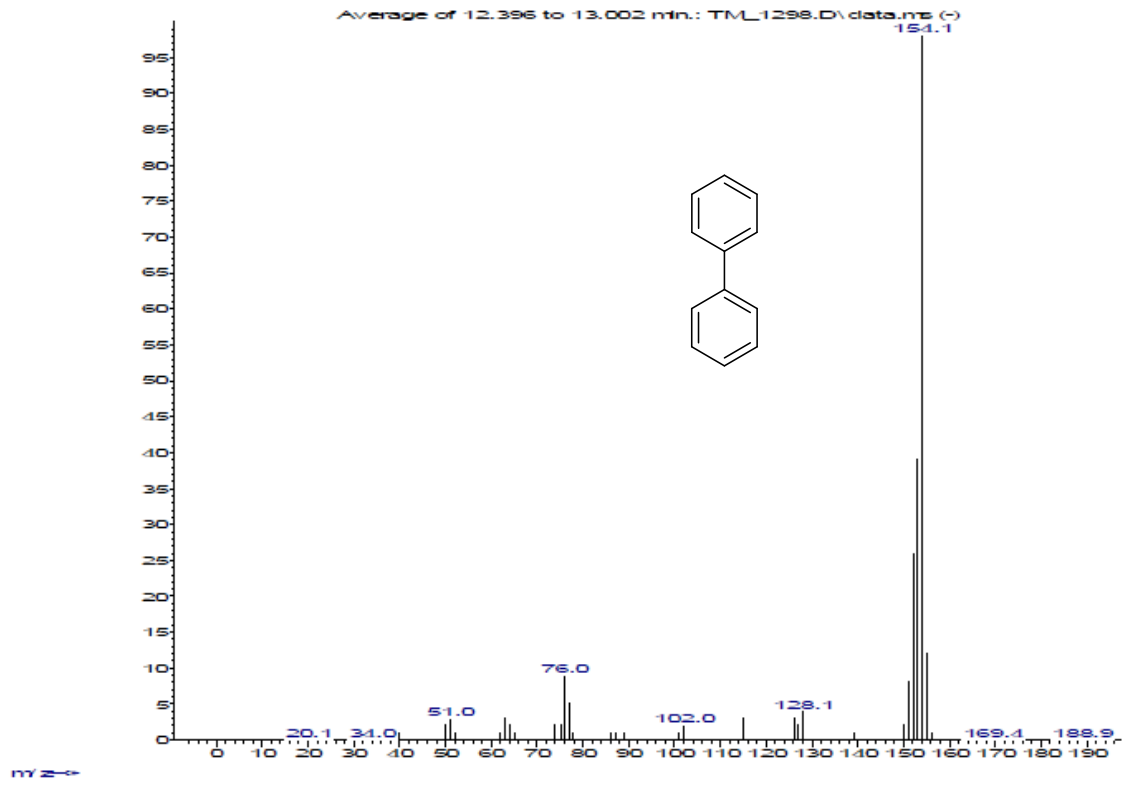
Abundance



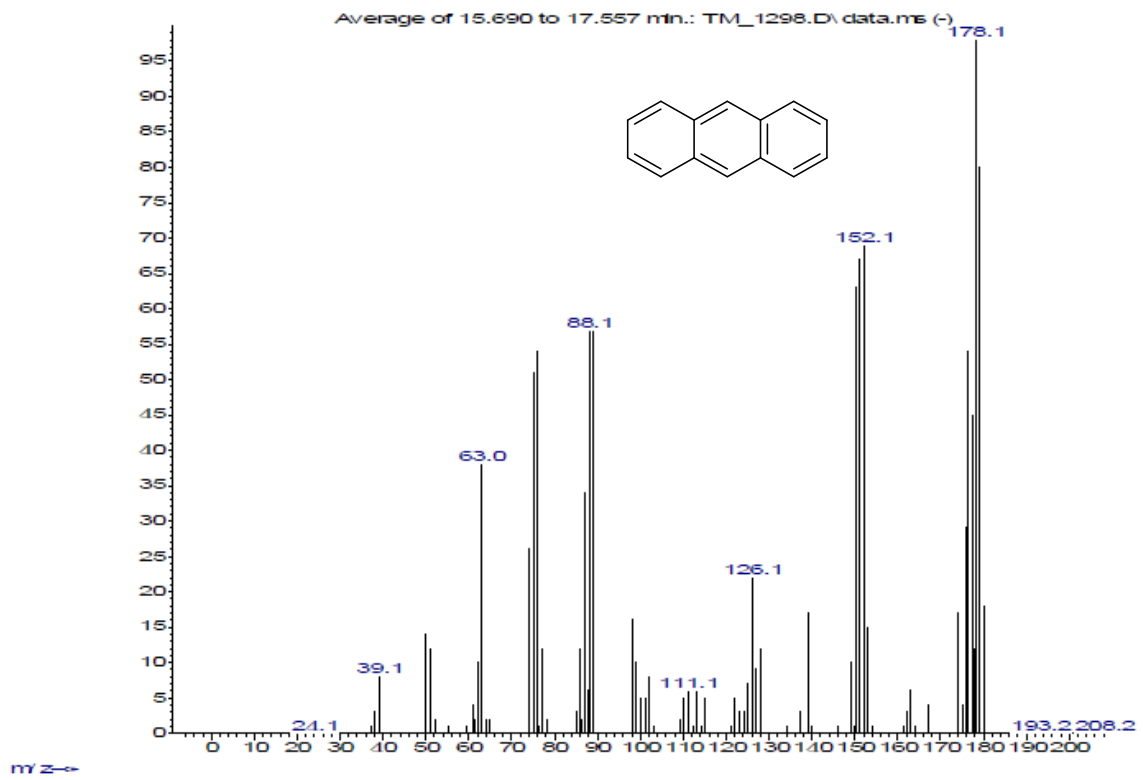
Abundance



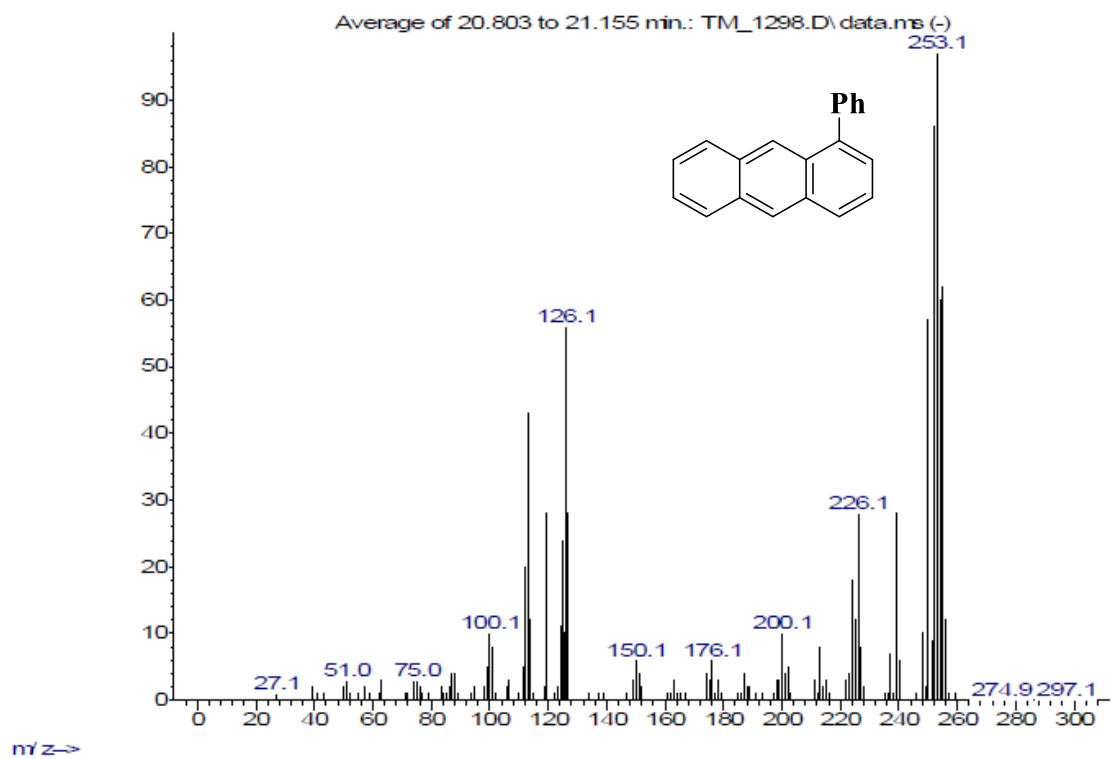
Abundance



Abundance



Abundance



Abundance

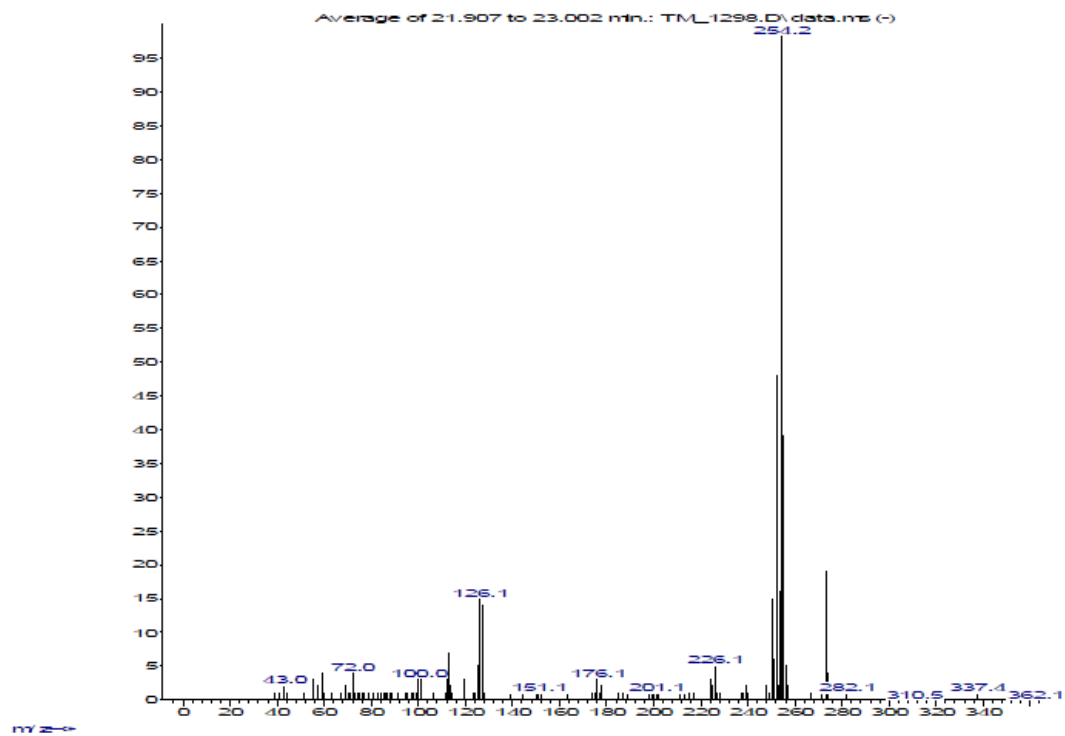


Figure S57. GCMS profile for the arylation of anthracene.

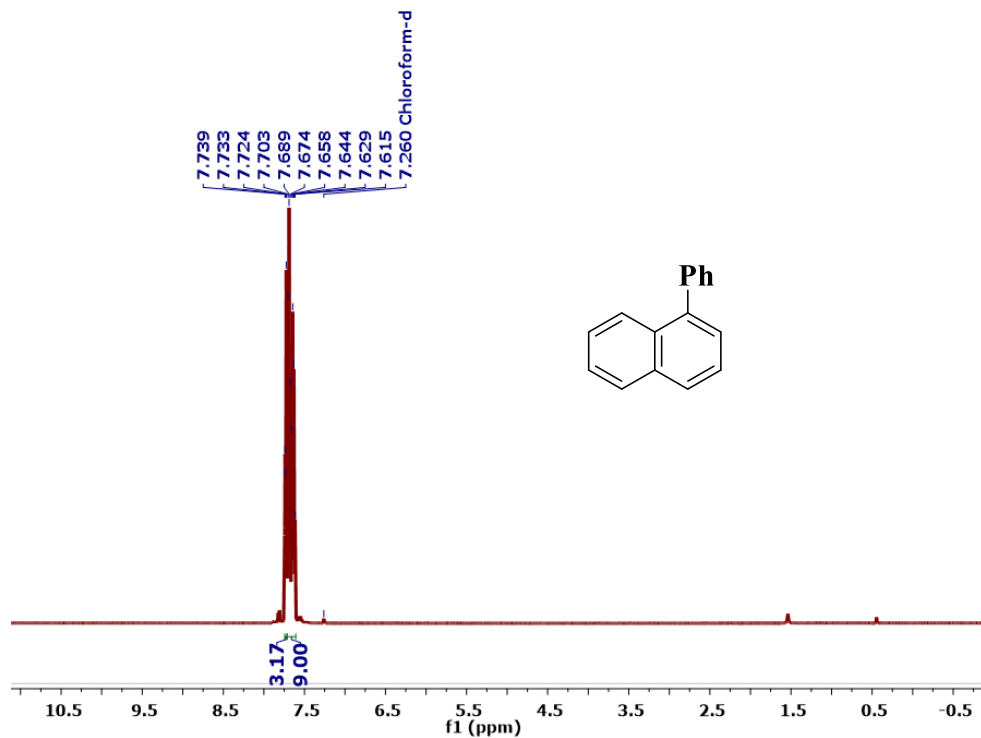


Figure S58.  $^1\text{H}$  NMR spectrum of 1-phenylnaphthalene (500 MHz,  $\text{CDCl}_3$ ).

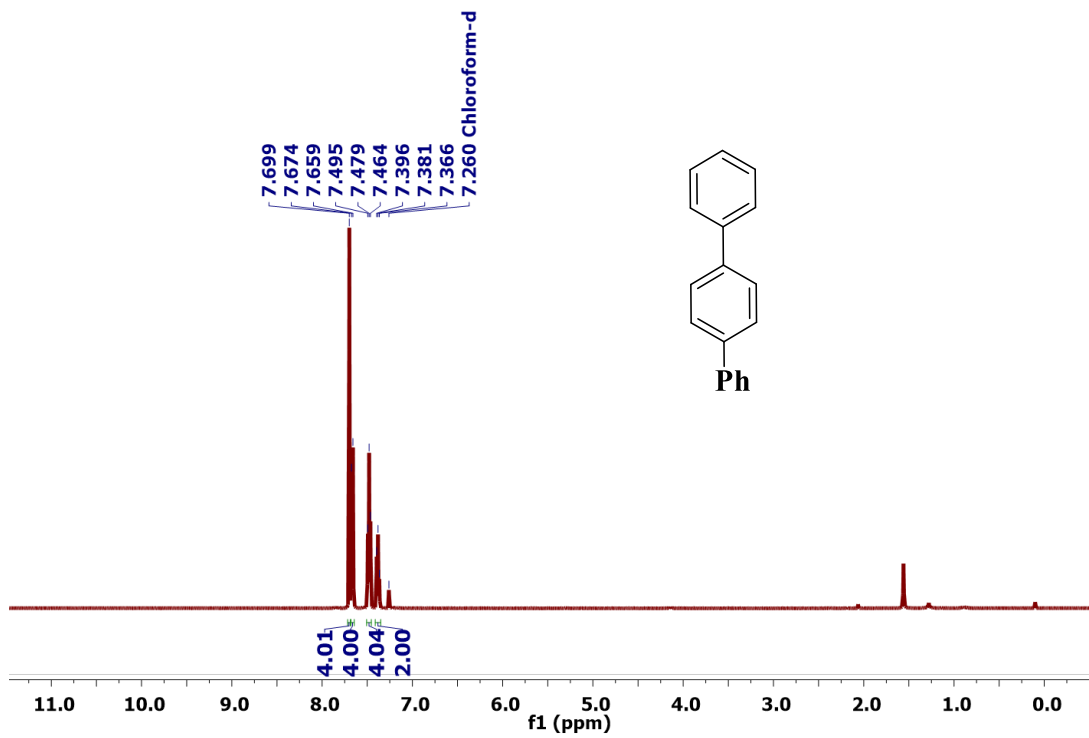


Figure S59.  $^1\text{H}$  NMR spectrum of 1,1':4',1''-terphenyl (500 MHz,  $\text{CDCl}_3$ ).



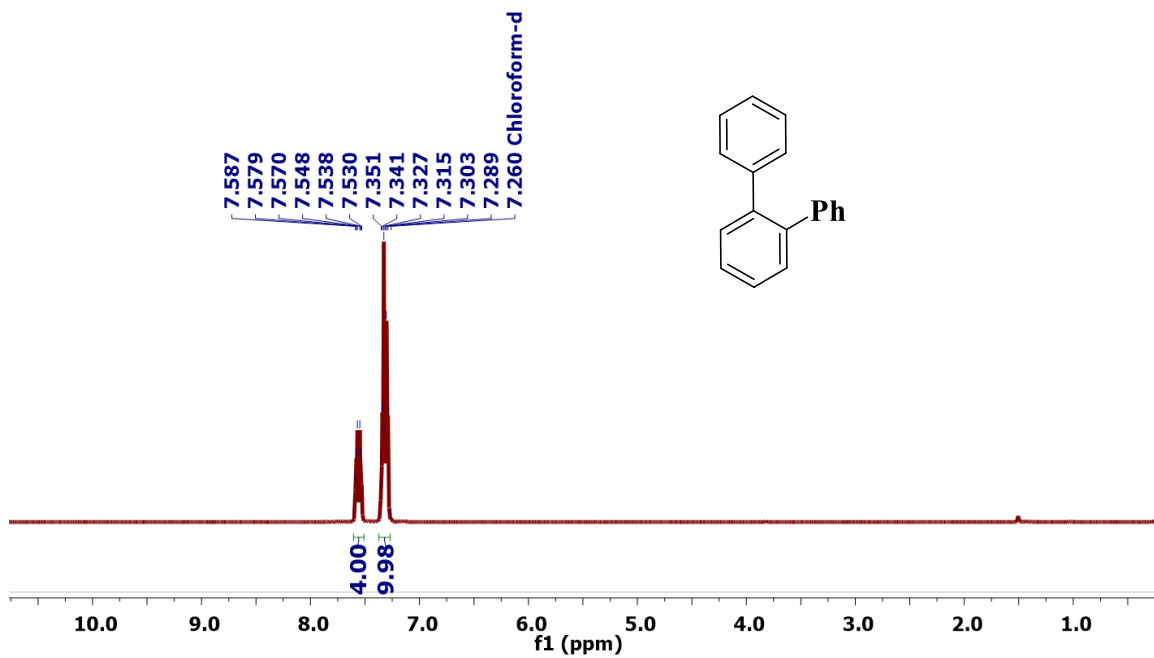


Figure S60.  $^1\text{H}$  NMR spectrum of 1,1':2',1''-terphenyl (500 MHz,  $\text{CDCl}_3$ ).

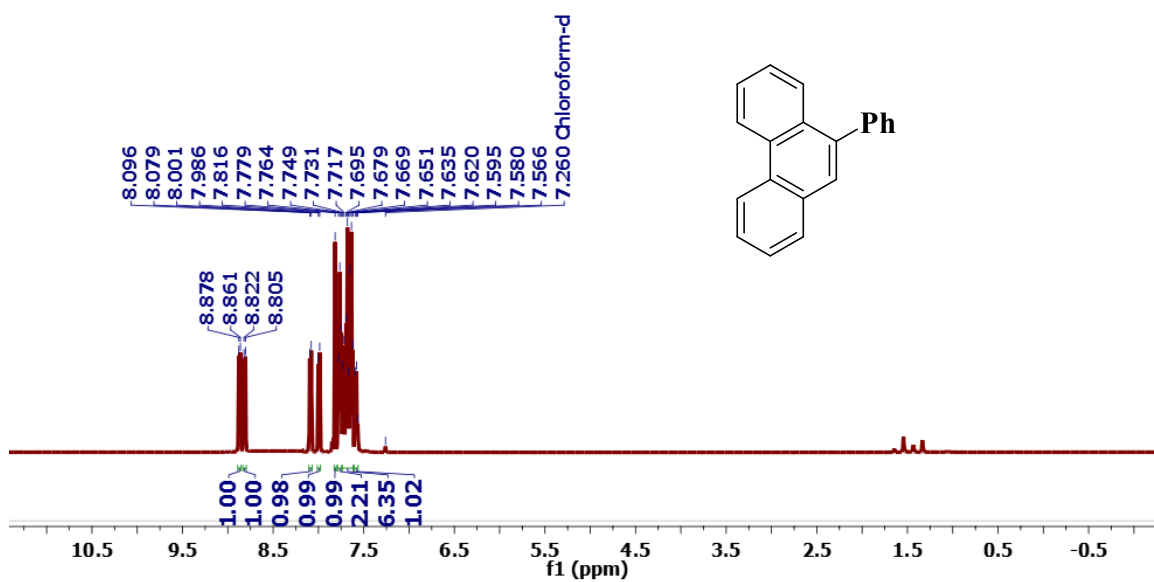
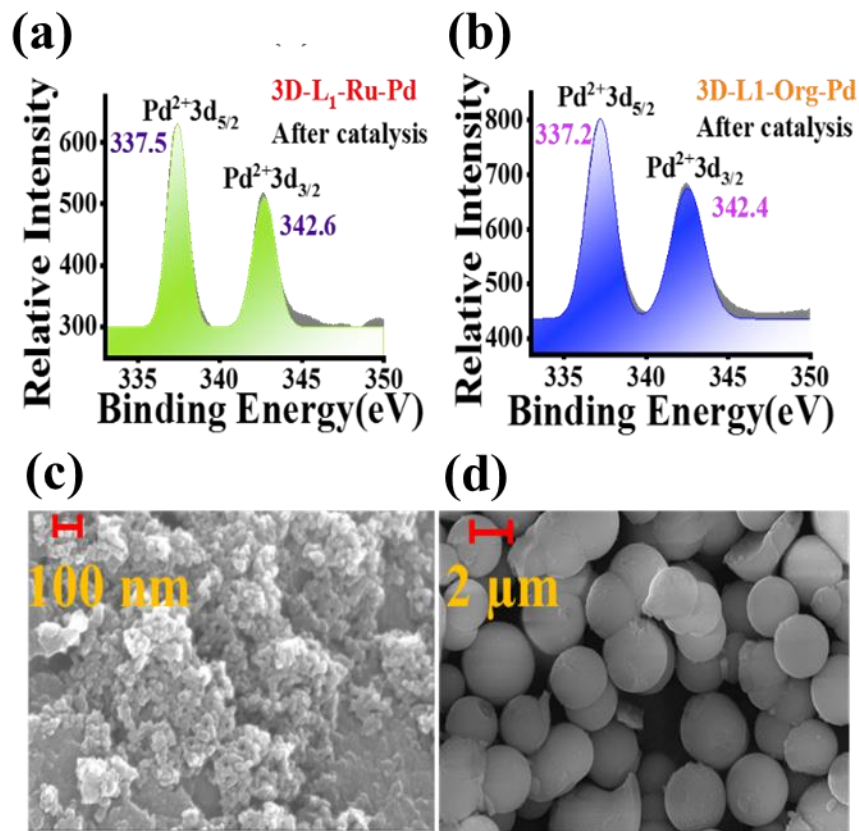


Figure S61.  $^1\text{H}$  NMR spectrum of 9-phenylphenanthrene (500 MHz,  $\text{CDCl}_3$ ).

## XV. XPS and SEM analysis of recovered catalysts



**Figure S62.** XPS spectra of the recovered catalysts (a) [TRIM-Ru-Pd]<sub>n</sub> and (b) [TRIM-Org-Pd]<sub>n</sub>. SEM images of the recovered catalysts (c) [TRIM-Ru-Pd]<sub>n</sub> and (d) [TRIM-Org-Pd]<sub>n</sub>.

## XVI. References

- S1. S. Korwar, K. Brinkley, A. R. Siamaki, B. F. Gupton and K. C. Ellis, *Org. Lett.*, 2015, **17**, 1782–1785
- S2. H. Fei and S. M. Cohen, *J. Am. Chem. Soc.*, 2015, **137**, 2191–2194
- S3. V. Pascanu, F. Carson, M. V. Solano, J. Su, X. Zou, M. J. Johansson and B. Martín-Matute, *Chem. – Eur. J.*, 2016, **22**, 3729–3737
- S4. M. Mondal, J. Joji and J. Choudhury, *Chem. Commun.*, 2017, **53**, 3185–3188
- S5. K. Kim, Y. Jung, S. Lee, M. Kim, D. Shin, H. Byun, S. J. Cho, H. Song and H. Kim, *Angew. Chem., Int. Ed.*, 2017, **56**, 6952–6956

S6. M. H. Majeed, P. Shayesteh, P. Tunå, A. R. Persson, R. Gritcenko, L. R. Wallenberg, L. Ye, C. Hulteberg, J. Schnadt and O. F. Wendt, *Chem. – Eur. J.*, 2019, **25**, 13591-13597

S7. D. Meng, J. Bi, Y. Dong, B. Hao, K. Qin, T. Li and D. Zhu, *Chem. Commun.*, 2020, **56**, 2889-2892

S8. H. Vardhan, A.M. Al-Enizi, A. Nafady, Y. Pan, Z. Yang, H.R. Gutierrez, X. Han, S. Ma, *Small* 2020, 2003970-2003979

S9. T. Mandal, M. Mondal, and J. Choudhury, *Organometallics*, 2021, **40**, 2443–2449

---